AN APPROACH TO MODELING AND IDENTIFICATION OF SYSTEMS WITH SIGNAL-DEPENDENT PARAMETERS

By

KU-CHIN LIN

Bachelor of Science
National Taiwan College of Marine
Science and Technology
Taiwan, R. O. C.
1981

Master of Science
National Cheng Kung University
Taiwan, R. O. C.
1984

Submitted to the Faculty of the
Graduate College of the
Oklahoma State University
in partial fulfillment of
the requirements for
the Degree of
DOCTOR OF PHILOSOPHY
May, 1992

AN APPROACH TO MODELING AND IDENTIFICATION OF SYSTEMS WITH SIGNAL-DEPENDENT PARAMETERS

Thesis Approved :

Karl N. Reid
Thesis Advisor

Dean of the Graduate College

PREFACE

The identification of systems with signal-dependent parameters is considered in this thesis. The main difficulty of such a problem is to estimate the dependence between the signal and system parameters which is usually not in an explicit or simple equation especially when working in the discrete-time domain.

One possible approach to solve the problem is to parameterize the signal dependence into a simplified function in the sense of curve-fitting approximation. Based on such an idea, previous identification methods were not sufficiently robust for a range of applications. Therefore, a new, systematic, and more robust method is introduced in this thesis.

The author would like to express sincere appreciation to Dr. Karl N. Reid for his invaluable advise and thoughtful understanding during the research period under his supervision. Many thanks also go to Dr. Lawrence L. Hoberock, Dr. Gary E. Young, Dr. Martin T. Hagen, and Dr. Eduardo A. Misawa for serving on the advisory committee; their teachings and suggestions brought this study to a successful conclusion.

The author appreciates Dr. M. L. Millett for his helpful guidance and comments during writing this thesis. The advise from Mr. Butch Taylor was so precious on writing and debugging the computer software used in the author's experimental work. Deep gratitude is expressed to Ms. Loi Taylor and Mr. Tom Stewart for their invaluable help in the spiritual phase.

My parents, Yi-zhi Lin and Kou Lyou, have been looking forward to my academic success for years. Their endless support is endlessly appreciated. Thanks to my wife, Tsuey-Fang, for her love and help to keep the end goal constantly in sight, and my lovely daughters, Ann and Joy.

TABLE OF CONTENTS

LIST OF TABLES

Table Page

LIST OF FIGURES

NOMENCLATURE

A	polynomial in q^{-1}
$\mathbf{A}$	system matrix
a_i	constant parameter in system input-output equation
$\mathcal{a}_i$	parameter function in system input-output equation
$\mathcal{a}_{ij}$	parameter function in system state-space equation
$\hat{\mathcal{a}}_i$	estimate of $\mathcal{a}_i$
B	polynomial in q^{-1}
$\mathfrak{B}_n$	a batch of identification data
$\mathfrak{B}_n^*$	a batch of data for model cross validation
$\underline{b}$	input vector
b_j	constant parameter in system input-output equation
$\mathcal{b}_j$	parameter function in system equation
$\mathcal{D}$	system dynamic variable
$\mathcal{D}_{min}$	lower bound of system dynamic variable
$\mathcal{D}_{max}$	upper bound of system dynamic variable
$\mathcal{F}$	Fourier transform
$\mathcal{M}$	membership function
$\mathfrak{M}_i$	model structure
m	system (model) order
n	system (model) order
q^{-1}	backward shift operator

$\mathcal{S}$	shape function
t	discrete time
u	system input
[u]	gated input signal
$\mathcal{W}$	weighting function
x_i	system state variable
$\underline{x}$	system state variable vector
y	system output
[y]	gated output signal
μ_i	constant parameter in membership function
σ_i	constant parameter in shape function
$\underline{\phi}$	regression vector
$\underline{\phi}^T$	transpose of $\underline{\phi}$
$\underline{\theta}$	parameter vector
∇_n	suggested system input signals

CHAPTER I

INTRODUCTION

Background

System identification theory has been well developed for linear systems for decades. The process of system identification basically includes three stages which are system modeling (or model structure selection), parameter estimation, and model validation [24]. However, problems may arise in each stage of the process if an extension of the linear theory to the identification of nonlinear systems is desired.

First, the stage of nonlinear systems modeling is difficult to be generalized since diverse nonlinear systems exist in real life. First principles and physical insights of systems are important to achieve a pertinent model structure in which the parameters can be adequately estimated using an estimator available.

Basically, nonlinear model structures can be classified into two categories which are linear and nonlinear in terms of the model parameters respectively. Parameters are more easily estimated by implementing many well-known

least-squares based estimators [46, 55] if a nonlinear system can be properly modeled into the former category. But, for some applications, it is necessary to consider a model structure which is nonlinear in its parameters.

Models resulting from the stages of system modeling and parameter estimation may still be inadequate for prediction accuracy or application purpose. The stage of model validation concerns the use or development of techniques to test the validity of the resulting models.

For linear models, many model validation methods such as correlation methods [11, 49], statistical hypothesis tests [24, 43] and the famous Akaike's Information Criterion [40, 42] have been well developed. However, the methods assume the system to be identified is within a selected model structure. Such an assumption is too restricting in the validation of nonlinear models [6, 8].

Literature Survey

The problem of nonlinear system identification is too broad to be treated in a general manner. It is the trend in literature to narrow down the problem for some specific classes of nonlinear systems which include :

1. Volterra series

$$y(t) = \sum_{i=1}^{\infty} \int_{\Omega} \cdots \int h_n(\tau_1, \ldots, \tau_n) \prod_{i=1}^{n} u(t-\tau_i)\, d\tau_i \qquad (1.1)$$

2. Bilinear systems

$$y(t) = \sum_{i=1}^{n} a_i \; y(t-i) + \sum_{j=1}^{m} b_j \; u(t-j) + \sum_{i=1}^{n} \sum_{j=1}^{m} c_{ij} \; y(t-i)u(t-j) \qquad (1.2)$$

3. Block-Oriented systems

   (a) Hammerstein systems

   (b) Wiener systems

   (c) Generalized Hammerstein (Wiener) systems

4. Nonlinear auto-regressive-moving-average (NARMA) systems

$$y(t) = \mathcal{F}^{\ell}(y(t-1),\ldots,y(t-n),u(t-1),\ldots,u(t-m)) \qquad (1.3)$$

5. "Linear" systems with signal-dependent parameters

Volterra series can be regarded as a generalization of impulse responses for linear systems [Volterra 1930, Sagaspe 1979, Parker 1982]. As shown in Equation (1.1), the series is a mapping from the system past inputs into present output. Such a modeling approach normally requires a large number of Volterra kernels h_n to characterize the system process that may cause problems in the estimation of Volterra kernels [Stoica 1982, Billings 1984].

Bilinear systems are a special class of nonlinear systems. Due to the mathematical simplicity and close

relation to linear systems, bilinear systems were considered good examples to exploit the problem of nonlinear system identification [Ahmed 1986, Gabr 1986, Fnaiech 1987].

Block-oriented systems form another special class of nonlinear systems where system nonlinearities are static and can be modeled separately from the system dynamics. Some typical block-oriented systems are shown in Figure 1, where the system nonlinearities are denoted by the functions f(u) and/or g(x).

A Hammerstein system can be conceived as a system with a nonlinear input component. Henceforth, the system dynamics will change as the input varies. Practical examples of Hammerstein systems can be found in [Hsia 1968] and [Corlis 1969].

The identification of Hammerstein systems was first investigated by Narendra et. al. [47]. Since then, the problem has received much attention from many researchers, for example, Chang [13], Haist [33], Gallman [22], Stoica [57], Greblicki [26-28], Hwang [35], Jiang [37], and Krzyzak [39]. However, most researchers assumed the nonlinear function f(u) is polynomial or can be approximated by a finite order polynomial. It can be shown that the assumption could be inadequate for some applications.

On the other hand, Wiener system nonlinearities can be conceived as due to the nonlinear output measurement device. Although the structure of a Wiener system is simply the

(a) Hammerstein Systems

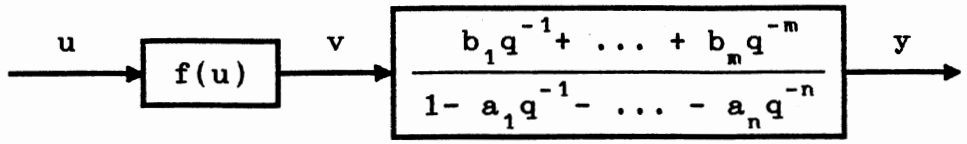

(b) Wiener Systems

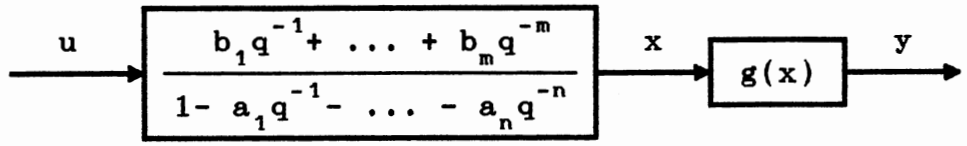

(c) Generalized Hammerstein (Wiener) Systems

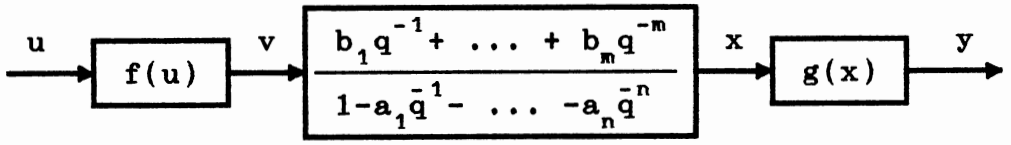

Figure 1. Typical Block-Oriented Systems.

reverse of that of a Hammerstein system, the identification problem for the former is in general more complicated than that for the latter [Billings 1982, Pajunen 1985] as explained in Chapter III of this thesis.

A generalized Hammerstein system has dynamics depending on the system input and the system output. Due to the complexity of system dynamics, it is difficult to develop a feasible identification algorithm for such a class of systems. Interested readers may refer to the paper by Falkner [18].

The class of NARMA systems was introduced by Billings et. al. [4, 6, 7, 8, 9], Chen [14] and Korenberg [38]. In Equation (1.3), ℓ denotes the degree of system nonlinearities and the function $\mathcal{F}$ is a linear combination of its arguments. Such a class of systems is more broad than the class of bilinear systems.

In practice, system identification using NARMA models works just like a "black-box" approach. A model validation method is required to determine proper values of m, n and ℓ. In this respect, Billings et. al. [6, 8] proposed a correlation-based validation method by testing higher-order correlation functions between the system inputs and outputs. But, the method could fail if the system concerned does not belong to the class of NARMA systems.

"Linear" systems with signal-dependent parameters are ubiquitous in real life. Indeed, system nonlinearities are

mostly caused by the variation of some signal such as system input, state variables and/or environmental temperature. Examples of such a class of systems are illustrated in Chapter IV and refer to [Haber, 1979] for more examples.

Modeling nonlinear systems using signal-dependent parameters is a more general approach than using block-oriented structures. For example, the nonlinearities of a Hammerstein system and Wiener system are caused by the variation of system inputs and outputs respectively. It will be shown in Chapter II that a Hammerstein system can be considered as a "linear" system with input-dependent parameters, whereas a Wiener system can be considered as a "linear" system with output-dependent parameters.

The so-called sinusoidal-input describing function models are input amplitude dependent [59-61]. Such a modeling approach is based on an assumption that the system nonlinearities can be lumped into an input-dependent function such as those of Hammerstein systems.

Also, the signal-dependent modeling concept gives a clear description of system dynamics. Many well-known terminologies such as system zeros/poles and damping ratio, and stability concept for linear systems can be extended for systems with signal dependent parameters.

Previous Studies

One approach to estimate system parameters is the use

of classical linear identification method by neglecting the signal dependence. But, the resulting model could be inadequate when the required working range is large.

Another approach called gate function method by Haber et. al. [30, 31] was developed based on the concept of piecewise linear modeling which fits a nonlinear system by using a number of linear models and each linear model is used to describe the system local dynamics.

In gate function method, the working range of the nonlinearity-related signal is quantified into intervals. For each quantification interval, a set of gated signals is extracted from the identification data collected. Then, a linear model is formed based on each set of gated signals by using a classical linear estimator such as the recursive least-squares. However, the quantification intervals cannot be too small to guarantee the success of parameter estimation for each model [Haber, 1985]. In other words, the number of linear models to fit the nonlinear system is limited. This means the global modeling accuracy could be limited (see Chapter III for further discussion).

The third possible approach to estimate system parameters having uncertain signal dependence is to assume the relationship between the system parameters and the signal is approximately polynomial. However, as mentioned earlier, such an assumption may not be adequate for a wide range of applications.

Scope of Study

The literature survey conducted by the author shows that although the modeling concept using signal-dependent parameters is more general than using block-oriented structures, the corresponding identification problem for the former have received much less attention from researchers than for the latter.

The signal-dependent modeling concept may not be well known or widely accepted. This study shows a favor to such a modeling concept by illustrating some industrial systems which have no block-oriented structures but can be adequately modeled into "linear" structures with signal-dependent parameters (Example 2 and Example 3 in Chapter IV).

Also, some promising advantages accompanied with the signal-dependent modeling concept are revealed. They include an useful insight into the system input design problem for persistent excitation and improvement of the robustness of classical model-based linear controllers to system nonlinearities. The former is practically important in the issue of nonlinear system identification. For the latter, a linear control methodology is used as an example to design a controller with signal-dependent gains. The demonstration of the robustness of such a signal-dependent controller to system nonlinearities was carried out

experimentally.

In the previous methods, the signal-dependent parameters were approximated by constants (i.e. classical linear method), piecewise constants (i.e. gate function method), or polynomials. It will be shown that those methods may not be adequate for systems with complicated signal-dependent parameters. In this respect, a new identification method with better flexibility to handle diverse complicated system nonlinearities is proposed (Appendix D).

In the proposed identification method, the approximation of system signal-dependent parameters is developed using the fuzzy linguistic description. The resulting model structure is a combination of the linguistic description and "linear" dynamic equation(s) (Chapter II). A parameter estimation method, which works cyclically and iteratively between the Complex Method [12, 53] and recursive least-squares estimator, is introduced to estimate the model parameters (Chapter III).

Finally, the scope of this study includes comparison studies among the above identification methods across a range of different systems which are conducted either by simulation or by experiment.

CHAPTER II

"LINEAR" SYSTEMS WITH SIGNAL-DEPENDENT PARAMETERS

A "linear" system with signal-dependent parameters means that the values of the system parameters (or coefficients) can change with some signal(s) which can be the system input, state variables and/or an environmental signal such as temperature. In other words, the system considered has signal-dependent dynamic properties, such as signal-dependent *poles*, *zeros*, *damping ratio* and so on.

System Equations and Definitions

It is assumed that the class of systems to be identified can be described by the following discrete input-output equation :

$$A(q^{-1},\mathcal{P})\ y(t) = B(q^{-1},\mathcal{P})\ u(t) \tag{2.1a}$$

where

$$A(q^{-1},\mathcal{P}) = 1 - a_1(\mathcal{P})q^{-1} - \ldots - a_n(\mathcal{P})q^{-n} \tag{2.1b}$$

$$B(q^{-1},\mathcal{P}) = b_1(\mathcal{P})q^{-1} + \ldots + b_m(\mathcal{P})q^{-m} \tag{2.1c}$$

or state-space equations :

$$\underline{x}(t+1) = \mathbf{A}(\mathcal{D})\ \underline{x}(t) + \underline{b}(\mathcal{D})\ u(t) \tag{2.2a}$$

where

$$\underline{x}(t) = [x_1(t),\ x_2(t),\ \ldots,\ x_n(t)]^T \tag{2.2b}$$

$$\mathbf{A}(\mathcal{D}) = \begin{bmatrix} a_{11}(\mathcal{D}) & a_{12}(\mathcal{D}) & \ldots & a_{1n}(\mathcal{D}) \\ a_{21}(\mathcal{D}) & a_{22}(\mathcal{D}) & \ldots & a_{2n}(\mathcal{D}) \\ \vdots & \vdots & \ddots & \vdots \\ a_{n1}(\mathcal{D}) & a_{n2}(\mathcal{D}) & \ldots & a_{nn}(\mathcal{D}) \end{bmatrix} \tag{2.2c}$$

$$\underline{b}(\mathcal{D}) = [\mathcal{b}_1(\mathcal{D}),\ \mathcal{b}_2(\mathcal{D}),\ \ldots,\ \mathcal{b}_n(\mathcal{D})]^T \tag{2.2d}$$

The script parameters $\mathcal{a}$s and $\mathcal{b}$s denote signal-dependent parameters.

The above system equations are very similar to their linear counterparts. The only difference is that the parameters involved depend on the signal $\mathcal{D}$ which is the system *dynamic variable*. Since the system parameters are functions of the dynamic variable, they are sometimes called *parameter functions* in the ensuing context.

The relation between the system parameters and the dynamic variable is assumed uncertain, and the functional forms of $\mathcal{a}$s and $\mathcal{b}$s are unknown.

Also, it is assumed that the system inputs are available for handling and design, and the system output (or the state variables if a state-space model is required) and the dynamic variable (if it differs from the signals already measured) are available for measure.

Practical Examples

Many physical systems have signal-dependent parameters. For instance, the parameters of a gas-turbine engine are direction dependent [23]. An aircraft flight system during the stall/post-stall regions has parameters which are functions of the angle of attack [56] (Example 2, Chapter IV). For a hydraulic system, the bulk modulus of the system working fluid depends on pressure and temperature [45] (Example 3, Chapter IV). Further examples can be found in [Haber 1979].

Special Examples : Block-Oriented Systems

As shown in Figure 1(a), a Hammerstein system has static nonlinearities on the input side. It can be easily shown that the system equations can be written in a "linear" structure with input-dependent parameters :

$$A(q^{-1})\, y(t) = B(q^{-1},u)\, u(t) \tag{2.3a}$$

where

$$A(q^{-1}) = 1 - a_1 q^{-1} - \ldots - a_n q^{-n} \tag{2.3b}$$

$$B(q^{-1},u) = \mathcal{B}_1(u(t-1))q^{-1} + \ldots + \mathcal{B}_m(u(t-m))q^{-m} \tag{2.3c}$$

$$\mathcal{B}_j(u(t-j)) = b_j f(u(t-j))/u(t-j),\ j = 1, \ldots, m \tag{2.3d}$$

In Equations (2.3), only part of the system parameters depend on the input or its past signals; the system poles are fixed but the zeros depend on the system inputs. The parameter functions have the same form and are related to the nonlinear element f(u) according to Equation (2.3d). Such information is useful in the later parameter estimation (Example 1, Chapter IV).

On the other hand, a Wiener system (Figure 1(b)) can be conceived as a linear system along with an output measurement device which has significant nonlinearities in the normal operating range. A practical example of Wiener systems is considered in Example 4, Chapter IV while the system equations are :

$$A(q^{-1},y)\ y(t) = B(q^{-1},y)\ u(t) \tag{2.4a}$$

where

$$A(q^{-1},y) = 1 - \alpha_1(y(t),y(t-1))q^{-1} - \ldots - \alpha_n(y(t),y(t-n))q^{-n} \tag{2.4b}$$

$$B(q^{-1},u) = \beta_1(y(t))q^{-1} + \ldots + \beta_m(y(t))q^{-m} \tag{2.4c}$$

$$\alpha_i(y(t),y(t-i)) = a_i g^*(y(t-i))/g^*(y(t)) ,\quad i = 1,\ldots,n \tag{2.4d}$$

$$\beta_j(y(t)) = b_j/g^*(y(t)) ,\ j = 1, \ldots,m \tag{2.4e}$$

$$g^*(y(t)) = g^{-1}(y(t))/y(t) \qquad (2.4f)$$

Note that the system nonlinear element g(x) is assumed invertible with the inverse denoted by $g^{-1}(y)$.

As shown in Equations (2.4), Wiener system parameters depend on the system output and/or its past signals. The dependence is characterized by the function $1/g^*(y)$ which is related to the reciprocal of the inverse of the nonlinear function g(x).

In general, the parameter functions of a Wiener system, compared with a corresponding Hammerstein system, are more complicated and difficult for estimation. Furthermore, for Wiener systems, the input design problem to guarantee persistent excitation is more complicated. This will be explained in Chapter III.

By combining Equations (2.3) with Equations (2.4), the system equations of a generalized Hammerstein system shown in Figure 1(c) are

$$A(q^{-1},y)\ y(t) = B(q^{-1},y,u)\ u(t) \qquad (2.5a)$$

where

$$A(q^{-1},y) = 1 - a_1(y(t),y(t-1))q^{-1} - \ldots - a_n(y(t),y(t-n))q^{-n} \qquad (2.5b)$$

$$B(q^{-1},u) = \ell_1(y(t),u(t-1))q^{-1} + \ldots + \ell_m(y(t),u(t-m))q^{-m} \qquad (2.5c)$$

$$a_i(y(t),y(t-i)) = a_i g^*(y(t-i))/g^*(y(t)) \ , \quad i = 1,\ldots,n \qquad (2.5d)$$

$$\ell_j(y(t),u(t-j)) = b_j f(u(t-j))/(u(t-j)g^*(y(t))) \ , \quad j = 1,\ldots,m \qquad (2.5e)$$

$$g^*(y(t)) = g^{-1}(y(t))/y(t) \qquad (2.5f)$$

It has been shown that typical block-oriented systems can be considered as "linear" systems with input- and/or output-dependent parameters. If the signal dependence is uncertain, the system parameter functions cannot be estimated unless they are parameterized. In this respect, some parameterization approaches such as curve-fitting approximation are considered in this study.

For instance, a possible approach is to parameterize each system parameter function in terms of a proper order polynomial. Also, one may fit a piecewise constant function in each parameter function (Chapter III). Both parameterization approaches are conceptually simple and easy to implement. However, it will be shown later that they are not adequate for a range of applications. For this reason, a more general parameterization approach is proposed.

Parameterization of System Parameter Functions Using Fuzzy Linguistic Description

Fuzzy linguistic description based on the pioneer work by Zadeh [64] has been applied in many engineering areas such as system identification and control [58]. In this study, fuzzy description is used to parameterize the uncertain relation between the system parameters and dynamic variable.

Consider the following linguistic rules :

If $\mathcal{D}$ is small then

$$\hat{a}_1(\mathcal{D}) = \mathcal{S}_S(\mathcal{D}) \tag{2.6a}$$

If $\mathcal{D}$ is large then

$$\hat{a}_1(\mathcal{D}) = \mathcal{S}_L(\mathcal{D}) \tag{2.6b}$$

where $\mathcal{D}$ is the input of the linguistic rules, $\hat{a}_1(\mathcal{D})$ denotes an estimate of $a_1(\mathcal{D})$ in Equation (2.1b) which is the output of the rules. "Small" and "large" are the so-called *membership functions* and are denoted by $\mathcal{M}_S(\mathcal{D})$ and $\mathcal{M}_L(\mathcal{D})$ respectively.

Note that each membership function will be accompanied by a function (i.e. $\mathcal{S}_S(\mathcal{D})$ or $\mathcal{S}_L(\mathcal{D})$ for this case) which is referred to as a *shape function*. By the definitions in the next section, each equal sign in Equations (2.6) does not

exactly hold unless either $M_S(\mathcal{D}) = 0$ or $M_L(\mathcal{D}) = 0$.

Definitions

The output of Equations (2.6) is defined to be a combination of $\mathcal{S}_S(\mathcal{D})$ and $\mathcal{S}_L(\mathcal{D})$ with signal-dependent weights, i.e. :

$$\hat{a}_1(\mathcal{D}) = W_S(\mathcal{D})\ \mathcal{S}_S(\mathcal{D}) + W_L(\mathcal{D})\ \mathcal{S}_L(\mathcal{D}) \tag{2.7a}$$

where

$$W_S(\mathcal{D}) = \begin{cases} \dfrac{M_S(\mathcal{D})}{M_S(\mathcal{D}) + M_L(\mathcal{D})}, & \text{if } M_S(\mathcal{D}) + M_L(\mathcal{D}) \neq 0 \\ 0, & \text{otherwise} \end{cases} \tag{2.7b}$$

$$W_L(\mathcal{D}) = \begin{cases} \dfrac{M_L(\mathcal{D})}{M_S(\mathcal{D}) + M_L(\mathcal{D})}, & \text{if } M_S(\mathcal{D}) + M_L(\mathcal{D}) \neq 0 \\ 0, & \text{otherwise} \end{cases} \tag{2.7c}$$

and $W_S(\mathcal{D})$ and $W_L(\mathcal{D})$ will be called *weighting functions*.

By the above definitions, the meaning of the linguistic description of Equations (2.6) should be clear. The degrees of truth of the premise statements are given by the images of the corresponding membership functions which are in turn used to calculate $W_S(\mathcal{D})$ and $W_L(\mathcal{D})$ according to Equations (2.7b) and (2.7c).

The result of Equations (2.6) is determined by the membership functions and shape functions to be used.

Although the selection of membership functions and shape functions could be application dependent, a simple and systematic approach which has been proven adequate for a range of applications is provided here.

Membership Functions

Typical membership functions considered in this study are shown in Figure 2.

(a) Linear membership functions

$$\mu_S(\mathcal{D}) = \begin{cases} \mathcal{L}_S(\mathcal{D}) & , \text{ if } \mathcal{D}_{min} \le \mathcal{D} < \mu_1 \\ 0 & , \text{ otherwise} \end{cases} \qquad (2.8a)$$

$$\mu_L(\mathcal{D}) = \begin{cases} \mathcal{L}_L(\mathcal{D}) & , \text{ if } \mu_2 < \mathcal{D} \le D_{max} \\ 0 & , \text{ otherwise} \end{cases} \qquad (2.8b)$$

(b) Quadratic membership functions

$$\mu_S(\mathcal{D}) = \begin{cases} (1-\mu_3)\ \mathcal{L}_S^2 + \mu_3\ \mathcal{L}_S & , \text{ if } \mathcal{D}_{min} \le \mathcal{D} < \mu_1 \\ 0 & , \text{ otherwise} \end{cases} \qquad (2.9a)$$

$$\mu_L(\mathcal{D}) = \begin{cases} (1-\mu_4)\ \mathcal{L}_L^2 + \mu_4\ \mathcal{L}_L & , \text{ if } \mu_2 < \mathcal{D} \le \mathcal{D}_{max} \\ 0 & , \text{ otherwise} \end{cases} \qquad (2.9b)$$

where

(a) Linear Membership Functions

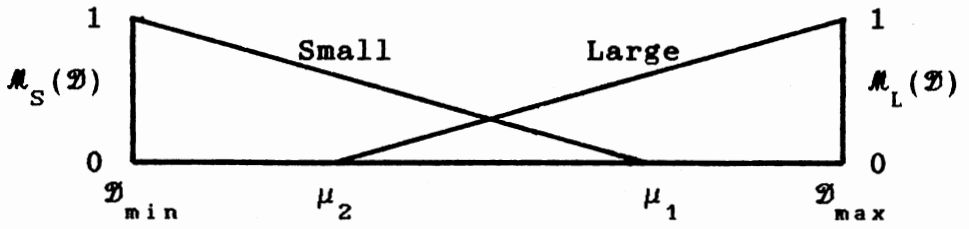

(b) Quadratic Membership Functions

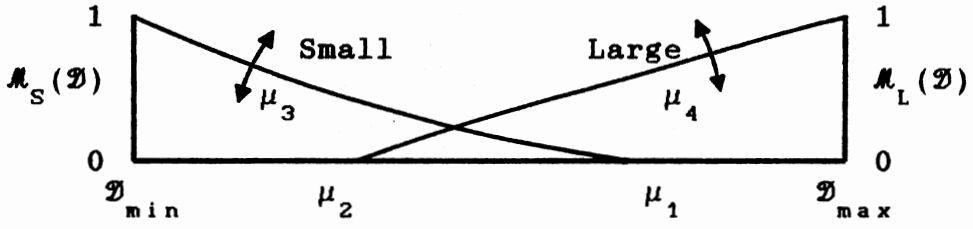

Figure 2. Typical Membership Functions.

$$\mathcal{L}_S(\mathcal{D}) = (\mu_1 - \mathcal{D})/(\mu_1 - \mathcal{D}_{min}) \qquad (2.10a)$$

$$\mathcal{L}_L(\mathcal{D}) = (\mathcal{D} - \mu_2)/(\mathcal{D}_{max} - \mu_2) \qquad (2.10b)$$

$$\mathcal{D}_{min} < \mu_1, \mu_2 < \mathcal{D}_{max} \qquad (2.11a)$$

$$0 \leq \mu_3, \mu_4 \leq 2 \qquad (2.11b)$$

Note that the bounds of the operating range of the dynamic variable (i.e. $\mathcal{D}_{min}$ and $\mathcal{D}_{max}$) are required in the above equations. If the bounds do not naturally arise as part of the problem formulation, then proper estimates are necessary.

Without loss of generality, the values of membership functions can be normalized between 0 and 1 as shown in Figure 2. A linear membership function is characterized by one parameter and a quadratic membership function by two.

Membership function $\mathcal{M}_L(\mathcal{D})$ is zero if $\mathcal{D}_{min} \leq \mathcal{D} \leq \mu_2$ (i.e. $\mathcal{D}$ is "very" small) that in turn means $\hat{a}_1(\mathcal{D}) = \mathcal{I}_S(\mathcal{D})$. Similarly, $\hat{a}_1(\mathcal{D}) = \mathcal{I}_L(\mathcal{D})$ if $\mathcal{D}$ is "very" large (i.e. $\mu_1 \leq \mathcal{D} \leq \mathcal{D}_{max}$). In Equation (2.11b), the constraints on μ_3 and μ_4 are just to assure $0 \leq \mathcal{M}_S(\mathcal{D}), \mathcal{M}_L(\mathcal{D}) \leq 1$. The best values of the parameter μs are still unknown but they will be determined (or estimated) with the constraints of Equations (2.11) in some optimal sense.

Shape Functions

The selection of shape functions cannot be arbitrary to be in tune with the parameter estimation algorithm proposed in Chapter III. First, adequate shape functions must be linear :

$$\mathcal{S}_S(\mathcal{D}) = \sigma_{S,0} + \sigma_{S,1}\varphi_{S,1}(\mathcal{D}) + \ldots + \sigma_{S,N}\varphi_{S,N}(\mathcal{D}) \qquad (2.12a)$$

$$\mathcal{S}_L(\mathcal{D}) = \sigma_{L,0} + \sigma_{L,1}\varphi_{L,1}(\mathcal{D}) + \ldots + \sigma_{L,N}\varphi_{L,N}(\mathcal{D}) \qquad (2.12b)$$

Secondly, in above equations $\{1,\varphi_{S,1},\ldots,\varphi_{S,N}\}$ and $\{1,\varphi_{L,1},\ldots,\varphi_{L,N}\}$ should be two bases in $\mathbb{R}^{N+1}$, i.e.

$$\text{if } \mathcal{S}_S(\mathcal{D}) = 0 \text{ then } \sigma_{S,0} = \sigma_{S,1} = \ldots = \sigma_{S,N} = 0 \qquad (2.13a)$$

$$\text{if } \mathcal{S}_L(\mathcal{D}) = 0 \text{ then } \sigma_{L,0} = \sigma_{L,1} = \ldots = \sigma_{L,N} = 0 \qquad (2.13b)$$

The requirements of Equations (2.12) and (2.13) can be simply satisfied by using polynomial shape functions so that

$$\varphi_{S,i}(\mathcal{D}) = \varphi_{L,i}(\mathcal{D}) = \mathcal{D}^i \quad , \; i = 1,\ldots,N \qquad (2.14)$$

In short, the result of Equations (2.6) along with the use of the membership functions shown in Figure 2 is summarized as :

(a) $\mu_1 > \mu_2$ (2.15)

$$\hat{a}_1(\mathcal{D}) = \begin{cases} \mathcal{S}_S(\mathcal{D}) & , \text{ if } \mathcal{D}_{min} \le \mathcal{D} \le \mu_2 \\ \mathcal{W}_S(\mathcal{D})\mathcal{S}_S(\mathcal{D}) + \mathcal{W}_L(\mathcal{D})\mathcal{S}_L(\mathcal{D}), & \text{ if } \mu_2 < \mathcal{D} < \mu_1 \\ \mathcal{S}_L(\mathcal{D}) & , \text{ if } \mu_1 \le \mathcal{D} \le \mathcal{D}_{max} \end{cases} \quad (2.16)$$

(b) $\mu_1 < \mu_2$ (2.17)

$$\hat{a}_1(\mathcal{D}) = \begin{cases} \mathcal{S}_S(\mathcal{D}) & , \text{ if } \mathcal{D}_{min} \le \mathcal{D} < \mu_1 \\ 0 & , \text{ if } \mu_1 \le \mathcal{D} \le \mu_2 \\ \mathcal{S}_L(\mathcal{D}) & , \text{ if } \mu_2 < \mathcal{D} \le \mathcal{D}_{max} \end{cases} \quad (2.18)$$

and some mathematical properties of the proposed linguistic description are summarized in the following remarks :

Remark 1. Geometrically, $\hat{a}_1(\mathcal{D})$ is composed of three elements. It can be piecewise continuous with the constraint of $\mu_1 > \mu_2$ or discontinuous with the constraint of $\mu_1 < \mu_2$.

Remark 2. An increase in the order of the membership functions only results in an improvement of $\hat{a}_1(\mathcal{D})$ at the subspace $[\mu_2, \mu_1]$ as shown in Equation (2.16). However, an increase in the order of the shape functions may lead to a global improvement of $\hat{a}_1(\mathcal{D})$.

Remark 3. An intriguing advantage of the proposed parameterization approach is its ease for extension. Indeed, the whole dynamic variable space can be first divided into two or more subspaces. Then, a pair of membership functions and shape functions are defined over each subspace. Such an extension is important in case the system parameter functions are very complicated or high accurate modeling is required (Examples 2 and 4, Chapter IV).

Proposed Nonlinear Model Structures

Perform the similar parameterization of $\hat{a}_1(\mathcal{D})$ as in the previous section for the estimates of the other system parameter functions. The following nonlinear model structures $\mathcal{R}_1$ and $\mathcal{R}_2$ are proposed for those systems expressed by Equations (2.1) and (2.2) respectively :

$$\mathcal{R}_1 : \quad \hat{A}(q^{-1},\mathcal{D})\, y(t) = \hat{B}(q^{-1},\mathcal{D})\, u(t) \tag{2.19a}$$

If $\mathcal{D}$ is small then

$$\begin{aligned} \hat{a}_1(\mathcal{D}) &= \mathcal{F}_{S,a_1}(\mathcal{D}) \\ &\vdots \quad\quad \vdots \\ \hat{a}_n(\mathcal{D}) &= \mathcal{F}_{S,a_n}(\mathcal{D}) \\ \hat{b}_1(\mathcal{D}) &= \mathcal{F}_{S,b_1}(\mathcal{D}) \\ &\vdots \quad\quad \vdots \\ \hat{b}_m(\mathcal{D}) &= \mathcal{F}_{S,b_m}(\mathcal{D}) \end{aligned} \tag{2.19b}$$

If $\mathcal{D}$ is large then

$$\begin{aligned}
\hat{a}_1(\mathcal{D}) &= \mathcal{I}_{L,a_1}(\mathcal{D}) \\
&\vdots \qquad\quad \vdots \\
\hat{a}_n(\mathcal{D}) &= \mathcal{I}_{L,a_n}(\mathcal{D}) \\
\hat{b}_1(\mathcal{D}) &= \mathcal{I}_{L,b_1}(\mathcal{D}) \\
&\vdots \qquad\quad \vdots \\
\hat{b}_m(\mathcal{D}) &= \mathcal{I}_{L,b_m}(\mathcal{D})
\end{aligned} \tag{2.19c}$$

where

$$\hat{A}(q^{-1},\mathcal{D}) = 1 - \hat{a}_1(\mathcal{D})q^{-1} - \ldots - \hat{a}_n(\mathcal{D})q^{-n} \tag{2.19d}$$

$$\hat{B}(q^{-1},\mathcal{D}) = \hat{b}_1(\mathcal{D})q^{-1} + \ldots + \hat{b}_m(\mathcal{D})q^{-m} \tag{2.19e}$$

and

$$\mathcal{R}_2 : \quad \underline{x}(t+1) = \hat{A}(\mathcal{D})\ \underline{x}(t) + \hat{\underline{b}}(\mathcal{D})\ u(t) \tag{2.20a}$$

If $\mathcal{D}$ is small then

$$\begin{aligned}
\hat{a}_{11}(\mathcal{D}) &= \mathcal{I}_{S,a_{11}}(\mathcal{D}) \\
&\vdots \qquad\quad \vdots \\
\hat{a}_{nn}(\mathcal{D}) &= \mathcal{I}_{S,a_{nn}}(\mathcal{D}) \\
\hat{b}_1(\mathcal{D}) &= \mathcal{I}_{S,b_1}(\mathcal{D}) \\
&\vdots \qquad\quad \vdots \\
\hat{b}_n(\mathcal{D}) &= \mathcal{I}_{S,b_n}(\mathcal{D})
\end{aligned} \tag{2.20b}$$

If $\mathcal{D}$ is large then

$$\begin{aligned}
\hat{a}_{11}(\mathcal{D}) &= \mathcal{F}_{L,a_{11}}(\mathcal{D}) \\
&\vdots \qquad\quad \vdots \\
\hat{a}_{nn}(\mathcal{D}) &= \mathcal{F}_{L,a_{nn}}(\mathcal{D}) \\
\hat{b}_1(\mathcal{D}) &= \mathcal{F}_{L,b_1}(\mathcal{D}) \\
&\vdots \qquad\quad \vdots \\
\hat{b}_n(\mathcal{D}) &= \mathcal{F}_{L,b_n}(\mathcal{D})
\end{aligned} \tag{2.20c}$$

where

$$\hat{\mathbf{A}}(\mathcal{D}) = \begin{bmatrix} \hat{a}_{11}(\mathcal{D}) & \hat{a}_{12}(\mathcal{D}) & \cdots & \hat{a}_{1n}(\mathcal{D}) \\ \hat{a}_{21}(\mathcal{D}) & \hat{a}_{22}(\mathcal{D}) & \cdots & \hat{a}_{2n}(\mathcal{D}) \\ \vdots & \vdots & \ddots & \vdots \\ \hat{a}_{n1}(\mathcal{D}) & \hat{a}_{n2}(\mathcal{D}) & \cdots & \hat{a}_{nn}(\mathcal{D}) \end{bmatrix} \tag{2.20d}$$

$$\hat{\underline{b}}(\mathcal{D}) = [\hat{b}_1(\mathcal{D}),\ \hat{b}_2(\mathcal{D}),\ \ldots,\ \hat{b}_n(\mathcal{D})]^T \tag{2.20e}$$

In the proposed model structures, it is not necessary for all estimated parameter functions to share the same set of membership functions. Theoretically, a different set of membership functions can be used to form each estimated parameter function. But, for computation efficiency and feasible estimation of parameters, this is not recommended.

Instead, the estimated parameter functions will be distinguished by using different shape functions as :

$$\mathcal{G}_{S,a_i}(\mathcal{D}) = \underline{\Sigma}^T_{S,a_i}\,\underline{\Delta} \quad , \; i = 1,\ldots,n \tag{2.21a}$$

$$\mathcal{G}_{L,a_i}(\mathcal{D}) = \underline{\Sigma}^T_{L,a_i}\,\underline{\Delta} \quad , \; i = 1,\ldots,n \tag{2.21b}$$

$$\mathcal{G}_{S,b_j}(\mathcal{D}) = \underline{\Sigma}^T_{S,b_j}\,\underline{\Delta} \quad , \; j = 1,\ldots,m \tag{2.21c}$$

$$\mathcal{G}_{L,b_j}(\mathcal{D}) = \underline{\Sigma}^T_{L,b_j}\,\underline{\Delta} \quad , \; j = 1,\ldots,m \tag{2.21d}$$

where

$$\underline{\Sigma}^T_{S,a_i} = [\sigma_{S,a_i,0},\ldots,\sigma_{S,a_i,N}] \quad , \; i = 1,\ldots,n \tag{2.22a}$$

$$\underline{\Sigma}^T_{L,a_i} = [\sigma_{L,a_i,0},\ldots,\sigma_{L,a_i,N}] \quad , \; i = 1,\ldots,n \tag{2.22b}$$

$$\underline{\Sigma}^T_{S,b_j} = [\sigma_{S,b_j,0},\ldots,\sigma_{S,b_j,N}] \quad , \; j = 1,\ldots,m \tag{2.22c}$$

$$\underline{\Sigma}^T_{L,b_j} = [\sigma_{L,b_j,0},\ldots,\sigma_{L,b_j,N}] \quad , \; j = 1,\ldots,m \tag{2.22d}$$

$$\underline{\Delta}^T = [1,\ \mathcal{D},\ \mathcal{D}^2,\ldots,\ \mathcal{D}^N] \tag{2.22e}$$

and

$$\mathcal{G}_{S,a_{ij}}(\mathcal{D}) = \underline{\Sigma}^T_{S,a_{ij}}\,\underline{\Delta} \quad , \; \begin{matrix} i = 1,\ldots,n \\ j = 1,\ldots,n \end{matrix} \tag{2.23a}$$

$$\mathcal{G}_{L,a_{ij}}(\mathcal{D}) = \underline{\Sigma}^T_{L,a_{ij}}\,\underline{\Delta} \quad , \; \begin{matrix} i = 1,\ldots,n \\ j = 1,\ldots,n \end{matrix} \tag{2.23b}$$

$$\mathcal{G}_{S,b_i}(\mathcal{D}) = \underline{\Sigma}^T_{S,b_i}\,\underline{\Delta} \quad , \; i = 1,\ldots,n \tag{2.23c}$$

$$\mathcal{G}_{L,b_i}(\mathcal{D}) = \underline{\Sigma}^T_{L,b_i}\,\underline{\Delta} \quad , \; i = 1,\ldots,n \tag{2.23d}$$

where

$$\underline{\Sigma}^T_{S,a_{ij}} = [\sigma_{S,a_{ij},0},\ldots,\sigma_{S,a_{ij},N}], \quad \begin{matrix} i = 1,\ldots,n \\ j = 1,\ldots,n \end{matrix} \qquad (2.24a)$$

$$\underline{\Sigma}^T_{L,a_{ij}} = [\sigma_{L,a_{ij},0},\ldots,\sigma_{L,a_{ij},N}], \quad \begin{matrix} i = 1,\ldots,n \\ j = 1,\ldots,n \end{matrix} \qquad (2.24b)$$

$$\underline{\Sigma}^T_{S,b_i} = [\sigma_{S,b_i,0},\ldots,\sigma_{S,b_i,N}] \ , \ i = 1,\ldots,n \qquad (2.24c)$$

$$\underline{\Sigma}^T_{L,b_i} = [\sigma_{L,b_i,0},\ldots,\sigma_{L,b_i,N}] \ , \ i = 1,\ldots,n \qquad (2.24d)$$

Pseudolinear Regression

For the presentation followed, the model structure $\mathbb{R}_1$ is rewritten in the following *regression* form :

$$\mathbb{R}_1 : \qquad y(t) = \underline{\phi}^T(t)\,\underline{\theta} \qquad (2.25a)$$

where

$$\begin{aligned} \underline{\phi}^T(t) = [&\mathbb{W}_S\, y(t-1)\,\underline{\Delta}^T,\ \mathbb{W}_L\, y(t-1)\,\underline{\Delta}^T,\ \ldots, \\ &\mathbb{W}_S\, y(t-n)\,\underline{\Delta}^T,\ \mathbb{W}_L\, y(t-n)\,\underline{\Delta}^T, \\ &\mathbb{W}_S\, u(t-1)\,\underline{\Delta}^T,\ \mathbb{W}_L\, u(t-1)\,\underline{\Delta}^T,\ \ldots, \\ &\mathbb{W}_S\, u(t-m)\,\underline{\Delta}^T,\ \mathbb{W}_L\, u(t-m)\,\underline{\Delta}^T] \end{aligned} \qquad (2.25b)$$

$$\begin{aligned} \underline{\theta}^T = [\ &\underline{\Sigma}^T_{S,a_1},\ \underline{\Sigma}^T_{L,a_1},\ \ldots,\ \underline{\Sigma}^T_{S,a_n},\ \underline{\Sigma}^T_{L,a_n}, \\ &\underline{\Sigma}^T_{S,b_1},\ \underline{\Sigma}^T_{L,b_1},\ \ldots,\ \underline{\Sigma}^T_{S,b_m},\ \underline{\Sigma}^T_{L,b_m}] \end{aligned} \qquad (2.25c)$$

The model structure $\mathbb{R}_1$ is in a *pseudolinear regression* form in that not only the parameters σs in the *parameter vector* $\underline{\theta}$ and the parameters μs in the *regression vector* $\underline{\phi}$ are unknown and must be estimated.

Similar pseudolinear regression form for model structure $\mathbb{R}_2$ can also be derived if all related state variables are available. The derivation of $\mathbb{R}_2$ follows the above straightforwardly.

Identifiability Properties

Identifiability is a concept that is central in identification problems. The concept concerns the unique representation of a given system description in a model structure. A framework on the proof of the identifiability of some linear model structures is given in [Ljung, 1987]. This framework will be followed to exploit the identifiability of the proposed model structures.

Consider the model structure $\mathbb{R}_1$ as an example. For convenience, introduce

$$\underline{\theta} = \underline{\theta}_L = [\mu_1, \mu_2, \underline{\theta}^T]^T \tag{2.26a}$$

or

$$\underline{\theta} = \underline{\theta}_N = [\mu_1, \mu_2, \mu_3, \mu_4, \underline{\theta}^T]^T \tag{2.26b}$$

where $\underline{\theta}$ is given in Equation (2.25c).

Definition 2.1. Two models $\mathbb{R}_1^{<1>}$, $\mathbb{R}_1^{<2>} \in \mathbb{R}_1$ are *equal* (i.e. $\mathbb{R}_1^{<1>} = \mathbb{R}_2^{<2>}$) if

$$\hat{a}_i^{<1>}(\mathcal{D}) = \hat{a}_i^{<2>}(\mathcal{D}) \quad , \quad i = 1,\ldots,n \tag{2.27a}$$

$$\hat{b}_j^{<1>}(\mathcal{D}) = \hat{b}_j^{<2>}(\mathcal{D}) \quad , \quad j = 1,\ldots,m \tag{2.27b}$$

Definition 2.2. The model structure $\mathbb{R}_1$ is *globally identifiable* at $\underline{\theta}^*$ if $\mathbb{R}_1(\underline{\theta}) = \mathbb{R}_1(\underline{\theta}^*)$, $\underline{\theta} \in \mathfrak{R}^M \Rightarrow \underline{\theta} = \underline{\theta}^*$ where $\mathfrak{R}^M$ denotes a set of values over which $\underline{\theta}$ ranges in the model structure $\mathbb{R}_1$.

Definition 2.3. The model structure $\mathbb{R}_1$ is strictly globally identifiable if it is globally identifiable at all $\underline{\theta}^* \in \mathfrak{R}^M$.

Definition 2.4. The model structure $\mathbb{R}_1$ is globally identifiable if it is globally identifiable at almost all $\underline{\theta}^* \in \mathfrak{R}^M$.

Definition 2.3 is quite demanding. It is difficult to construct model structures that are strictly globally identifiable. This is especially true for nonlinear cases. Definition 2.4 is weaker but more realistic. It means that $\mathbb{R}_1$ is globally identifiable at all $\underline{\theta}^* \in \hat{\mathfrak{R}}^M \subset \mathfrak{R}^M$ where

$$\delta\mathfrak{R}_M = \{ \underline{\theta} \mid \underline{\theta} \in \mathfrak{R}^M; \ \underline{\theta} \notin \hat{\mathfrak{R}}^M \} \tag{2.28}$$

is a set of Lebesgue measure zero in $\mathbb{R}^n$ where $n = \dim(\underline{\theta})$.

Theorem 2.1. The model structure $\mathfrak{R}_1$ with linear membership functions and the parameters μs subject to Equation (2.11a), is globally identifiable at almost all $\underline{\theta}_L^* \in \mathfrak{R}_L^M$ where

$$\delta\mathfrak{R}_L^M = \{ \underline{\theta}_L \mid \text{the elements of } \underline{\theta}_L \text{ subject to Equations (2.30)} \} \tag{2.29}$$

$$\underline{\Sigma}^T_{S,a_i} = 0 \quad \text{and} \quad \underline{\Sigma}^T_{S,b_j} = 0 \,, \quad i = 1,\ldots,n \text{ and } j = 1,\ldots,m \tag{2.30a}$$

$$\underline{\Sigma}^T_{L,a_i} = 0 \quad \text{and} \quad \underline{\Sigma}^T_{L,b_j} = 0 \,, \quad i = 1,\ldots,n \text{ and } j = 1,\ldots,m \tag{2.30b}$$

$$\underline{\Sigma}^T_{S,a_i} = \underline{\Sigma}^T_{L,a_i} \quad \text{and} \quad \underline{\Sigma}^T_{S,b_j} = \underline{\Sigma}^T_{L,b_j} \,, \quad i = 1,\ldots,n \text{ and } j = 1,\ldots,m \tag{2.30c}$$

Theorem 2.2. The model structure $\mathfrak{R}_1$, with quadratic membership functions and the parameters μs subject to Equations (2.11) and (2.15), is globally identifiable at almost all $\underline{\theta}_N^* \in \mathfrak{R}_N^M$ where

$$\delta\mathfrak{R}_N^M = \{ \underline{\theta}_N \mid \text{the elements of } \underline{\theta}_N \text{ subject to Equations (2.30)} \} \tag{2.31}$$

Proofs of Theorems 2.1 and 2.2 are given in Appendix A.

Also, it can be shown that the model structure $\mathcal{R}_2$ is globally identifiable since each state-space equation can be handled independently and the concept for proof exactly follows that given in Appendix A.

Models with More Than One Dynamic Variables

It is possible to extend the linguistic description introduced in Equations (2.6) for systems with more than one dynamic variable such as generalized Hammerstein systems Suppose the system parameters depend on $\mathcal{D}_1$ and $\mathcal{D}_2$. An extension of Equations (2.6) could be

If $\mathcal{D}_1$ is small and $\mathcal{D}_2$ is small then

$$\hat{a}_1(\mathcal{D}_1,\mathcal{D}_2) = \mathcal{S}_{SS}(\mathcal{D}_1,\mathcal{D}_2) \qquad (2.32a)$$

If $\mathcal{D}_1$ is large and $\mathcal{D}_2$ is small then

$$\hat{a}_1(\mathcal{D}_1,\mathcal{D}_2) = \mathcal{S}_{LS}(\mathcal{D}_1,\mathcal{D}_2) \qquad (2.32b)$$

If $\mathcal{D}_1$ is small and $\mathcal{D}_2$ is large then

$$\hat{a}_1(\mathcal{D}_1,\mathcal{D}_2) = \mathcal{S}_{SL}(\mathcal{D}_1,\mathcal{D}_2) \qquad (2.32c)$$

If $\mathcal{D}_1$ is large and $\mathcal{D}_2$ is large then

$$\hat{a}_1(\mathcal{D}_1,\mathcal{D}_2) = \mathcal{S}_{LL}(\mathcal{D}_1,\mathcal{D}_2) \qquad (2.32d)$$

Here, both $\mathcal{D}_1$ and $\mathcal{D}_2$ are the inputs of the linguistic description whose output can be defined :

$$\hat{a}_1(\mathcal{D}_1,\mathcal{D}_2) = \mathcal{W}_{SS}(\mathcal{D}_1,\mathcal{D}_2)\ \mathcal{S}_{SS}(\mathcal{D}_1,\mathcal{D}_2) + \mathcal{W}_{LS}(\mathcal{D}_1,\mathcal{D}_2)\ \mathcal{S}_{LS}(\mathcal{D}_1,\mathcal{D}_2) + \mathcal{W}_{SL}(\mathcal{D}_1,\mathcal{D}_2)\ \mathcal{S}_{SL}(\mathcal{D}_1,\mathcal{D}_2) + \mathcal{W}_{LL}(\mathcal{D}_1,\mathcal{D}_2)\ \mathcal{S}_{LL}(\mathcal{D}_1,\mathcal{D}_2) \tag{2.33}$$

where

$$\mathcal{W}_{SS}(\mathcal{D}_1,\mathcal{D}_2) = \begin{cases} \dfrac{\mathcal{M}_{S1}(\mathcal{D}_1)\ \mathcal{M}_{S2}(\mathcal{D}_2)}{S_M} & \text{, if } S_M \neq 0 \\ 0 & \text{, otherwise} \end{cases} \tag{2.34a}$$

$$\mathcal{W}_{LS}(\mathcal{D}_1,\mathcal{D}_2) = \begin{cases} \dfrac{\mathcal{M}_{L1}(\mathcal{D}_1)\ \mathcal{M}_{S2}(\mathcal{D}_2)}{S_M} & \text{, if } S_M \neq 0 \\ 0 & \text{, otherwise} \end{cases} \tag{2.34b}$$

$$\mathcal{W}_{SL}(\mathcal{D}_1,\mathcal{D}_2) = \begin{cases} \dfrac{\mathcal{M}_{S1}(\mathcal{D}_1)\ \mathcal{M}_{L2}(\mathcal{D}_2)}{S_M} & \text{, if } S_M \neq 0 \\ 0 & \text{, otherwise} \end{cases} \tag{2.34c}$$

$$\mathcal{W}_{LL}(\mathcal{D}_1,\mathcal{D}_2) = \begin{cases} \dfrac{\mathcal{M}_{L1}(\mathcal{D}_1)\ \mathcal{M}_{L2}(\mathcal{D}_2)}{S_M} & \text{, if } S_M \neq 0 \\ 0 & \text{, otherwise} \end{cases} \tag{2.34d}$$

$$S_M = \mathcal{M}_{S1}(\mathcal{D}_1)\ \mathcal{M}_{S2}(\mathcal{D}_2) + \mathcal{M}_{L1}(\mathcal{D}_1)\ \mathcal{M}_{S2}(\mathcal{D}_2) + \mathcal{M}_{S1}(\mathcal{D}_1)\ \mathcal{M}_{L2}(\mathcal{D}_2) + \mathcal{M}_{L1}(\mathcal{D}_1)\ \mathcal{M}_{L2}(\mathcal{D}_2) \tag{2.34e}$$

Note that for each dynamic variable space a set of membership functions is required (e.g. $\mathcal{M}_{S1}(\mathcal{D})$, $\mathcal{M}_{L1}(\mathcal{D})$ for $\mathcal{D}_1$-space and $\mathcal{M}_{S2}(\mathcal{D})$, $\mathcal{M}_{L2}(\mathcal{D})$ for $\mathcal{D}_2$-space). The membership

functions can be linear or quadratic as in Equations (2.8) or (2.9).

On the selection of shape functions, recall that the requirements of Equations (2.12) and (2.13) must be fulfilled. Based on this, a natural option might be

$$\mathcal{S}_{SS}(\mathcal{D}_1,\mathcal{D}_2) = \sum_{i=0}^{N} \sum_{j=0}^{M} \sigma_{SS,i,j}\, \mathcal{D}_1^i\, \mathcal{D}_2^j \qquad (2.35a)$$

$$\mathcal{S}_{LS}(\mathcal{D}_1,\mathcal{D}_2) = \sum_{i=0}^{N} \sum_{j=0}^{M} \sigma_{LS,i,j}\, \mathcal{D}_1^i\, \mathcal{D}_2^j \qquad (2.35b)$$

$$\mathcal{S}_{SL}(\mathcal{D}_1,\mathcal{D}_2) = \sum_{i=0}^{N} \sum_{j=0}^{M} \sigma_{SL,i,j}\, \mathcal{D}_1^i\, \mathcal{D}_2^j \qquad (2.35c)$$

$$\mathcal{S}_{LL}(\mathcal{D}_1,\mathcal{D}_2) = \sum_{i=0}^{N} \sum_{j=0}^{M} \sigma_{LL,i,j}\, \mathcal{D}_1^i\, \mathcal{D}_2^j \qquad (2.35d)$$

Some mathematical properties of the above linguistic description are given in [Lin 1990]. Further discussion on the identifiability of model structures with more than one dynamic variable is beyond the scope of this study.

CHAPTER III

PARAMETER ESTIMATION METHODS

Some previous parameter estimation methods and a proposed new method for the class of systems described by Equations (2.1) or (2.2) are introduced. Among all the methods, it is assumed that a batch of data $\mathfrak{Z}_n$ has been collected for the need of parameter estimation and

$$\mathfrak{Z}_n = \{u(t), y(t), \mathfrak{D}(t) \mid t = 1, \ldots, n\} \tag{3.1a}$$

or

$$\mathfrak{Z}_n = \{u(t), \underline{x}(t), \mathfrak{D}(t) \mid t = 1, \ldots, n\} \tag{3.1b}$$

where n denotes the number of data points collected.

It is understood that the data $\mathfrak{Z}_n$ play a dominant role on the identification results. Roughly speaking, good identification data should contain sufficient information about the system dynamics. A proper selection (or design) of system inputs is required to generate such informative identification data. In this respect, a new point of view based on the signal-dependent modeling concept is presented in this chapter.

Previous Methods

It is a common idea to fit a nonlinear system using piecewise linear models each of which governs a part of the working range. Applying such an idea to systems with signal-dependent parameters, Haber et. al. [30, 31] proposed the so-called gate function method.

The gate function method begins by quantifying $[\mathcal{D}_{min}, \mathcal{D}_{max}]$ into some intervals.

$$[\mathcal{D}_{min},\mathcal{D}_{max}] = [\mathcal{D}^{[0]},\mathcal{D}^{[1]}] \cup [\mathcal{D}^{[1]},\mathcal{D}^{[2]}] \cup \ldots \cup [\mathcal{D}^{[d-1]},\mathcal{D}^{[d]}] \tag{3.2a}$$

where

$$\mathcal{D}_{min} = \mathcal{D}^{[0]} < \mathcal{D}^{[1]} \ldots < \mathcal{D}^{[d]} = \mathcal{D}_{max} \tag{3.2b}$$

and d denotes the number of intervals quantified.

For each quantification interval, a locally linear model is to be formed, i. e., within each quantification interval the system parameter functions are treated as constants.

In Haber's paper [31], a locally linear model was called an elementary gate model (EGM). The parameters of each EGM were estimated based on data called gated signals which were extracted from the original identification data

$\mathcal{B}_n$.

For instance, the gated input and output signals corresponding to the i^{th} quantification interval are defined as

$$[u(t)]_i = \begin{cases} u(t) & , \text{ if } \mathcal{D}^{[i-1]} \le \mathcal{D} \le \mathcal{D}^{[i]} \\ 0 & , \text{ otherwise} \end{cases} \tag{3.3a}$$

$$[y(t)]_i = \begin{cases} y(t) & , \text{ if } \mathcal{D}^{[i-1]} \le \mathcal{D} \le \mathcal{D}^{[i]} \\ 0 & , \text{ otherwise} \end{cases} \tag{3.3b}$$

So, there are d sets of gated signals as a result of the quantification in Equations (3.2). Theoretically, each set of gated signals can be used to form an EGM model. For the system described by Equations (2.1), it seems reasonable to consider the following model structures :

$$\hat{A}_i(q^{-1})\,[y(t)]_i = \hat{B}_i(q^{-1})\,[u(t)]_i \,, \qquad i = 1,\ldots,d \tag{3.4a}$$

where

$$\hat{A}_i(q^{-1}) = 1 - \hat{a}_1^{[i]}q^{-1} - \ldots - \hat{a}_n^{[i]}q^{-n} \tag{3.4b}$$

$$\hat{B}_i(q^{-1}) = \hat{b}_1^{[i]}q^{-1} + \ldots + \hat{b}_m^{[i]}q^{-m} \tag{3.4c}$$

It is a well-known problem to estimate the parameters in Equations (3.4). Many classical estimators developed for linear systems [43, 44, 55] such as the recursive least-squares estimator are adequate for use.

The gate function method is simple and requires no further effort to develop new parameter estimation algorithms. Theoretically, the overall modeling accuracy seems able to be improved by increasing d. Unfortunately, such a hypothesis is not correct as explained in the next two paragraphs.

As shown in Equations (3.3), the gated signals are formed by intermittent subsets of zero and non-zero signals. Every non-zero subset to be useful for parameter estimation must have sufficient length (here, the length of a subset is defined as the number of data points contained in the subset). The minimum length required depends on the model order chosen. For Equations (3.4), the minimum length required is n+1 or m, whichever is larger.

Due to the above minimum length requirement, the quantification intervals cannot be arbitrarily small. Such a limitation cannot be effectively reduced by increasing the number of identification data $\mathfrak{B}_n$. As pointed out by Haber et. al. [31], to permit a successful parameter estimation procedure between the gated input/output signals, the quantification intervals have to be chosen sufficiently

large.

Another approach to handle the uncertainty of signal dependence is to parameterize the dependence into a polynomial. For convenience, this approach is called polynomial function method in the ensuing context.

For the system described by Equations (2.1), a model structure with polynomial parameter functions is

$$\hat{A}(q^{-1},\mathcal{D})\ y(t) = \hat{B}(q^{-1},\mathcal{D})\ u(t) \tag{3.5a}$$

where

$$\hat{A}(q^{-1},\mathcal{D}) = 1 - \hat{a}_1(\mathcal{D})q^{-1} - \ldots - \hat{a}_n(\mathcal{D})q^{-n} \tag{3.5b}$$

$$\hat{B}(q^{-1},\mathcal{D}) = \hat{\ell}_1(\mathcal{D})q^{-1} - \ldots - \hat{\ell}_m(\mathcal{D})q^{-m} \tag{3.5c}$$

$$\hat{a}_i(\mathcal{D}) = \hat{a}_{i,0} + \hat{a}_{i,1}\,\mathcal{D} + \ldots + \hat{a}_{i,N}\,\mathcal{D}^N\ , \qquad i = 1,\ldots,n \tag{3.5d}$$

$$\hat{\ell}_j(\mathcal{D}) = \hat{b}_{j,0} + \hat{b}_{j,1}\,\mathcal{D} + \ldots + \hat{b}_{j,N}\,\mathcal{D}^N\ , \qquad j = 1,\ldots,m \tag{3.5e}$$

which also can be written in a linear regression form :

$$y(t) = \underline{\phi}^T(t)\ \underline{\theta} \tag{3.6a}$$

where

$$\underline{\phi}^T(t) = [y(t-1), \mathcal{D}\, y(t-1), \ldots, \mathcal{D}^N\, y(t-1),$$
$$\vdots \qquad\qquad\qquad\qquad \vdots$$
$$y(t-n), \mathcal{D}\, y(t-n), \ldots, \mathcal{D}^N\, y(t-n),$$
$$u(t-1), \mathcal{D}\, u(t-1), \ldots, \mathcal{D}^N\, u(t-1),$$
$$\vdots \qquad\qquad\qquad\qquad \vdots$$
$$u(t-m), \mathcal{D}\, u(t-m), \ldots, \mathcal{D}^N\, u(t-m)] \qquad (3.6b)$$

$$\underline{\theta}^T = [\hat{a}_{1,0}, \hat{a}_{1,1}, \ldots, \hat{a}_{1,N},$$
$$\vdots \qquad\qquad \vdots$$
$$\hat{a}_{n,0}, \hat{a}_{n,1}, \ldots, \hat{a}_{n,N},$$
$$\hat{b}_{1,0}, \hat{b}_{1,1}, \ldots, \hat{b}_{1,N},$$
$$\vdots \qquad\qquad \vdots$$
$$\hat{b}_{m,0}, b_{m,1}, \ldots, \hat{b}_{m,N}] \qquad (3.6c)$$

One advantage to parameterizing system parameter functions into polynomials is the resulting linearity in model parameters. Henceforth, least-squares based estimators can be used in a straightforward manner to estimate the parameters in Equation (3.6c). However, as illustrated in Chapter IV, many system parameter functions are too complicated to be adequately approximated by polynomial expansions. Despite its simplicity, the polynomial function method may be adequate only for a limited range of applications.

Proposed Method

In Chapter II, it has been shown that parameterization

of system signal-dependent parameters using fuzzy linguistic rules is more flexible than that using polynomial functions. But, the model structures resulting from the use of fuzzy parameterization are no longer in linear regression forms. A new and reliable parameter estimation method is proposed in this section to estimate the model parameters.

In Equations (2.25), the unknown parameters μs in the weighting functions of the regression vector $\underline{\phi}$ cause the difficulty to use classical linear estimators. However, if the parameters μs are pre-determined by some method, the linear estimators become applicable and can be incorporated to estimate the remaining parameters.

The above idea was borrowed from Takagi et. al. [1985] where the identification of static nonlinear systems using fuzzy linguistic rules was studied. The model structures presented in Takagi's paper have the basic form similar to Equations (2.19b) and (2.19c), but have no dynamic equation such as Equation (2.19a). Henceforth, this study may be considered as an extension of Takagi's work to the identification of nonlinear systems with dynamics.

The parameter estimation algorithm proposed by Takagi et. al. is a combination of the so-called Complex Method [12, 53] and the recursive least-squares estimator. For this application, the Complex Method is used to optimize the values of the parameters μs while the recursive

least-squares estimator is used to estimate the parameters in Equation (2.25c). The estimation of parameters is performed in a cyclically iterative manner.

In the Complex Method, the set of parameters μs is called a point in the μ-space. If the point is within the domain satisfying the constraints such as Equations (2.11), (2.15), or (2.17), it is referred to as a feasible point. Then, the task of parameter estimation is to ultimately seek a feasible point in the μ-space and this point, in turn, results in a model with the best performance.

For seeking such a "best" point, the Complex Method begins with a proper number of working points which are pre-assigned in the feasible domain. During the Complex Method's searching, each feasible point can be conceived as a model with a performance index indicating its prediction accuracy. The upgrade of these working points is based on their corresponding performance indices and feasibility involved.

A flowchart of the proposed parameter estimation method is shown in Figure 3. Further details about the Complex Method are presented in Appendix B.

Convergent Properties

As with most optimization methods, there is no

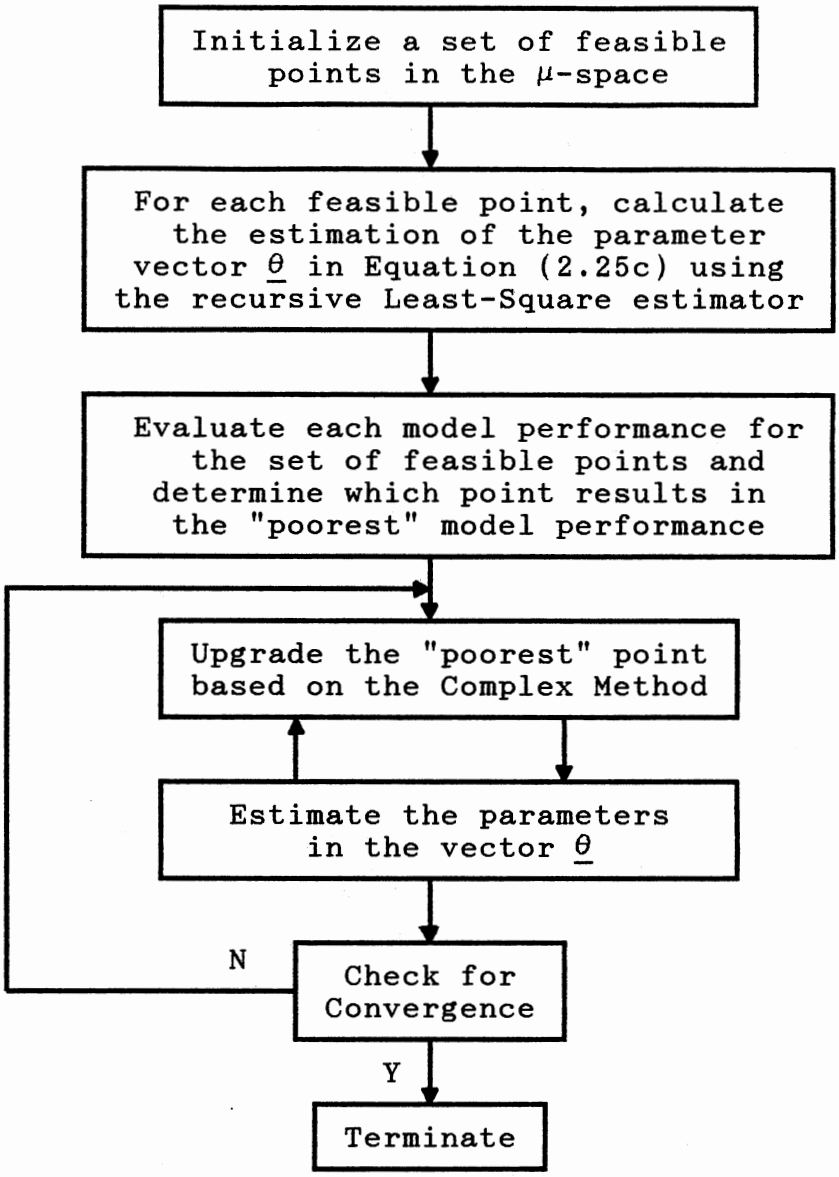

Figure 3. A Flowchart of the Proposed Parameter Estimation Method.

guarantee the Complex Method will always converge to a local minimum. Indeed, the original version of the Complex Method [53] sometimes would fail to converge. A minor modification of the Complex Method is necessary to prevent such a failure of convergence (Remark B1 in Appendix B).

Since no gradient of any problem function is required in the Complex Method, the convergent rate is, in general, slow especially when the dimension of the μ-space is large. The computational time required in the proposed method may be 5-100 times (Table XIV) that required in other parameter estimation methods.

The Complex Method permits several terminations and subsequent restarts to occur before actually terminating the search. Thus, the "best" point in the previous searching, even it is not the globally best, can be saved and assigned as one of initial points for the subsequent searching. This device is useful to improve the overall convergence rate of the algorithm.

If computer time is not the major concern, a comprehensive grid net covering the whole working domain can be defined and then for each grid point the corresponding model performance is evaluated. By doing such exhaustive searching, it seems more likely to result in the globally optimal point.

Persistence of System Excitation

The issue of persistence of system excitation as a result of the design of system inputs to generate a batch of data is vital to provide sufficient information about the system dynamics. A relative question is whether the data generated permits one to distinguish between different models in the chosen model structure.

Consider a linear regression model structure such as :

$$y(t) = \underline{\phi}^T(t)\ \underline{\theta} \tag{3.7a}$$

where

$$\underline{\phi}^T(t) = [\phi_1(t),\ \phi_2(t),\ \ldots,\ \phi_n(t)] \tag{3.7b}$$

$$\underline{\theta}^T = [\theta_1,\ \theta_2,\ \ldots,\ \theta_n] \tag{3.7c}$$

A persistent excitation condition [3, 25, 44] is that the matrix

$$\Phi^T(t)\Phi(t) \text{ is positive definite} \tag{3.8a}$$

where

$$\Phi(t) = \begin{bmatrix} \phi_1(1), & \phi_2(1), & \ldots, & \phi_n(1) \\ \vdots & \vdots & & \vdots \\ \phi_1(t), & \phi_2(t), & \ldots, & \phi_n(t) \end{bmatrix} \tag{3.8b}$$

The above excitation condition is less meaningful for a pseudolinear regression model structure such as Equations

(2.25). As some elements in the matrix $\Phi^T(t)\Phi(t)$ are still unknown, it is not possible to determine whether Equation (3.8a) holds. However, one can present a new insight into the input design problem based on the signal-dependent modeling concept.

First, consider a system with a signal-dependent parameter described by

$$y(t) = a(u(t-1))\ y(t-1) + u(t-1) \tag{3.9a}$$

where

$$a(u) = a_1\ u^2 + a_2\ u + a_3 \tag{3.9b}$$

and for illustrative purpose, the exact system structure is used as the model structure, i.e.

$$y(t) = \hat{a}(u(t-1))\ y(t-1) + u(t-1) \tag{3.10a}$$

where

$$\hat{a}(u) = \hat{a}_1\ u^2 + \hat{a}_2\ u + \hat{a}_3 \tag{3.10b}$$

If pseudo-random binary signals with magnitude, say u_1 and u_2, are used as system inputs, the estimates will not be unique, because the following inference does not necessarily hold :

$$\hat{a}(u_1) = a(u_1) \text{ and } \hat{a}(u_2) = a(u_2) \longrightarrow$$

$$\hat{a}_1 = a_1,\ \hat{a}_2 = a_2 \text{ and } \hat{a}_3 = a_3 \qquad (3.11)$$

What the system inputs should be to achieve persistent excitation obviously depends on the shapes of system parameter functions. From the above example, a necessary condition for the data $\mathfrak{Z}_n$ to be informative is that $\mathfrak{Z}_n$ must be able to distinguish among different sub-functions within the structure of $a(u)$.

In practice, the shapes or structures of system parameter functions are normally not known beforehand and they will not be as simple as that in Equation (3.9b). It might be a good idea to have the system inputs uniformly distributed over the whole input domain of interest to assure Equation (3.11) holds.

Henceforth, if the system to be identified has input-dependent parameters such as a Hammerstein system, the input design problem may be easily solved by choosing uniformly distributed pseudo-random signals as the system inputs. But, for those systems with a non-input dynamic variable (e.g. Wiener systems), it would be difficult to generate uniformly distributed dynamic variable.

Although the distribution of the system dynamic variable is not so controllable, its variation range under

excitation may be extended to cover the entire range of interest. It should be understood that the data generated with a large variation of the dynamic variable would be more informative than those generated with a small variation of the dynamic variable.

Assume that the dynamic variable is one of the system states. In the design of system inputs, a suggested class of signals which are synthesized from uniformly distributed random signals with proper "time re-scaling" will be used.

By time re-scaling, each input signal is permitted to excite the system for more than one sampling interval. An example of the suggested class of input signals is shown in Figure 4. The subscript of ∇_n denotes the number of sampling intervals for which each input signal acts. In the ensuing context, the suggested class of input signals will be named ∇_n-class signals.

The aim of time re-scaling of the system input signals is to achieve a large ratio of the system dynamic variable to the input. By doing so, more information about the system parameter functions can be gained.

The concept to achieve a large system output-to-input ratio through input time re-scaling can be explained in the frequency domain. Let the discrete Fourier transform of ∇_n-class signals denoted by $\mathcal{F}_n(f)$.

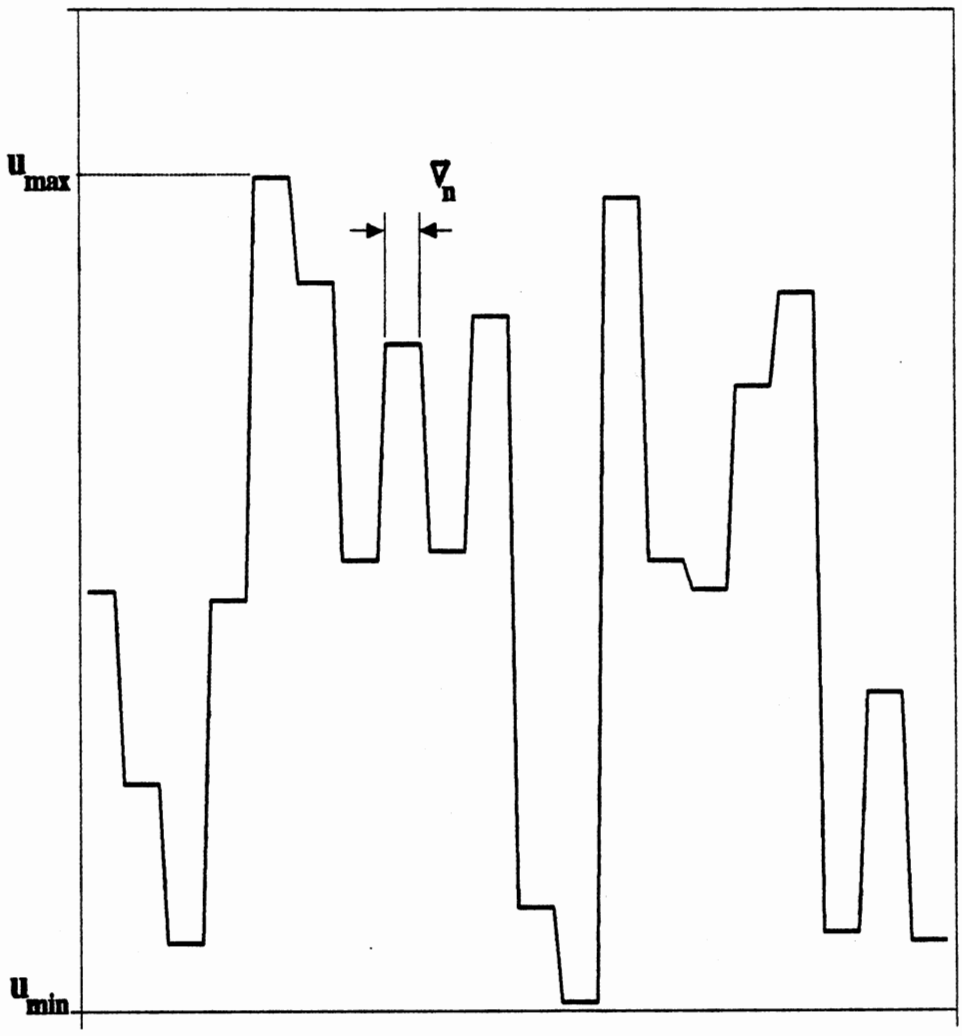

Figure 4. The Suggested Class of Input Excitation Signals for Nonlinear System Identification.

$$\mathcal{F}_n(f) = h \sum_{t=0}^{N-1} \nabla_n(t) \exp(j2\pi tf) \qquad (3.12)$$

where h denotes the sampling interval, f the frequency.

From Equation (3.12), it can be shown that the following equation holds :

$$\mathcal{F}_n(f) = n\, \mathcal{F}_1(nf) \qquad (3.13)$$

Equation (3.13) states that a time scaling of signals results in a frequency scaling of the signal spectrum. As n increases, the spectrum of ∇_n-class signals will be "compressed" to the side with lower frequency and the power of the spectrum is increased proportionally (Figure 24). In other words, the dominant frequency band of ∇_n-class signals is shifted. It will eventually converge to the system resonant frequency (i.e. the frequency at which the peak resonance occurs) if sampling time interval has been properly chosen. Therefore, large output-to-input signal ratios can be achieved.

Certainly, the use of ∇_n-class signals as system inputs is just a suboptimal solution. However, ∇_n-class signals have been found quite promising in a practical application (Example 3, Chapter IV).

Finally, it must be emphasized that the problem of input design in nonlinear system identification is still not

completely solved.

Model Validation

In the process of system identification, once model structures have been chosen, parameter estimation methods provide several models in competition, and which model among all competitive ones is the best, or whether the "best" model is good enough for the intended application purpose. Such testing is known as model validation.

Since by hypothesis, system parameter function forms are not known, model structure errors due to the parameterization of system parameter functions are inevitable. Classical linear model validation tests [11, 24], or higher-order correlation tests [6, 8] have been found inadequate. Indeed, a model which fails to pass those tests does not necessarily mean it is an unacceptable model.

A simple alternative for model validation is called cross-validation method [44]. The model performance is evaluated based on a batch of "fresh" data $\mathfrak{Z}_n^*$ which were not used in the estimation of parameters.

$$\mathfrak{Z}_n^* = \{u^*(t), y^*(t), \mathfrak{D}^*(t) \mid t = 1, \ldots, n^*\} \tag{3.14a}$$

or

$$\mathfrak{B}_n^* = \{u^*(t), \underline{x}^*(t), \mathfrak{D}^*(t) \mid t = 1, \ldots, n^*\} \qquad (3.14b)$$

The idea of model cross validation can be implemented in the identification method proposed in this chapter. During the Complex Method's searching, the evaluation of model performance for each feasible point can be done based on a batch of fresh data. The incorporation of such on-line model validation sometimes is advantageous to prevent falsely data fitting.

In the use of cross validation, the selection of fresh data certainly is problem dependent. Normally, the data can be generated with standard input signals (e.g. a step input) but should cover the entire working range of the system dynamic variable.

The model validation methods mentioned above only serve to pick the "best" model from the competitive models. In practice, there is always an intended purpose behind system identification such as for system control. It would be necessary to check whether the "best" model is sufficiently good for the purpose (Example 3, Chapter IV, for an illustration).

CHAPTER IV

ILLUSTRATIVE EXAMPLES

In this chapter, the identification methods presented in Chapter III are investigated through some illustrative examples. The example studies include simulations and an experiment (Example 3). The systems considered are a Hammerstein system, a simplified nonlinear stall/post-stall aircraft system, a hydraulic servovalve/motor system and an industrial Ph process.

In the ensuing context, Equations (2.19) and (2.20), or their corresponding pseudolinear regressions (e.g. Equations (2.25)) are referred to as the proposed model structures. Fuzzy linguistic description of system parameter functions such as Equations (2.6) is the proposed parameterization approach. The proposed (identification) method means that the estimation of the parameters in the proposed model structures is performed using the recursive least-square routine and Complex Method (Chapter III).

Throughout this chapter, the proposed parameterization approach is very flexible to meet diverse applications. Among the identification methods considered, the proposed method has good robustness across a range of different

systems and henceforth deserves to receive the most attention.

Example 1 - Hammerstein System with Saturating Gain

Assume the system to be identified is described as (Figure 1(a)) :

$$n = m = 3 \tag{4.1a}$$

$$a_1 = -0.9 \ , \ a_2 = -0.15 \ , \ a_3 = -0.002 \tag{4.1b}$$

$$b_1 = 1.0 \ , \ b_2 = 0.7 \ , \ b_3 = -1.5 \tag{4.1c}$$

and

$$f(u) = \begin{cases} u & , \text{ for } -0.5 < u < 0.5 \\ 0.5 & , \text{ for } 0.5 \leq |u| \leq 1.0 \end{cases} \tag{4.2}$$

where the system data are excerpted from the Narendra's paper [47].

Assume Equation (4.1a) is known. The working range of the system inputs is [-1, 1] (i.e. $u_{min} = -1$ and $u_{max} = 1$) in that the nonlinearities due to input saturation have been considered.

Gate Function Method

Assume four EGMs are to be formed. Each of them has the same model structure as :

$$[y(t)]_i = \hat{a}_1^{[i]}[y(t-1)]_i + \hat{a}_2^{[i]}[y(t-2)]_i + \hat{a}_3^{[i]}[y(t-3)]_i + \hat{b}_1^{[i]}[u(t-1)]_i + \hat{b}_2^{[i]}[u(t-2)]_i + \hat{b}_3^{[i]}[u(t-3)]_i \quad , \quad i = 1,\ldots,4 \tag{4.3a}$$

where

$$[u(t)]_i = \begin{cases} u(t) & , \text{ if } u^{[i-1]} \le u(t) \le u^{[i]} \\ 0 & , \text{ otherwise} \end{cases} \tag{4.3b}$$

$$[y(t)]_i = \begin{cases} y(t) & , \text{ if } u^{[i-1]} \le u(t) \le u^{[i]} \\ 0 & , \text{ otherwise} \end{cases} \tag{4.3c}$$

$$u^{[i]} = (u_{max} - u_{min})\, i/d + u_{min} \tag{4.3d}$$

Polynomial Function Method

Let f(u) be parameterized into a fourth-order polynomial function without constant term, i.e.

$$\hat{f}(u) = p_1 u + p_2 u^2 + p_3 u^3 + p_4 u^4 \tag{4.4}$$

Of course, in practice some efforts are required to investigate other possible polynomial parameterization with different order. However, the determination of the use of Equation (4.4) simply follows Narendra et. al. [47].

Replace f(u) in Equations (2.3) by the above $\hat{f}(u)$.

After arrangement,

$$y(t) = \underline{\phi}^T(t)\ \underline{\theta} \tag{4.5a}$$

where

$$\underline{\phi}^T(t) = [y(t-1),y(t-2),y(t-3),u(t-1),u^2(t-1), u^3(t-1),u^4(t-1),\hat{f}(u(t-2)),\hat{f}(u(t-3))] \tag{4.5b}$$

$$\underline{\theta}^T = [\hat{a}_1,\hat{a}_2,\hat{a}_3,p_1,p_2,p_3,p_4,\hat{b}_2,\hat{b}_3] \tag{4.5c}$$

Strictly speaking, Equation (4.5a) is not a linear regression because $\hat{f}(u(t-2))$ and $\hat{f}(u(t-3))$ in the regression vector $\underline{\phi}(t)$ are not known. However, during the recursive least-squares estimation they can be approximated by their existing available estimates.

Proposed Method

Assume f(u) is parameterized by

If u(t-1) is small then

$$\hat{f}(u(t-1) = \sigma_1 \tag{4.6a}$$

If u(t-1) is large then

$$\hat{f}(u(t-1) = \sigma_2 \tag{4.6b}$$

where linear membership functions and constant shape functions are appropriate for use. However, such understanding requires knowledge of the mathematical

properties of the proposed linguistic description.

From Equations (2.3) and (4.6), the proposed model structure has the following pseudo-linear regression form :

$$y(t) = \underline{\phi}^T(t)\ \underline{\theta} \tag{4.7a}$$

where

$$\underline{\phi}^T(t) = [y(t-1), y(t-2), y(t-3), \mathcal{W}_S(u(t-1)), \mathcal{W}_L(u(t-1)), \hat{f}(u(t-2)), \hat{f}(u(t-3))] \tag{4.7b}$$

$$\underline{\theta}^T = [\hat{a}_1, \hat{a}_2, \hat{a}_3, \sigma_1, \sigma_2, \hat{b}_2, \hat{b}_3] \tag{4.7c}$$

$$\hat{f}(u(t-1)) = \mathcal{W}_S(u(t-1))\ \sigma_1 + \mathcal{W}_L(u(t-1))\ \sigma_2 \tag{4.7d}$$

and $\mathcal{W}_S(u)$ and $\mathcal{W}_L(u)$ are given in Equations (2.7b), (2.7c), (2.8), and (2.10) with $\mathcal{D}$ replaced by u.

Simulation Results

The estimation of parameters was performed based on 300 input/output data points. Uniformly distributed measurement noise with zero mean, and variance 0.00342 was assumed additive to the system real output.

For the simulation of the proposed method and polynomial function method, ∇_1-class signals distributed over the range of [-1, 1] were used as the system inputs. But, for the simulation of the gate function method ∇_4-class input signals were used to guarantee each nonzero subset of

gated signals has enough length.

The simulation results of using the above identification methods are summarized in Tables I, II and III respectively. Comparison of $f(u)$ and $\hat{f}(u)$ is shown in Figure 5.

The gate function method was found not appropriate. First, the estimation results based on part of identification data are more sensitive to measurement noise than those based on the whole identification data (compare the estimates for $i = 2, 3$ in Table I with those in Table II and III). Another reason is that in the use of the gate function method the parameter function to be estimated is not $f(u)$ but $f(u)/u$ which has hyperbolic shapes at the saturation intervals (i.e. $-1 \leq u < -0.5$ and $0.5 < u \leq 1$). Obviously, the number of EGMs is extremely demanding to achieve reasonable modeling accuracy for system saturation dynamics.

The mean square errors between the system and model outputs produced by the proposed method and polynomial function method are 0.006538 and 0.009357 respectively (compared with the additive noise variance 0.00342). As shown in Figure 5, the estimates of $f(u)$ for both methods are equivalent in accuracy. But, the proposed method is more promising if measurement noise can be reduced or a noise model is considered.

TABLE I

A SUMMARY OF SIMULATION RESULTS OF EXAMPLE 1
(GATE FUNCTION METHOD)

	$\hat{a}_1^{[i]}$	$\hat{a}_2^{[i]}$	$\hat{a}_3^{[i]}$	$\hat{b}_1^{[i]}$	$\hat{b}_2^{[i]}$	$\hat{b}_3^{[i]}$
i=1	-0.427	0.282	0.064	0.069	-0.088	0.097
i=2	-0.540	0.171	0.079	0.991	0.475	-1.365
i=3	-0.807	-0.190	0.033	1.351	0.054	-1.148
i=4	-0.341	0.355	0.104	0.174	-0.002	-0.123

1 : $-1.0 \leq u < -0.5$ 3 : $0.0 \leq u < 0.5$
2 : $-0.5 \leq u < 0.0$ 4 : $0.5 \leq u \leq 1.0$

TABLE II

A SUMMARY OF SIMULATION RESULTS OF EXAMPLE 1
(POLYNOMIAL FUNCTION METHOD)

$\hat{a}_1$	$\hat{a}_2$	$\hat{a}_3$	$\hat{b}_2$	$\hat{b}_3$
-0.89937	-0.14961	-0.00070	0.66658	-1.42761

P_1	P_2	P_3	P_4
1.03984	0.03265	-0.57089	-0.00448

TABLE III

A SUMMARY OF SIMULATION RESULTS OF EXAMPLE 1
(THE PROPOSED METHOD)

$\hat{a}_1$	$\hat{a}_2$	$\hat{a}_3$	$\hat{b}_2$	$\hat{b}_3$
-0.92197	-0.17386	-0.00983	0.72466	-1.47982

μ_1	μ_2	σ_1	σ_2
0.51974	-0.51755	-0.53242	0.43958

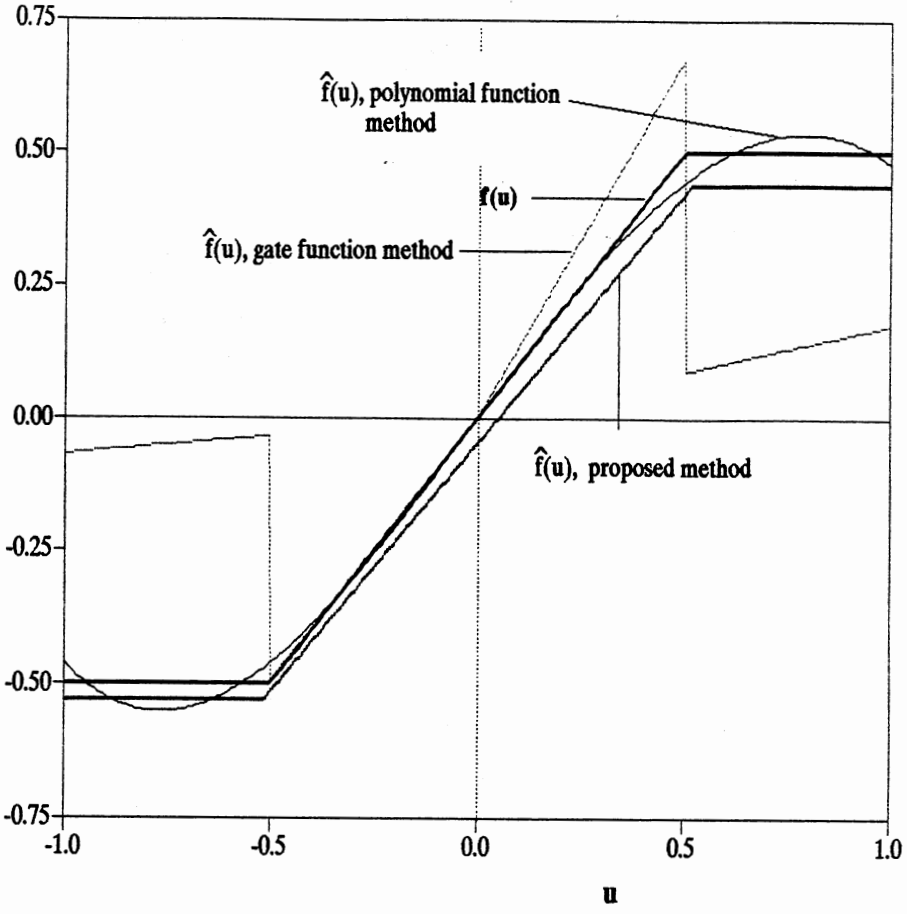

Figure 5. A Comparison Between f(u) and Its Estimates Obtained Using the Specific Identification Methods.

Example 2 - Simplified Nonlinear Stall/Post-Stall Aircraft System

The identification of an aircraft dynamic system in a large range of angle-of-attack flights is studied in this example. The following empirical model (excerpted from [Stalford, 1987]) determined from measured wind tunnel values of a T-2C airplane is the system to be identified :

$$\dot{x}_1 = 9.168\ c(x_1) + x_2 - 1.8336\ u - 5.473296 \qquad (4.8a)$$

$$\dot{x}_2 = -5.73\ x_1 - 8.595\ u + 2.865 \qquad (4.8b)$$

where

x_1 : the angle of attack in degrees

x_2 : the pitch rate in degrees per second

u : the elevator control in degrees

In Equation (4.8a), $c(x_1)$ denotes the system plunging force coefficient and

1. $x_1 \leq 14.36$ (the pre-stall region)

$$c(x_1) = -0.07378494\ x_1 \qquad (4.9a)$$

2. $14.36 \leq x_1 \leq 15.6$ (the stall region)

$$c(x_1) = 0.09722\ x_1^2 - 2.8653\ x_1 + 20.03846 \qquad (4.9b)$$

3. $15.6 \leq x_1 \leq 19.6$ (the stall/post-stall region)

$$c(x_1) = -0.01971\ x_1^2 + 0.74391\ x_1 - 7.80753 \qquad (4.9c)$$

4. $19.6 \leq x_1 \leq 28.0$ (the post-stall region)

$$c(x_1) = -0.47333 - 0.01667\, x_1 \qquad (4.9d)$$

It would require much wind tunnel and flight test time to measure the system coefficients and achieve the above empirical model.

In Stalford's paper, there is another piecewise linear model available which is described by Equations (4.8) but with the following piecewise linear plunging force coefficient :

1. $x_1 \leq 14.74$ (the pre-stall region)

$$c(x_1) = -0.07281587\, x_1 \qquad (4.10a)$$

2. $14.74 \leq x_1 \leq 17.4$ (the stall region)

$$c(x_1) = 0.088470922(x_1-14.74) - 1.073305924 \qquad (4.10b)$$

3. $17.4 \leq x_1 \leq 18.87$ (the stall/post-stall region)

$$c(x_1) = 0.03309905(x_1-17.4) - 0.8308956 \qquad (4.10c)$$

4. $18.87 \leq x_1 \leq 28.0$ (the post-stall region)

$$c(x_1) = -0.016633734(x_1-18.87) - 0.7882234 \qquad (4.10d)$$

How accurate the piecewise linear model matches the system can be seen from a plot of Equations (4.9) and (4.10) in Figure 6. Now, can one estimate the system coefficients including the plunging force coefficient simply by measuring the system inputs and outputs ? This problem will be

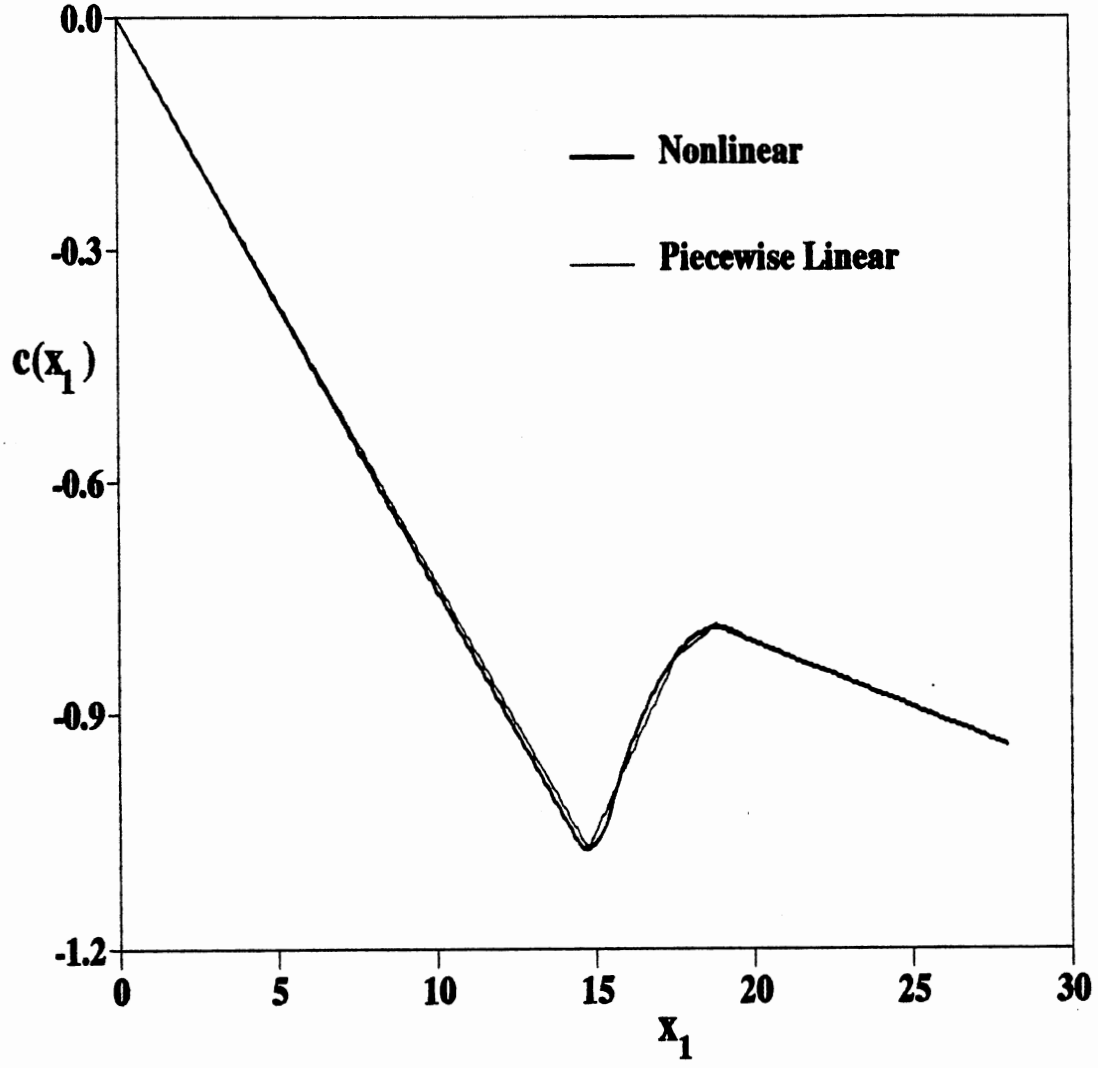

Figure 6. Nonlinear and Piecewise Linear Plunging Force Coefficients.

investigated in the discrete-time domain.

First, applying the z transform to Equations (4.8),

$$\begin{bmatrix} x_1 \\ x_2 \end{bmatrix}_{t+1} = \begin{bmatrix} a_{11} & a_{12} \\ a_{21} & a_{22} \end{bmatrix}_t \begin{bmatrix} x_1 \\ x_2 \end{bmatrix}_t + \begin{bmatrix} b_1 \\ b_2 \end{bmatrix}_t u(t) + \begin{bmatrix} c_1 \\ c_2 \end{bmatrix}_t \tag{4.11}$$

and all the discrete parameters above depend on x_1. The dependence is in general more complicated than that in the continuous-time domain. For instance,

$$a_{11}(x_1) = 9.168\ k_1(x_1)\ c(x_1)/x_1 + k_2(x_1) \tag{4.12a}$$

where

$$k_1 = \frac{1}{\lambda_1 + \lambda_2}\left(e^{\lambda_1 h} - e^{\lambda_2 h}\right) \tag{4.12b}$$

$$k_2 = \frac{1}{\lambda_1 + \lambda_2}\left(\lambda_1 e^{\lambda_2 h} - \lambda_2 e^{\lambda_1 h}\right) \tag{4.12c}$$

and h denotes the sampling time interval, λ_1 and λ_2 are the system signal-dependent poles in the continuous-time domain, i.e.

$$\lambda_{1,2} = \frac{\gamma \pm \sqrt{\gamma^2 - 22.92}}{2} \tag{4.12d}$$

where

$$\gamma = 9.168\ c(x_1)/x_1 + 1.0 \tag{4.12e}$$

In this example, h = 0.1 second is considered. Step-input responses of the system and piecewise linear model for u = -9.2 and -9.4 with initial conditions $x_1(0)$ = 11.0 and $x_2(0)$ = 0.0 are shown in Figure 7. It is obvious that the system would exhibit a longitudinal limit cycle when it is excited by a step input with magnitude somewhere in between -9.2 and -9.4. But, it is surprising that even though it is so accurate, the piecewise linear model does not provide a good prediction of the system longitudinal limit cycle. So, it is conceivable that the estimation accuracy for this example would be quite demanding if an improvement of the above prediction of the longitudinal limit cycle is required.

It should also be noted that although exact parameterization of system parameter functions can be derived as shown in Equations (4.12), they are too complicated to be useful. The problem is the difficulty to estimate the coefficients involved if the system parameter functions are parameterized in that manner. Simplified parameterization in the sense of system approximation seems necessary to render the problem useful.

Gate Function Method

Assume the dynamic variable space $[x_{1,min}, x_{1,max}]$ is quantified into d intervals with equal length. Each EGM has

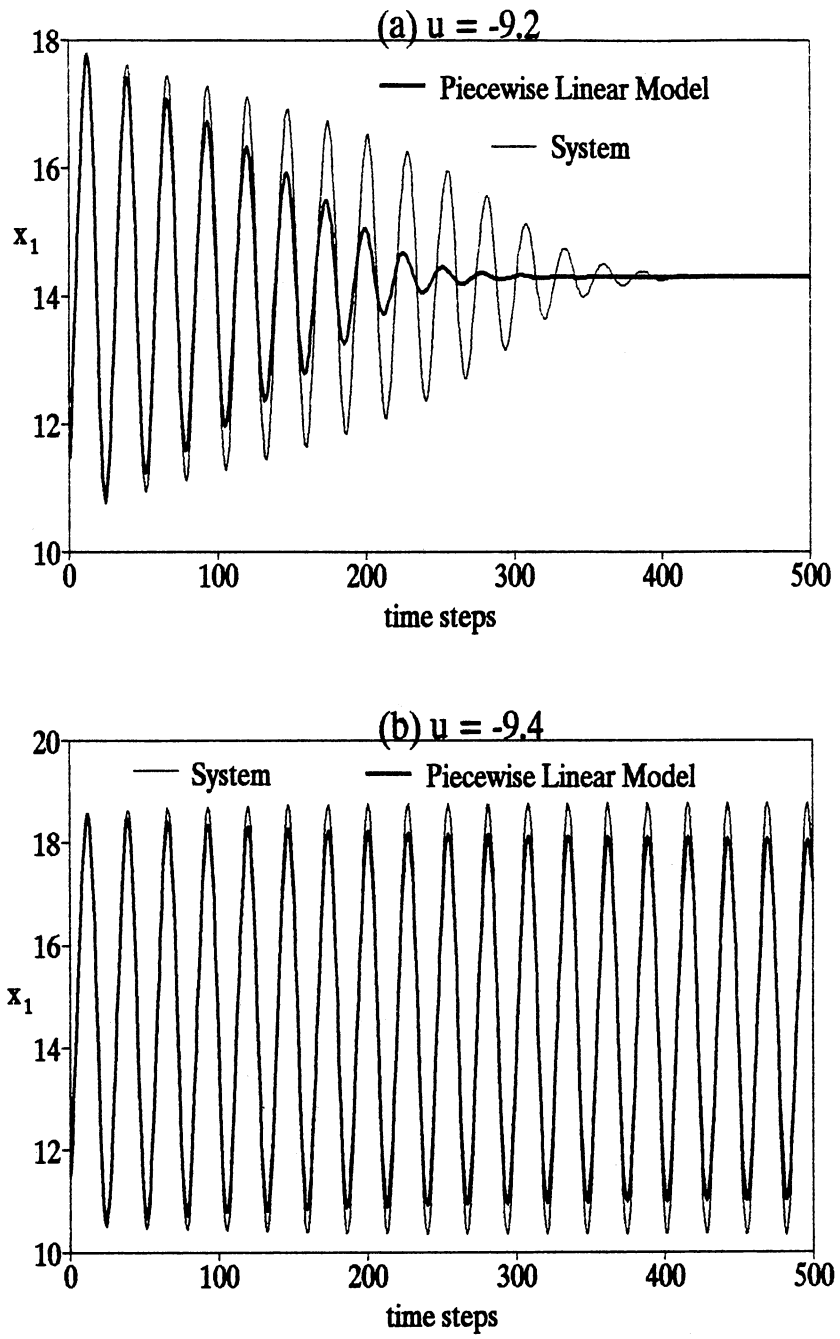

Figure 7. Step-Input Responses of the System and the Piecewise Linear Model.

the same model structure :

$$\begin{bmatrix} [x_1]_i \\ [x_2]_i \end{bmatrix}_{t+1} = \begin{bmatrix} \hat{a}_{11}^{[i]} & \hat{a}_{12}^{[i]} \\ \hat{a}_{21}^{[i]} & \hat{a}_{22}^{[i]} \end{bmatrix} \begin{bmatrix} [x_1]_i \\ [x_2]_i \end{bmatrix}_t + \begin{bmatrix} \hat{b}_1^{[i]} \\ \hat{b}_2^{[i]} \end{bmatrix} [u(t)]_i + \begin{bmatrix} \hat{c}_1^{[i]} \\ \hat{c}_2^{[i]} \end{bmatrix}, \quad i = 1,\ldots,d \qquad (4.13a)$$

where

$$[u(t)]_i = \begin{cases} u(t) & , \text{ if } x_1^{[i-1]} \le x_1(t) \le x_1^{[i]} \\ 0 & , \text{ otherwise} \end{cases} \qquad (4.13b)$$

$$[x_j(t)]_i = \begin{cases} x_j(t) & , \text{ if } x_1^{[i-1]} \le x_1(t) \le x_1^{[i]} \\ 0 & , \text{ otherwise} \end{cases}, \quad j = 1,2 \qquad (4.13c)$$

$$x_1^{[i]} = (x_{1,max} - x_{1,min})\, i/d + x_{1,min} \qquad (4.13d)$$

Polynomial Function Method

Consider the following model structure :

$$\begin{bmatrix} x_1 \\ x_2 \end{bmatrix}_{t+1} = \begin{bmatrix} \hat{a}_{11} & \hat{a}_{12} \\ \hat{a}_{21} & \hat{a}_{22} \end{bmatrix}_t \begin{bmatrix} x_1 \\ x_2 \end{bmatrix}_t + \begin{bmatrix} \hat{b}_1 \\ \hat{b}_2 \end{bmatrix}_t u(t) + \begin{bmatrix} \hat{c}_1 \\ \hat{c}_2 \end{bmatrix}_t \qquad (4.14)$$

where the parameter functions $\hat{a}$s and $\hat{b}$s are parameterized in terms of third-order polynomial functions :

$$\hat{a}_{11}(t) = p_{1,1} + p_{1,2}x_1(t) + p_{1,3}x_1^2(t) + p_{1,4}x_1^3(t) \qquad (4.15a)$$

$$\hat{a}_{12}(t) = p_{1,5} + p_{1,6}x_1(t) + p_{1,7}x_1^2(t) + p_{1,8}x_1^3(t) \qquad (4.15b)$$

$$\hat{b}_1(t) = p_{1,9} + p_{1,10}x_1(t) + p_{1,11}x_1^2(t) + p_{1,12}x_1^3(t) \qquad (4.15c)$$

$$\hat{a}_{21}(t) = p_{2,1} + p_{2,2}x_1(t) + p_{2,3}x_1^2(t) + p_{2,4}x_1^3(t) \qquad (4.15d)$$

$$\hat{a}_{22}(t) = p_{2,5} + p_{2,6}x_1(t) + p_{2,7}x_1^2(t) + p_{2,8}x_1^3(t) \qquad (4.15e)$$

$$\hat{b}_2(t) = p_{2,9} + p_{2,10}x_1(t) + p_{2,11}x_1^2(t) + p_{2,12}x_1^3(t) \qquad (4.15f)$$

Note that in Equation (4.14), the signal dependence of $c_1(x_1)$ and $c_2(x_1)$ have been assumed negligible. Such an assumption is for ensuring the identifiability of the model structure chosen.

Substituting Equations (4.15) into Equation (4.14) :

$$x_i(t+1) = \underline{\phi}^T(t)\,\underline{\theta}_i \quad , \quad i = 1,2 \qquad (4.16a)$$

where

$$\underline{\phi}^T(t) = [x_1(t), x_1^2(t), x_1^3(t), x_1^4(t), x_2(t), x_2(t)x_1(t), x_2(t)x_1^2(t), x_2(t)x_1^3(t), u(t), u(t)x_1(t), u(t)x_1^2(t), u(t)x_1^3(t), 1.0] \qquad (4.16b)$$

$$\underline{\theta}_i^T = [p_{i,1}, p_{i,2}, p_{i,3}, p_{i,4}, p_{i,5}, p_{i,6}, p_{i,7}, p_{i,8}, p_{i,9}, p_{i,10}, p_{i,11}, p_{i,12}, \hat{c}_i] \qquad (4.16c)$$

Equations (4.16) are two linear regressions. For each linear regression, the estimation of parameters can be

performed independently.

Proposed Method

Equation (4.14) along with the following linguistic parameterization of system parameter functions is considered as the proposed model structure :

If $x_1(t)$ is small then

$$\hat{a}_{11}(t) = \sigma_{1,1}$$
$$\hat{a}_{12}(t) = \sigma_{1,8}$$
$$\hat{b}_1(t) = \sigma_{1,15}$$
$$\hat{a}_{21}(t) = \sigma_{2,1}$$
$$\hat{a}_{22}(t) = \sigma_{2,8}$$
$$\hat{b}_2(t) = \sigma_{2,15} \qquad (4.17a)$$

If $x_1(t)$ is medium-1 then

$$\hat{a}_{11}(t) = \sigma_{1,2} + \sigma_{1,3}\, x_1(t)$$
$$\hat{a}_{12}(t) = \sigma_{1,9} + \sigma_{1,10}\, x_1(t)$$
$$\hat{b}_1(t) = \sigma_{1,16} + \sigma_{1,17}\, x_1(t)$$
$$\hat{a}_{21}(t) = \sigma_{2,2} + \sigma_{2,3}\, x_1(t)$$
$$\hat{a}_{22}(t) = \sigma_{2,9} + \sigma_{2,10}\, x_1(t)$$
$$\hat{b}_2(t) = \sigma_{2,16} + \sigma_{2,17}\, x_1(t) \qquad (4.17b)$$

If $x_1(t)$ is medium-2 then

$$\hat{a}_{11}(t) = \sigma_{1,4} + \sigma_{1,5}\, x_1(t)$$
$$\hat{a}_{12}(t) = \sigma_{1,11} + \sigma_{1,12}\, x_1(t)$$
$$\hat{b}_1(t) = \sigma_{1,18} + \sigma_{1,19}\, x_1(t)$$

$$\hat{a}_{21}(t) = \sigma_{2,4} + \sigma_{2,5}\, x_1(t)$$
$$\hat{a}_{22}(t) = \sigma_{2,11} + \sigma_{2,12}\, x_1(t)$$
$$\hat{b}_2(t) = \sigma_{2,18} + \sigma_{2,19}\, x_1(t) \qquad (4.17c)$$

If $x_1(t)$ is large then

$$\hat{a}_{11}(t) = \sigma_{1,6} + \sigma_{1,7}\, x_1(t)$$
$$\hat{a}_{12}(t) = \sigma_{1,13} + \sigma_{1,14}\, x_1(t)$$
$$\hat{b}_1(t) = \sigma_{1,20} + \sigma_{1,21}\, x_1(t)$$
$$\hat{a}_{21}(t) = \sigma_{2,6} + \sigma_{2,7}\, x_1(t)$$
$$\hat{a}_{22}(t) = \sigma_{2,13} + \sigma_{2,14}\, x_1(t)$$
$$\hat{b}_2(t) = \sigma_{2,20} + \sigma_{2,21}\, x_1(t) \qquad (4.17d)$$

where the membership functions are shown in Figure 8.

The introduction of additional membership functions "medium-1" and "medium-2" is intended to improve modeling accuracy of the proposed method. Such an intention, however, causes an increase of the μ-space dimension and henceforth would sacrifice the convergent rate in the Complex Method's optimization.

Moreover, the use of constant shape functions in Equation (4.17a) is warranted by the assumed linear system pre-stall dynamics (Figure 6).

The parameter functions in Equations (4.17) will be defined similar to those defined in Equations (2.7). For instance,

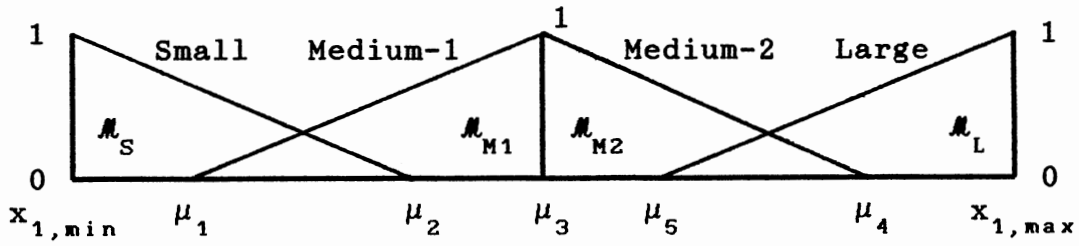

Figure 8. The Membership Functions Defined in Example 2, Chapter IV.

$$\hat{a}_{11}(t) \equiv \pi_S(t)\,\sigma_1 + \pi_{M1}(t)(\sigma_2 + \sigma_3 x_1(t)) + \pi_{M2}(t)(\sigma_4 + \sigma_5 x_1(t)) + \pi_L(t)(\sigma_6 + \sigma_7 x_1(t)) \qquad (4.18a)$$

where

$$\pi_S(t) \equiv \mu_S(t)/S_M(t) \qquad (4.18b)$$

$$\pi_{M1}(t) \equiv \mu_{M1}(t)/S_M(t) \qquad (4.18c)$$

$$\pi_{M2}(t) \equiv \mu_{M2}(t)/S_M(t) \qquad (4.18d)$$

$$\pi_L(t) \equiv \mu_L(t)/S_M(t) \qquad (4.18e)$$

$$S_M(t) \equiv \mu_S(t) + \mu_{M1}(t) + \mu_{M2}(t) + \mu_L(t) \qquad (4.18f)$$

$$\mu_S = \begin{cases} (\mu_1 - x_1)/(\mu_1 - x_{1,min}), & \text{if } x_{1,min} \le x_1 < \mu_1 \\ 0, & \text{otherwise} \end{cases} \qquad (4.18g)$$

$$\mu_{M1} = \begin{cases} (x_1 - \mu_2)/(\mu_3 - \mu_2), & \text{if } \mu_2 < x_1 \le \mu_3 \\ 0, & \text{otherwise} \end{cases} \qquad (4.18h)$$

$$\mu_{M2} = \begin{cases} (\mu_4 - x_1)/(\mu_4 - \mu_3), & \text{if } \mu_3 \le x_1 < \mu_4 \\ 0, & \text{otherwise} \end{cases} \qquad (4.18i)$$

$$\mu_L = \begin{cases} (x_1 - \mu_5)/(x_{1,max} - \mu_5), & \text{if } \mu_5 < x_1 \le x_{1,max} \\ 0, & \text{otherwise} \end{cases} \qquad (4.18j)$$

and the following constraints must hold to ensure S_M is nonzero :

$$x_{1,min} < \mu_2 < \mu_1 < \mu_3 < \mu_5 < \mu_4 < x_{1,max} \qquad (4.19)$$

Finally, Equations (4.14) and (4.17) can be combined and arranged into two pseudo-linear regressions :

$$x_i(t+1) = \underline{\phi}^T(t)\,\underline{\theta}_i \quad , \; i = 1,2 \tag{4.20a}$$

where

$$\begin{aligned}\underline{\phi}^T(t) = [&\mathcal{W}_S(t)x_1(t), \mathcal{W}_{M1}(t)x_1(t), \mathcal{W}_{M1}(t)x_1^2(t),\\ &\mathcal{W}_{M2}(t)x_1(t), \mathcal{W}_{M2}(t)x_1^2(t), \mathcal{W}_L(t)x_1(t),\\ &\mathcal{W}_L(t)x_1^2(t), \mathcal{W}_S(t)x_2(t), \mathcal{W}_{M1}(t)x_2(t),\\ &\mathcal{W}_{M1}(t)x_1(t)x_2(t), \mathcal{W}_{M2}(t)x_2(t), \mathcal{W}_{M2}(t)x_1(t)x_2(t),\\ &\mathcal{W}_L(t)x_2(t), \mathcal{W}_L(t)x_1(t)x_2(t), \mathcal{W}_S(t)u(t), \mathcal{W}_{M1}(t)u(t),\\ &\mathcal{W}_{M1}(t)x_1(t)u(t), \mathcal{W}_{M2}(t)u(t), \mathcal{W}_{M2}(t)x_1(t)u(t),\\ &\mathcal{W}_L(t)u(t), \mathcal{W}_L(t)x_1(t)u(t), 1.0]\end{aligned} \tag{4.20b}$$

$$\begin{aligned}\underline{\theta}_i^T = [&\sigma_{i,1}, \sigma_{i,2}, \sigma_{i,3}, \sigma_{i,4}, \sigma_{i,5}, \sigma_{i,6}, \sigma_{i,7}, \sigma_{i,8}, \sigma_{i,9},\\ &\sigma_{i,10}, \sigma_{i,11}, \sigma_{i,12}, \sigma_{i,13}, \sigma_{i,14}, \sigma_{i,15}, \sigma_{i,16},\\ &\sigma_{i,17}, \sigma_{i,18}, \sigma_{i,19}, \sigma_{i,20}, \sigma_{i,21}, \hat{c}_i]\end{aligned} \tag{4.20c}$$

Simulation Results

∇_2-class signals distributed over [-8.0,-11.0] were used as the system inputs. All the identification methods considered were performed based on the same identification data which are plotted in Figure 9.

First of all, from the collected x_1 data, arbitrarily choose $x_{1,min} = 0.0$ and $x_{1,max} = 28.0$. For gate function method, two sub-cases with d = 5 and d = 10 in Equations

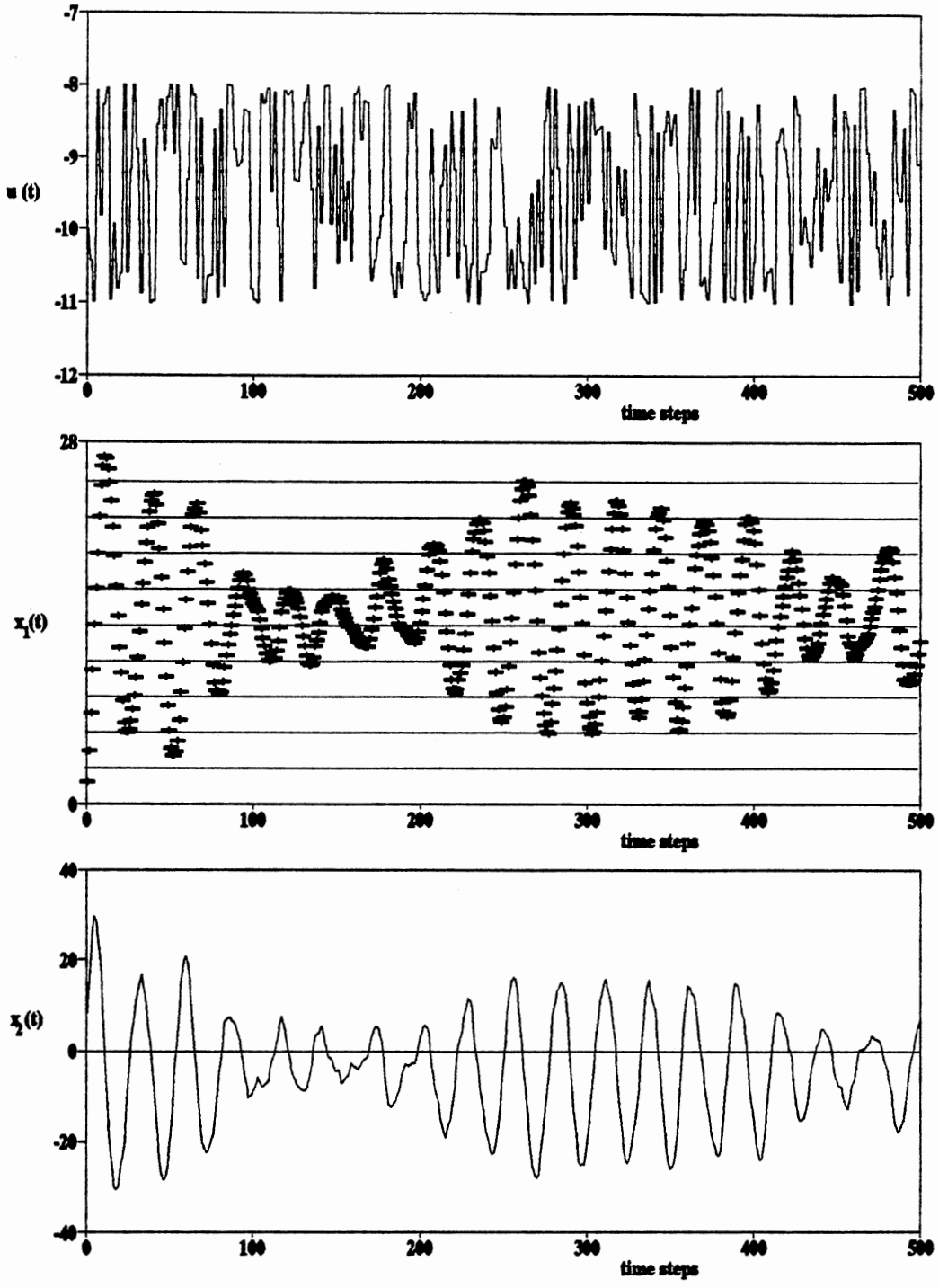

Figure 9. The Data Used for the Parameter Estimation in Example 2.

(4.13) were considered. As shown in Figure 9, x_1 vs. t data was plotted as symbols and with 10 quantification intervals so that one may have a rough idea about the number of data in each set of gated signals.

Simulation results for the studying identification methods are summarized in Table IV, V and VI respectively. As shown in Table IV, the quantification of $[x_{1,min}, x_{1,max}]$ into 10 intervals results in a meaningless EGM (i.e. d = 10 and i = 1). Such a situation is not uncommon in the use of gate function method if the quantification intervals are too small.

For comparison reason, a new term called estimation error function is introduced. For each system parameter function, it is defined :

$$\Delta a_{11}(x_1) = (a_{11}(x_1)-\hat{a}_{11}(x_1))/|a_{11}(x_1)| \qquad (4.21a)$$

$$\Delta a_{12}(x_1) = (a_{12}(x_1)-\hat{a}_{12}(x_1))/|a_{12}(x_1)| \qquad (4.21b)$$

$$\Delta a_{21}(x_1) = (a_{21}(x_1)-\hat{a}_{21}(x_1))/|a_{21}(x_1)| \qquad (4.21c)$$

$$\Delta a_{22}(x_1) = (a_{22}(x_1)-\hat{a}_{22}(x_1))/|a_{22}(x_1)| \qquad (4.21d)$$

$$\Delta b_1(x_1) = (b_1(x_1)-\hat{b}_1(x_1))/|b_1(x_1)| \qquad (4.21e)$$

$$\Delta b_2(x_1) = (b_2(x_1)-\hat{b}_2(x_1))/|b_2(x_1)| \qquad (4.21f)$$

$$\Delta c_1(x_1) = (c_1(x_1)-\hat{c}_1(x_1))/|c_1(x_1)| \qquad (4.21g)$$

$$\Delta c_2(x_1) = (c_2(x_1)-\hat{c}_2(x_1))/|c_2(x_1)| \qquad (4.21h)$$

TABLE IV

A SUMMARY OF SIMULATION RESULTS OF EXAMPLE 2
(GATE FUNCTION METHOD)

	$\hat{a}_{11}^{[i]}$	$\hat{a}_{12}^{[i]}$	$\hat{b}_{1}^{[i]}$	$\hat{c}_{1}^{[i]}$
d=5				
i=1	0.90732560	0.09577142	-0.21742235	-0.51015185
i=2	0.90733185	0.09577199	-0.21742975	-0.51023933
i=3	0.95108825	0.09542130	-0.21583963	-1.05756369
i=4	0.97001668	0.09714150	-0.21763249	-1.18167471
i=5	0.95690338	0.09742015	-0.22085342	-0.94101728
d=10				
i=1	0.00000000	0.00000000	0.00000000	0.00000000
i=2	0.90732848	0.09577067	-0.21741736	-0.51012899
i=3	0.90732682	0.09577181	-0.21742807	-0.51019086
i=4	0.90732879	0.09577188	-0.21742843	-0.51019743
i=5	0.90732987	0.09577186	-0.21742946	-0.51021083
i=6	1.04045997	0.09573199	-0.21958527	-2.46837741
i=7	0.99597572	0.09707773	-0.21877153	-1.66383482
i=8	0.95705884	0.09729108	-0.22071813	-0.94361770
i=9	0.95692184	0.09740083	-0.22084484	-0.94141759
i=10	0.93997860	0.09773161	-0.15707872	0.02678130

TABLE IV (Continued)

	$\hat{a}_{21}^{[i]}$	$\hat{a}_{22}^{[i]}$	$\hat{b}_{2}^{[i]}$	$\hat{c}_{2}^{[i]}$
d=5				
i=1	-0.54876886	0.97211852	-0.80033281	0.43635802
i=2	-0.54877322	0.97211815	-0.80032790	0.43641695
i=3	-0.56156581	0.97223421	-0.80080108	0.59637444
i=4	-0.56704457	0.97185794	-0.80056949	0.62983565
i=5	-0.56327776	0.97179958	-0.79969116	0.56035060
d=10				
i=1	0.00000000	0.00000000	0.00000000	0.00000000
i=2	-0.54876989	0.97211879	-0.80033460	0.43634980
i=3	-0.54876935	0.97211828	-0.80032910	0.43638050
i=4	-0.54877083	0.97211823	-0.80032887	0.43638479
i=5	-0.54877162	0.97211825	-0.80032812	0.43639411
i=6	-0.58748238	0.97217364	-0.79978076	1.00492537
i=7	-0.57456103	0.97186487	-0.80021272	0.76967075
i=8	-0.56330412	0.97182456	-0.79971451	0.56080816
i=9	-0.56327390	0.97180380	-0.79969027	0.56028161
i=10	-0.55417667	0.97166729	-0.83337221	0.04482194

TABLE V

A SUMMARY OF SIMULATION RESULTS OF EXAMPLE 2
(POLYNOMIAL FUNCTION METHOD)

	x_1^0	x_1^1	x_1^2	x_1^3
$\hat{a}_{11}$	1.19719465	-0.03760372	0.00196954	-0.00003221
$\hat{a}_{12}$	0.09806675	-0.00066150	0.00004907	-0.00000094
$\hat{b}_1$	-0.28680735	0.01797868	-0.00141486	0.00003434
$\hat{a}_{21}$	-0.63302178	0.01091652	-0.00057205	0.00000935
$\hat{a}_{22}$	0.97167922	0.00012984	-0.00000954	0.00000018
$\hat{b}_2$	-0.78005512	-0.00522606	0.00041012	-0.00000997
$\hat{c}_1 = -1.30534990$		$\hat{c}_2 = 0.66849212$		

TABLE VI

A SUMMARY OF SIMULATION RESULTS OF EXAMPLE 2
(THE PROPOSED METHOD)

$\sigma_{1,1} \rightarrow \sigma_{1,7}$	$\sigma_{1,8} \rightarrow \sigma_{1,14}$	$\sigma_{1,15} \rightarrow \sigma_{1,21}$	$\sigma_{2,1} \rightarrow \sigma_{2,7}$
0.90742266	0.09576598	-0.21769196	-0.54879983
0.86629843	0.09277416	-0.25877918	-0.53678030
0.00293430	0.00021786	0.00292692	-0.00085762
0.90720378	0.08612706	-0.02112072	-0.54842878
0.00065796	0.00063288	-0.01239269	-0.00021476
0.93395594	0.09470412	-0.17724961	-0.55661942
0.00012834	0.00012287	-0.00204623	-0.00003922

$\mu_1 = 14.57666$
$\mu_2 = 13.39307$
$\mu_3 = 14.93013$
$\mu_4 = 18.09663$
$\mu_5 = 15.37638$

$\hat{c}_1 = -0.51359686$
$\hat{c}_2 = 0.43739901$

$\sigma_{2,8} \rightarrow \sigma_{2,14}$	$\sigma_{2,15} \rightarrow \sigma_{2,21}$
0.97211993	-0.80025126
0.97293421	-0.78819312
-0.00005937	-0.00085902
0.97437652	-0.85664371
-0.00014657	0.00354794
0.97245908	-0.81208475
-0.00003022	0.00058257

The estimation error functions for each model are plotted in Figure 10 through Figure 17. From the figures (notice the change of the vertical scales), the results produced by polynomial function method are the poorest among all. No improvement of the estimation accuracy can be achieved by increasing the order of the polynomials in Equations (4.15). Therefore, it is not advisable to search for a single polynomial relationship which governs flight behavior in the total envelope spanning pre-stall, stall, and post-stall flight.

The gate function method is adequate for the pre-stall region where the system parameter functions are constant. However, as shown in Figures 10, 12, 16, and 17, the estimation accuracy for the stall and post-stall regions is poor. Further improvement is possible by quantifying the regions into finer intervals. But, the improvement is limited due to the required minimum length of nonzero gated signals.

In the proposed method, the dynamic variable space indeed was quantified into six intervals (Figure 8). The length and position of each interval is not determined by the user as in gate function method but by an optimization method. For each quantification interval, shape functions or their combinations with weighting functions are used to fit the system parameter functions instead of just using a

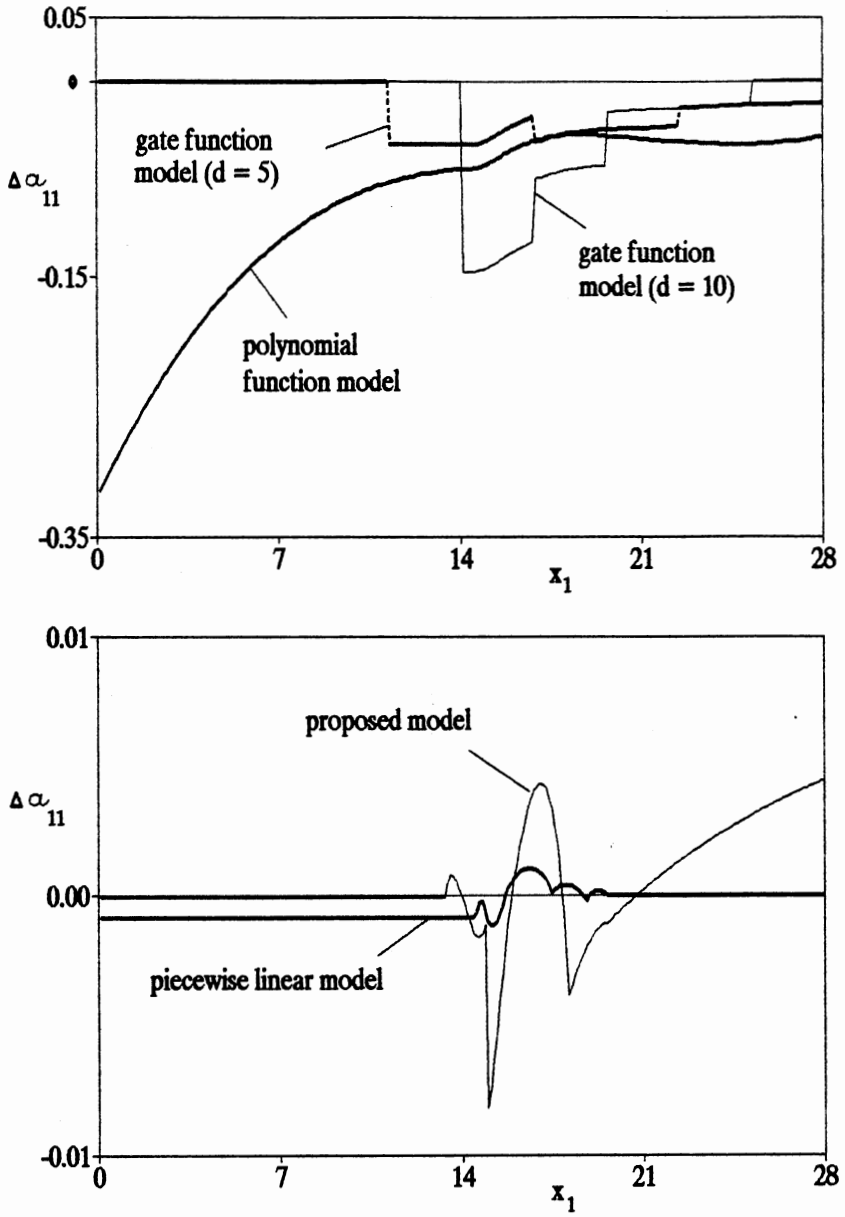

Figure 10. Comparison of the Estimation Error Function, Equation (4.21a).

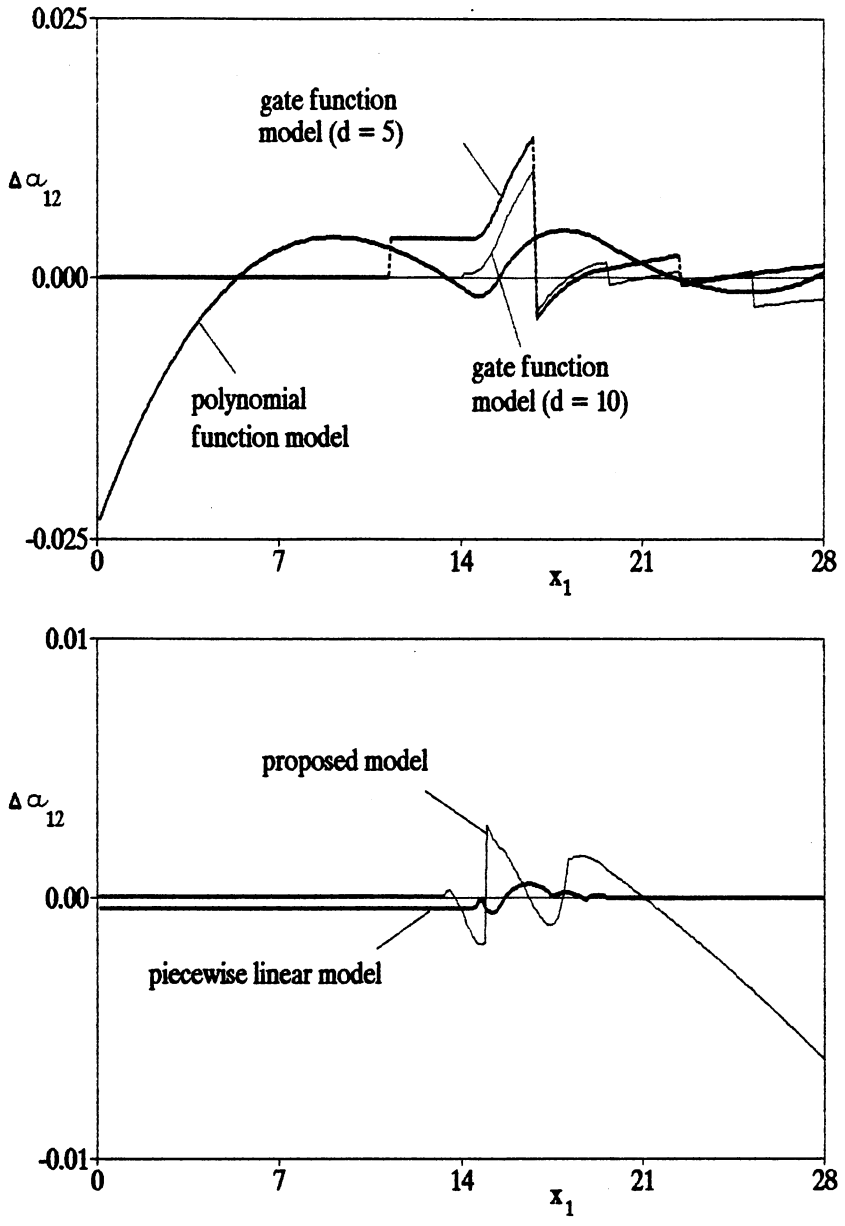

Figure 11. Comparison of the Estimation Error Function, Equation (4.21b).

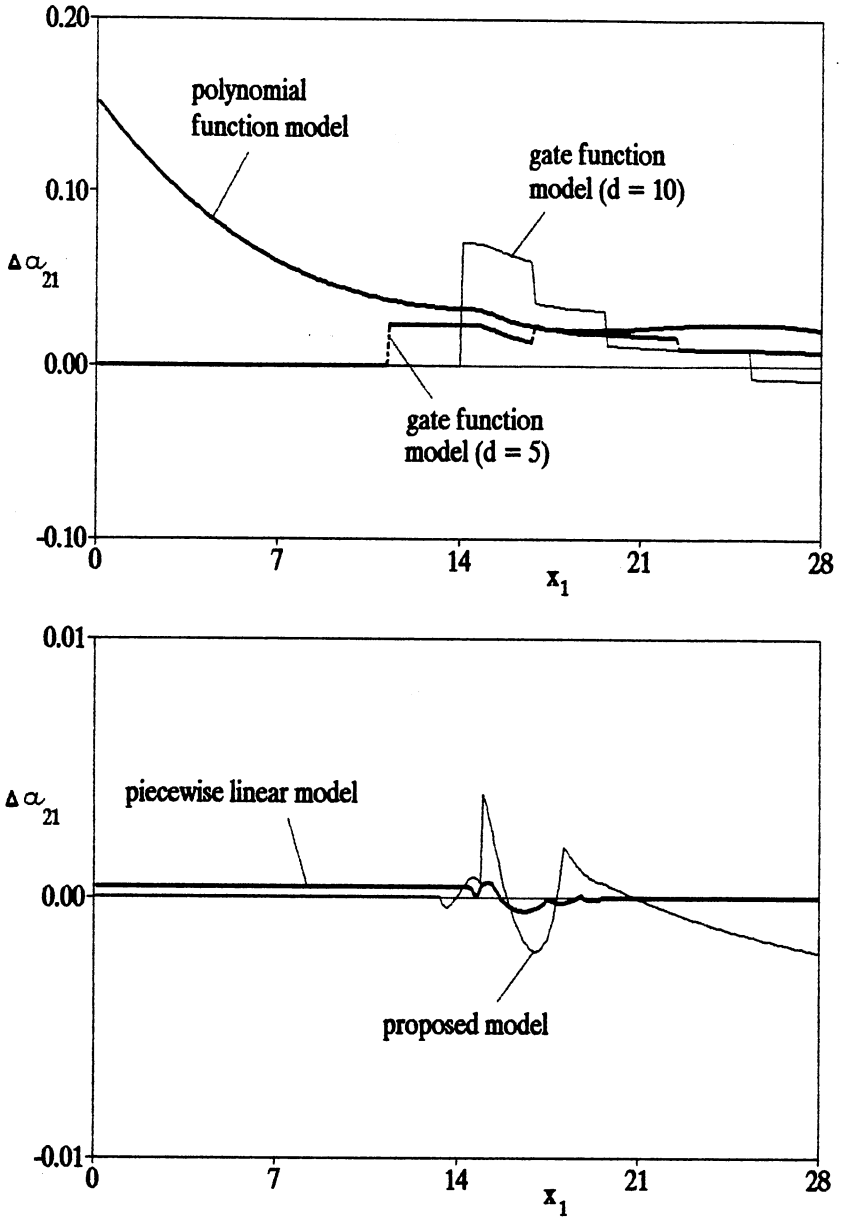

Figure 12. Comparison of the Estimation Error Function, Equation (4.21c).

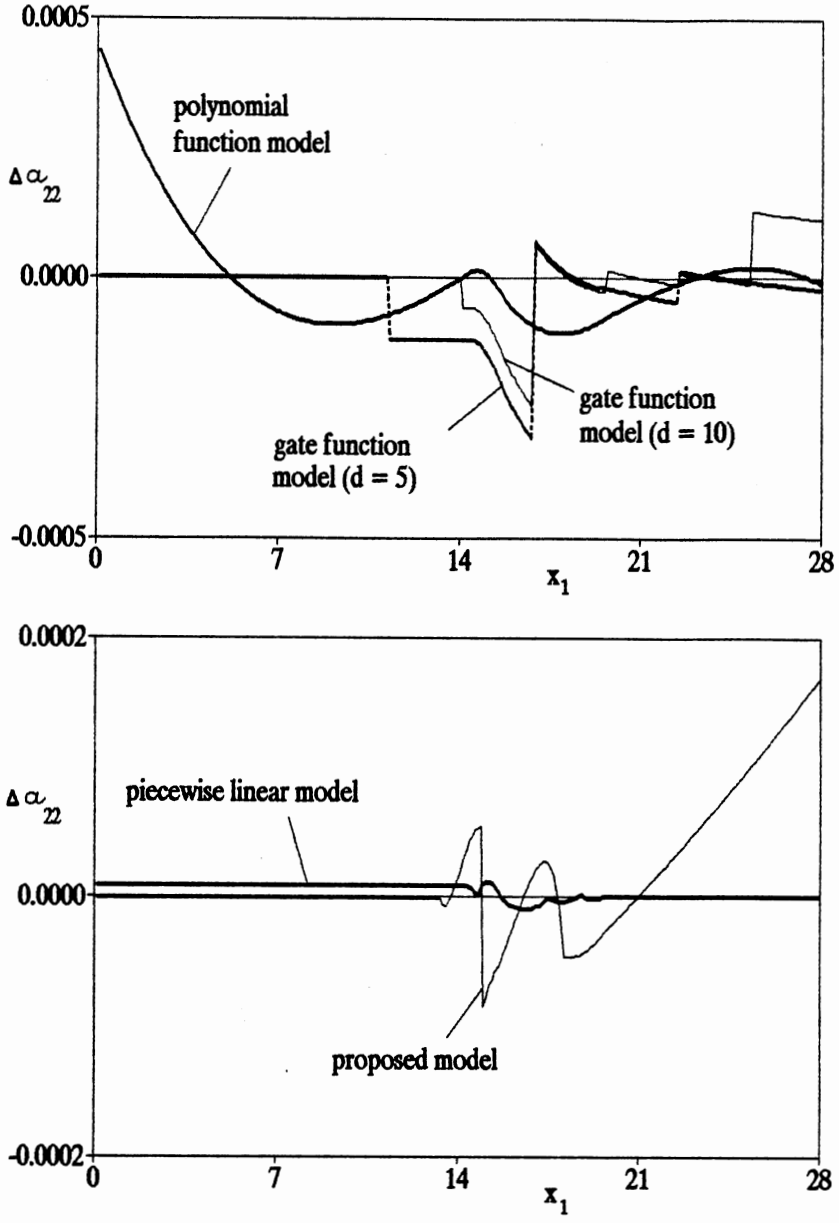

Figure 13. Comparison of the Estimation Error Function, Equation (4.21d).

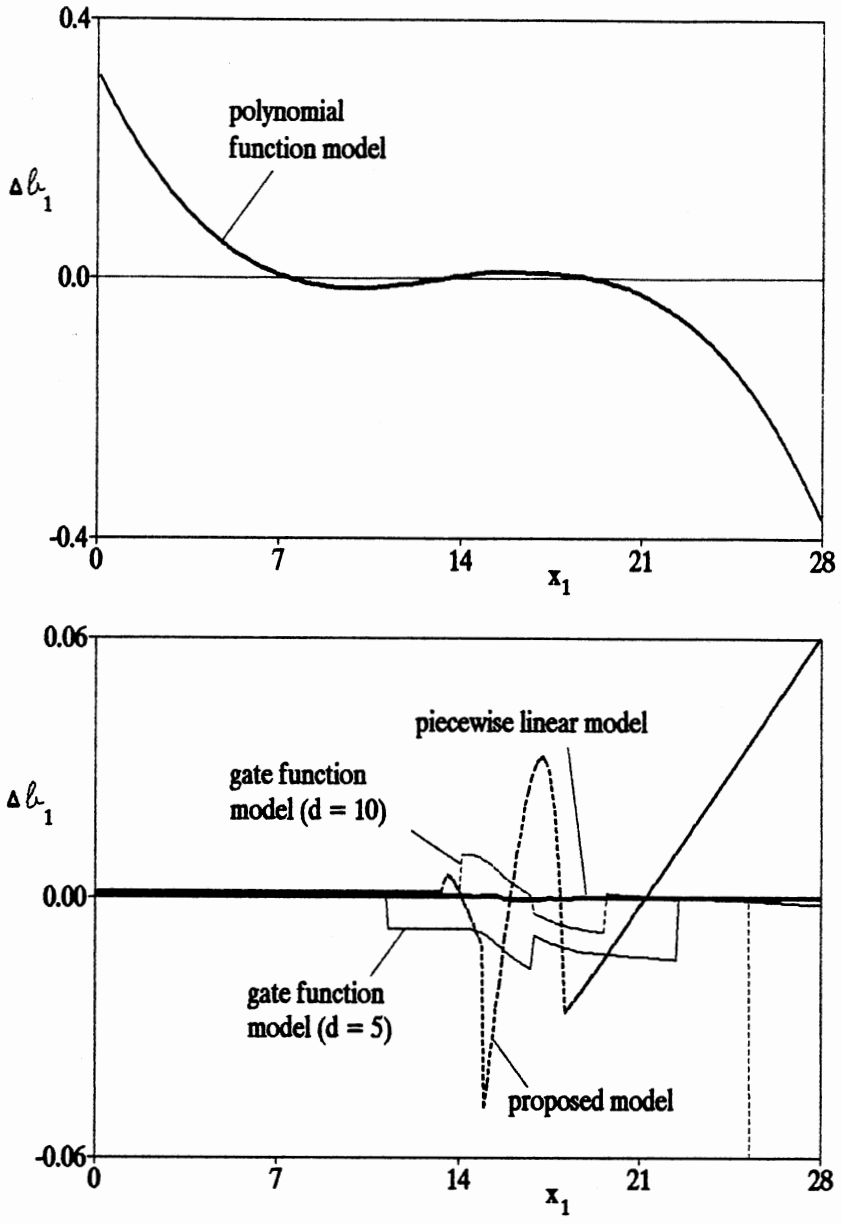

Figure 14. Comparison of the Estimation Error Function, Equation (4.21e).

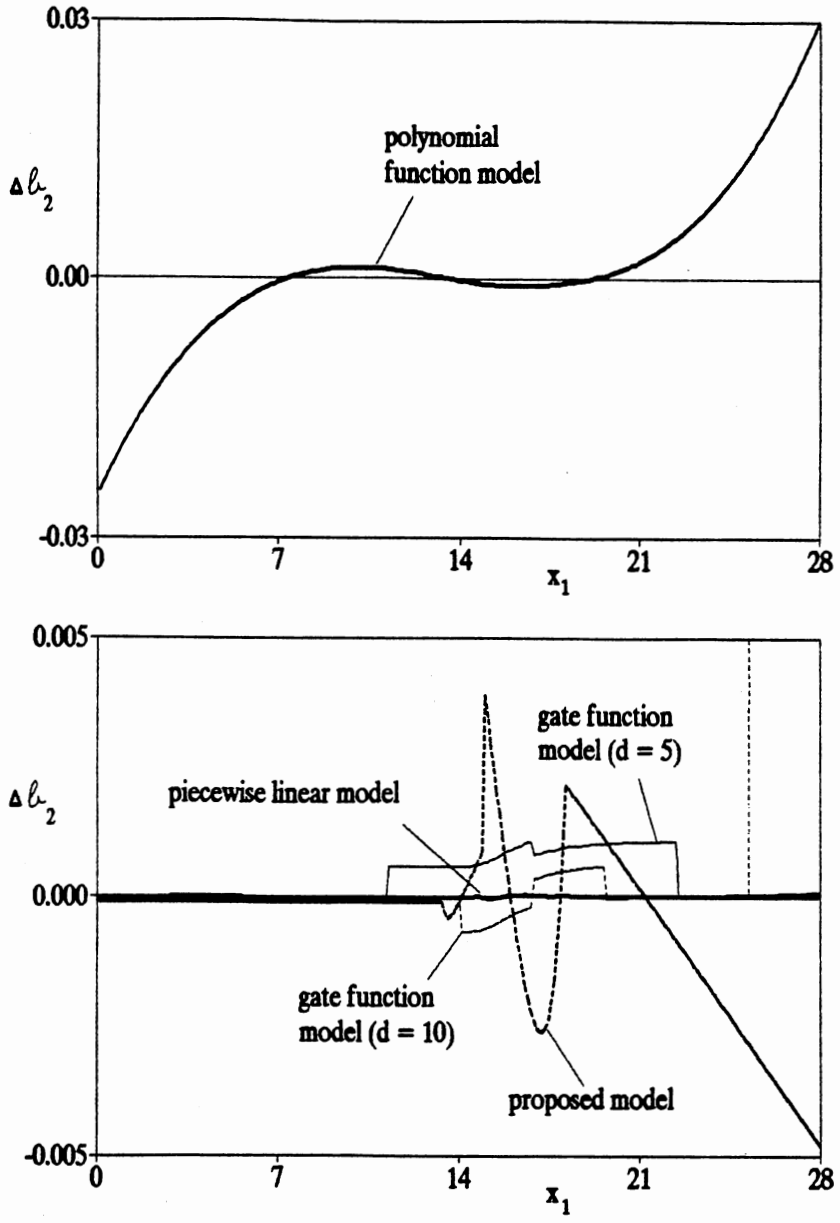

Figure 15. Comparison of the Estimation Error Function, Equation (4.21f).

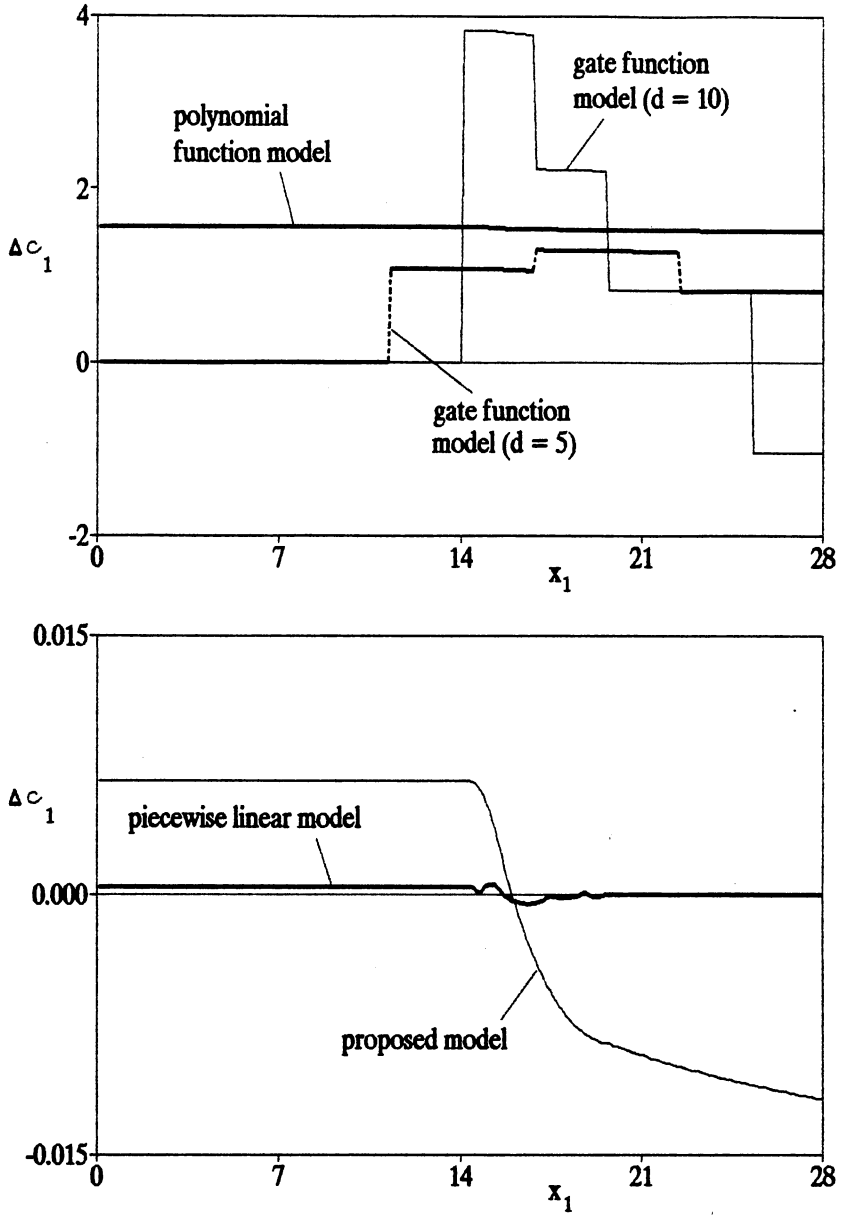

Figure 16. Comparison of the Estimation Error Function, Equation (4.21g).

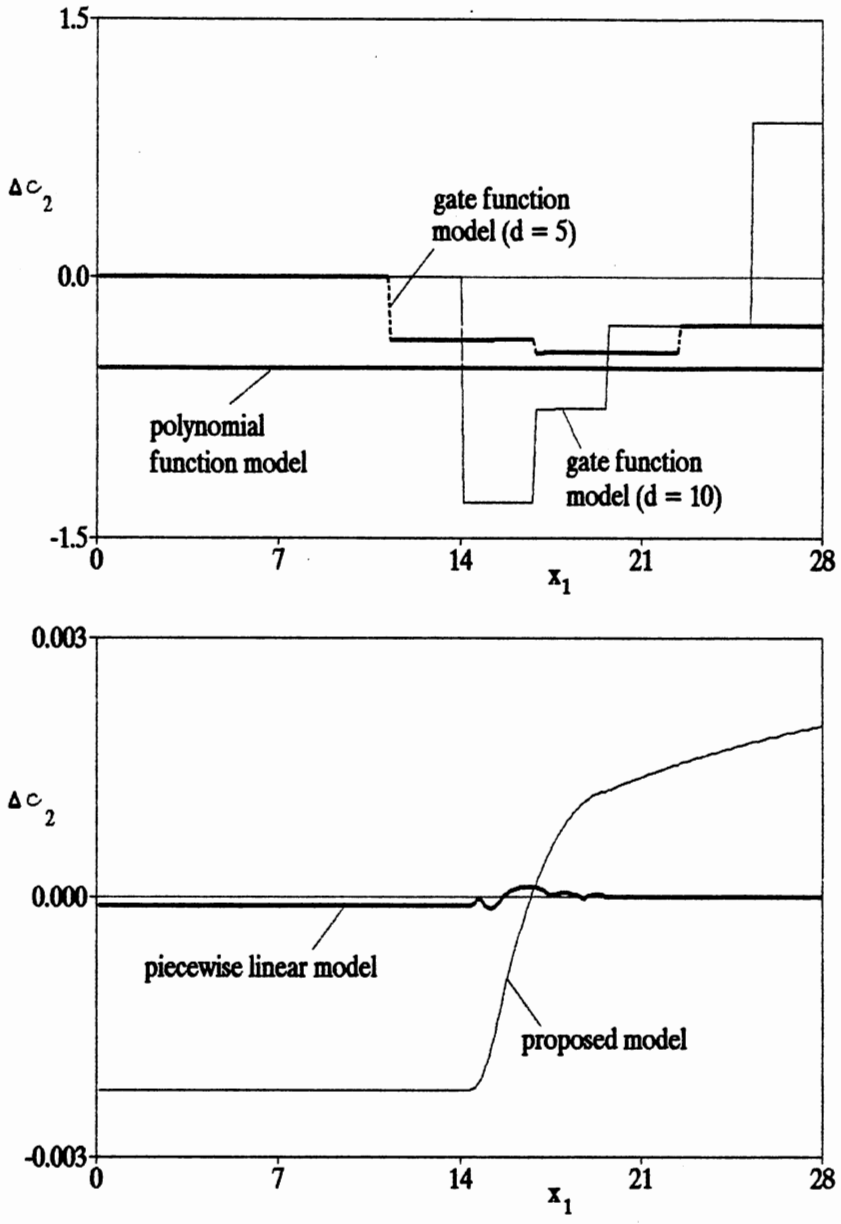

Figure 17. Comparison of the Estimation Error Function, Equation (4.21h).

constant. Although the proposed method may not produce the best estimates for all system parameter functions as shown in Figures 14 and 15, it is globally the best among the system identification methods.

For further investigating model predictions of the system longitudinal limit cycle, let a prediction error be defined by

$$\Delta x_1 \equiv x_1 - \hat{x}_1 \tag{4.22}$$

where $\hat{x}_1$ denote a model output.

The prediction errors for u = -9.2 and -9.4 are shown in Figures 18 and 19 respectively. As expected, the model achieved by the proposed method has better prediction accuracy than those achieved by the other methods. But, it is surprising that the model achieved by the proposed method is superior to the piecewise linear model. The reason is that the latter does a poor job in modeling of system pre-stall dynamics (Figures 10, 11, 12 and 13) and results in a poor prediction of the system longitudinal limit cycle.

Example 3 - Hydraulic Servovalve/Motor System

An experimental study of the identification of an hydraulic servovalve/motor system (Figure 20) is provided in this example including a follow-up control application. The study will examine the adequacy of those identification

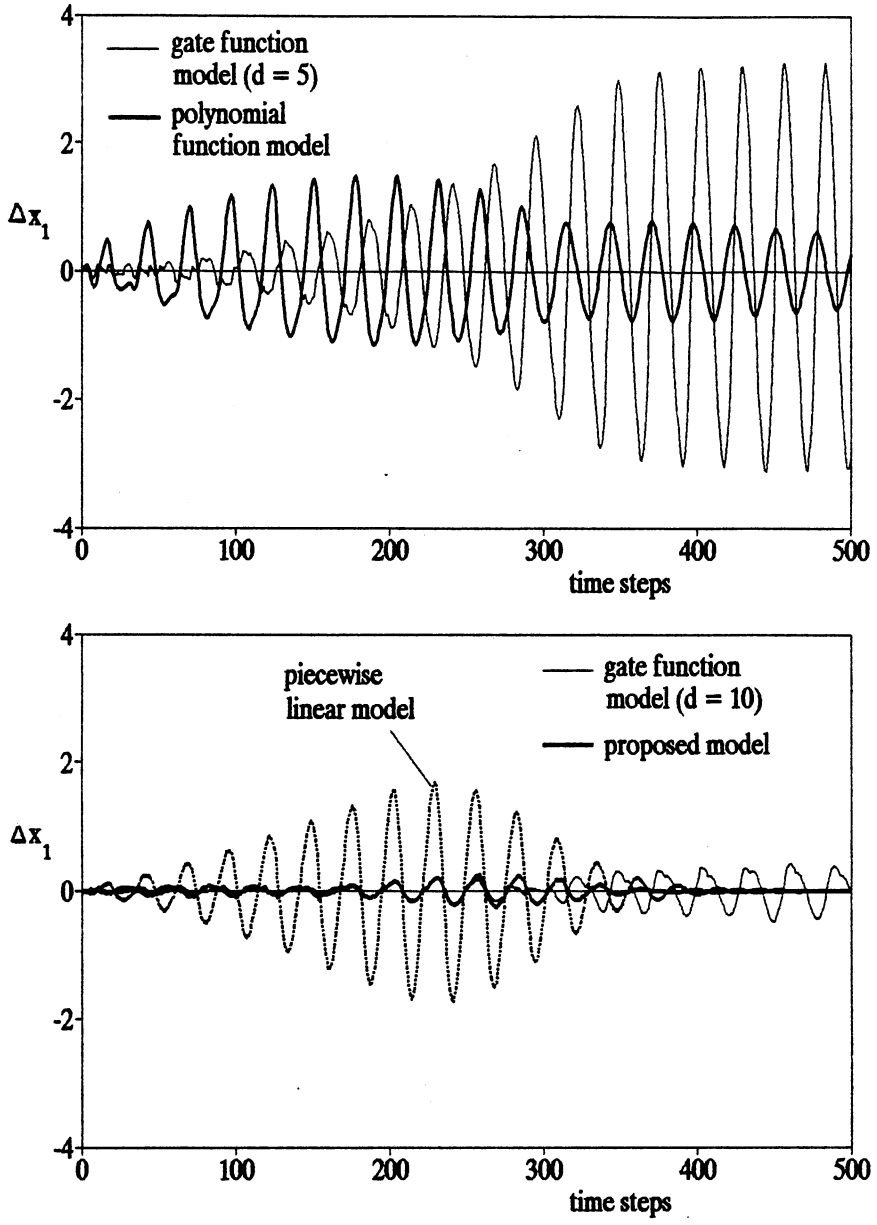

Figure 18. Comparison of the Prediction Errors of the System Step-Input Response (u = -9.2).

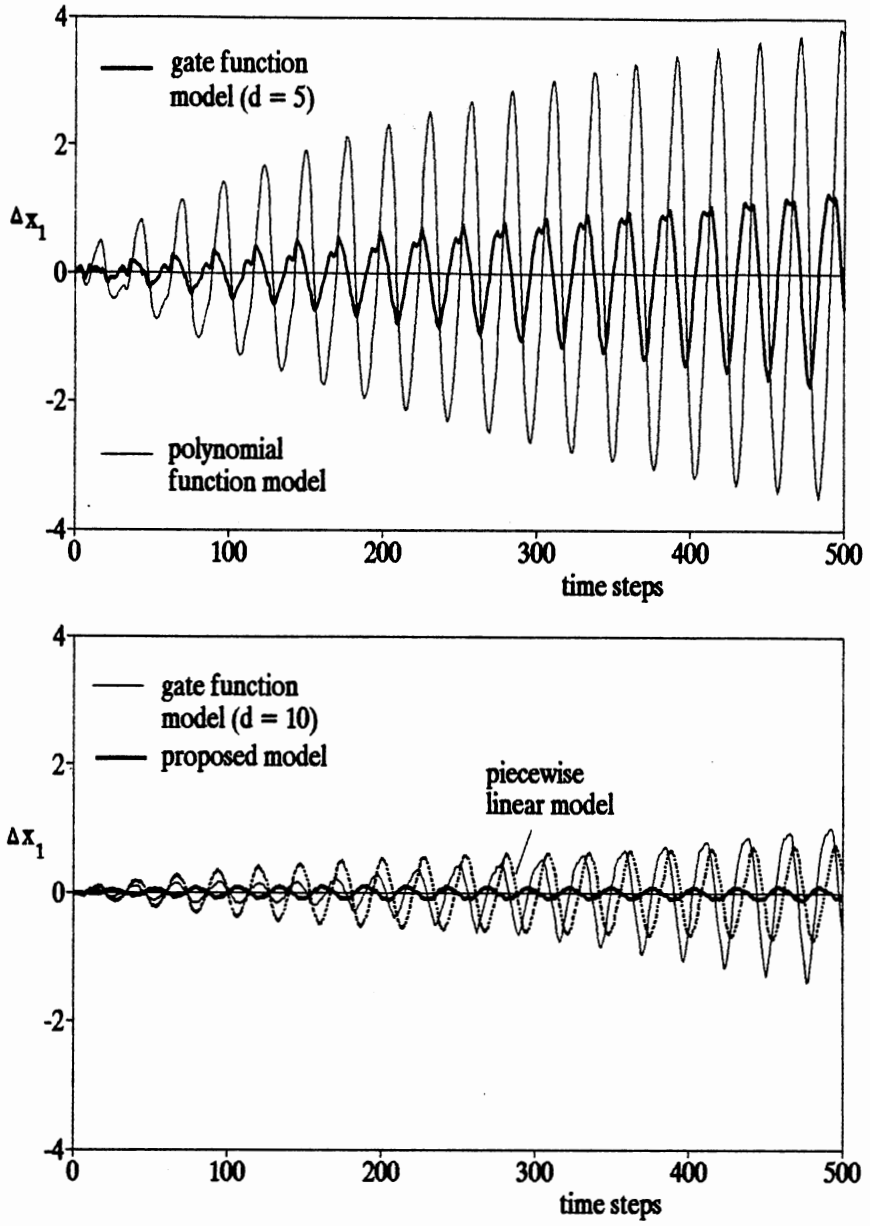

Figure 19. Comparison of the Prediction Errors of the System Step-Input Response (u = -9.4).

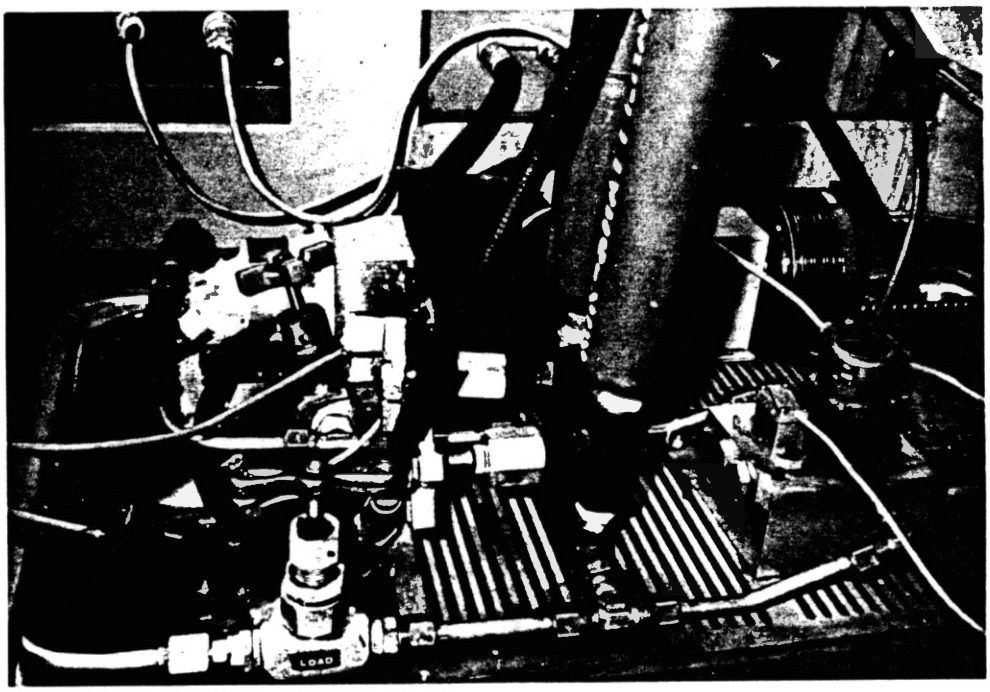

Figure 20. The Hydraulic Servovalve/Motor System Studied in Example 3, Chapter IV.

methods mentioned previously and a classical linear identification method.

The system is described by [45] :

$$\dot{N} = \frac{1}{J_t}(-C_d\ D_m\ \mu\ N + D_m\ P - T_t) \qquad (4.23a)$$

$$\dot{P} = \frac{2\ \beta}{V_o}(Q - D_m\ N - \frac{C_s\ D_m}{\mu} P) \qquad (4.23b)$$

$$Q = C_v\ I\ (P_s - |P|)^{\tau} \qquad (4.23c)$$

where

N : angular velocity, the system output (rad/sec)

P : load pressure (psig)

I : valve input current, the system input (mA);

P_s: supply pressure (psig)

Q : load flow rate (in^3/sec)

T_t: total friction torque (in-lb)

and J_t, C_d, D_m, μ, V_o, C_s, C_v, τ, and β denote system coefficients with proper units.

Temperature effects are assumed negligible here. The above coefficients are assumed constant except the bulk modulus β which is considered to be pressure dependent. Coulomb and viscous frictions can be considered and included in the friction term T_t in Equation (4.23a).

First, neglect T_t temporarily and rewrite Equations

(4.23) into the following matrix form :

$$\begin{bmatrix} \dot{N} \\ \dot{P} \end{bmatrix} = \begin{bmatrix} a_{11}^* & a_{12}^* \\ a_{21}^* & a_{22}^* \end{bmatrix} \begin{bmatrix} N \\ P \end{bmatrix} + \begin{bmatrix} 0 \\ \ell_2^* \end{bmatrix} I \qquad (4.24a)$$

where

$$a_{11}^* = - C_d D_m \mu/J_t \qquad (4.24b)$$

$$a_{12}^* = D_m/J_t \qquad (4.24c)$$

$$a_{21}^* = - 2 D_m \beta(|P|)/V_o \qquad (4.24d)$$

$$a_{22}^* = - 2 C_s D_m \beta(|P|)/(\mu V_o) \qquad (4.24e)$$

$$\ell_2^* = 2 C_v \beta(|P|)(P_s-|P|)^{\tau}/V_o \qquad (4.24f)$$

Taking the z transform of Equation (4.24a) gives

$$\begin{bmatrix} N \\ P \end{bmatrix}_{t+1} = \begin{bmatrix} \tilde{a}_{11} & \tilde{a}_{12} \\ \tilde{a}_{21} & \tilde{a}_{22} \end{bmatrix}_t \begin{bmatrix} N \\ P \end{bmatrix}_t + \begin{bmatrix} \tilde{\ell}_1 \\ \tilde{\ell}_2 \end{bmatrix}_t I(t) \qquad (4.25)$$

From the system input/output point of view, Equation (4.25) is equivalent to :

$$\begin{bmatrix} N \\ P \end{bmatrix}_{t+1} = \begin{bmatrix} a_{11} & a_{12} \\ a_{21} & a_{22} \end{bmatrix}_t \begin{bmatrix} N \\ P \end{bmatrix}_t + \begin{bmatrix} \ell_1 \\ \ell_2 \end{bmatrix}_t I(t) \qquad (4.26)$$

if

$$\ell_1 = \tilde{\ell}_1 \qquad (4.27a)$$

$$a_{11} + a_{22} = \tilde{a}_{11} + \tilde{a}_{22} \qquad (4.27b)$$

$$a_{11}a_{22} = a_{12}a_{21} + \tilde{a}_{11}\tilde{a}_{22} - \tilde{a}_{12}\tilde{a}_{21} \qquad (4.27c)$$

$$\ell_1 a_{22} + a_{12}\ell_2 = \tilde{\ell}_1\tilde{a}_{22} + \tilde{a}_{12}\tilde{\ell}_2 \qquad (4.27d)$$

Note that the solutions a_{11}, a_{22}, ℓ_1 and ℓ_2 exist uniquely for any given $\tilde{a}$s, $\tilde{\ell}$s, a_{12} and a_{21}.

Moreover, the pressure dependence of β is usually measured under an experimental condition. When the condition changes, the measured pressure dependence could no longer be adequate due to the change of the amount of gas entrained in the working fluid. So, the dependence must be treated as unknown and parameterized.

The structure of Equation (4.26) instead of that of Equation (4.25) will be selected as the working model structure in the use of the proposed method and polynomial function method. Such a selection of model structure is beneficial to the resulting model accuracy since the mean-square estimation error typically increases with the number of estimated parameters.

Classical Linear Method

The identification of systems based on a linear model structure is a classical method. For this example, a linear model structure can be formed by neglecting the pressure dependence involved and linearizing Equation (4.23c) around a nominal working point. With further consideration of the

process delay, one has

$$\begin{bmatrix} N \\ P \end{bmatrix}_{t+1} = \begin{bmatrix} \hat{a}_{11} & \hat{a}_{12} \\ \hat{a}_{21} & \hat{a}_{22} \end{bmatrix} \begin{bmatrix} N \\ P \end{bmatrix}_t + \begin{bmatrix} \hat{b}_1 \\ \hat{b}_2 \end{bmatrix} I(t-t_d) \qquad (4.28)$$

where t_d denotes the process delay time hereafter.

Gate Function Method

The dynamic variable space $[|P|_{min}, |P|_{max}]$ is quantified into d intervals with equal length. Each EGM has the same model structure :

$$\begin{bmatrix} [N]_i \\ [P]_i \end{bmatrix}_{t+1} = \begin{bmatrix} \hat{a}_{11}^{[i]} & \hat{a}_{12}^{[i]} \\ \hat{a}_{21}^{[i]} & \hat{a}_{22}^{[i]} \end{bmatrix} \begin{bmatrix} [N]_i \\ [P]_i \end{bmatrix}_t + \begin{bmatrix} \hat{b}_1^{[i]} \\ \hat{b}_2^{[i]} \end{bmatrix} [I(t-t_d)]_i \ ,$$

$$i = 1,\ldots,d \qquad (4.29a)$$

where

$$[N(t)]_i = \begin{cases} N(t), & \text{if } P^{[i-1]} \le |P(t)| \le P^{[i]} \\ 0 \quad , & \text{otherwise} \end{cases} \qquad (4.29b)$$

$$[P(t)]_i = \begin{cases} P(t), & \text{if } P^{[i-1]} \le |P(t)| \le P^{[i]} \\ 0 \quad , & \text{otherwise} \end{cases} \qquad (4.29c)$$

$$[I(t)]_i = \begin{cases} I(t), & \text{if } P^{[i-1]} \le |P(t)| \le P^{[i]} \\ 0 \quad , & \text{otherwise} \end{cases} \qquad (4.29d)$$

$$P^{[i]} = (|P|_{max} - |P|_{min})\ i/d + |P|_{min} \qquad (4.29e)$$

Polynomial Function Method

Consider the following model structure and parameterize each parameter function involved into a third-order polynomial in terms of |P(t)| :

$$\begin{bmatrix} N \\ P \end{bmatrix}_{t+1} = \begin{bmatrix} \hat{a}_{11} & \hat{a}_{12} \\ \hat{a}_{21} & \hat{a}_{22} \end{bmatrix}_t \begin{bmatrix} N \\ P \end{bmatrix}_t + \begin{bmatrix} \hat{\ell}_1 \\ \hat{\ell}_2 \end{bmatrix}_t I(t-t_d) \qquad (4.30)$$

where

$$\hat{a}_{11}(t) = p_{1,1}+p_{1,2}|P(t)|+p_{1,3}\ P^2(t)+p_{1,4}|P^3(t)| \qquad (4.31a)$$

$$\hat{\ell}_1(t) = p_{1,5}+p_{1,6}|P(t)|+p_{1,7}\ P^2(t)+p_{1,8}|P^3(t)| \qquad (4.31b)$$

$$\hat{a}_{22}(t) = p_{2,1}+p_{2,2}|P(t)|+p_{2,3}\ P^2(t)+p_{2,4}|P^3(t)| \qquad (4.31c)$$

$$\hat{\ell}_2(t) = p_{2,5}+p_{2,6}|P(t)|+p_{2,7}\ P^2(t)+p_{2,8}|P^3(t)| \qquad (4.31d)$$

Proposed Method

Two model structures are considered. One includes friction but the other does not. For the latter, the proposed model structure is the same as that of Equation (4.30) with the following linguistic parameterizations :

If $|P(t)|$ is small then

$$\hat{a}_{11} = \sigma_{1,1} + \sigma_{1,2}|P(t)|$$
$$\hat{b}_1 = \sigma_{1,5} + \sigma_{1,6}|P(t)|$$
$$\hat{a}_{22} = \sigma_{2,1} + \sigma_{2,2}|P(t)|$$
$$\hat{b}_2 = \sigma_{2,5} + \sigma_{2,6}|P(t)| \qquad (4.32a)$$

If $|P(t)|$ is large then

$$\hat{a}_{11} = \sigma_{1,3} + \sigma_{1,4}|P(t)|$$
$$\hat{b}_1 = \sigma_{1,7} + \sigma_{1,8}|P(t)|$$
$$\hat{a}_{22} = \sigma_{2,3} + \sigma_{2,4}|P(t)|$$
$$\hat{b}_2 = \sigma_{2,7} + \sigma_{2,8}|P(t)| \qquad (4.32b)$$

For the former, the following model structure is considered.

$$\begin{bmatrix} N \\ P \end{bmatrix}_{t+1} = \begin{bmatrix} \hat{a}_{11} & \hat{a}_{12} \\ \hat{a}_{21} & \hat{a}_{22} \end{bmatrix}_t \begin{bmatrix} N \\ P \end{bmatrix}_t + \begin{bmatrix} \hat{b}_1 \\ \hat{b}_2 \end{bmatrix}_t I(t-t_d) - \begin{bmatrix} \hat{c}_1 \\ \hat{c}_2 \end{bmatrix}_t \mathrm{sgn}(N(t)) \qquad (4.33)$$

If $|P(t)|$ is small then

$$\hat{a}_{11} = \sigma_{1,1} + \sigma_{1,2}|P(t)|$$
$$\hat{b}_1 = \sigma_{1,5} + \sigma_{1,6}|P(t)|$$
$$\hat{c}_1 = \sigma_{1,9} + \sigma_{1,10}|P(t)|$$
$$\hat{a}_{22} = \sigma_{2,1} + \sigma_{2,2}|P(t)|$$
$$\hat{b}_2 = \sigma_{2,5} + \sigma_{2,6}|P(t)|$$
$$\hat{c}_2 = \sigma_{2,9} + \sigma_{2,10}|P(t)| \qquad (4.34a)$$

If $|P(t)|$ is large then

$$\hat{a}_{11} = \sigma_{1,3} + \sigma_{1,4}|P(t)|$$
$$\hat{b}_1 = \sigma_{1,7} + \sigma_{1,8}|P(t)|$$
$$\hat{c}_1 = \sigma_{1,11} + \sigma_{1,12}|P(t)|$$
$$\hat{a}_{22} = \sigma_{2,3} + \sigma_{2,4}|P(t)|$$
$$\hat{b}_2 = \sigma_{2,7} + \sigma_{2,8}|P(t)|$$
$$\hat{c}_2 = \sigma_{2,11} + \sigma_{2,12}|P(t)| \qquad (4.34b)$$

For both proposed model structures, the membership functions defined are shown in Figure 21. The bounds of dynamic variable space are defined $|P|_{max} = P_s$ and $|P|_{min} = 0$ and will be used in Equation (4.29e).

Preliminary Considerations

System identification in practice usually requires some preliminary work. For the example, in addition to the analysis work mentioned above, some issues such as measurement of process delay, selection of sampling time interval, and system input design deserve contemplation beforehand.

Theoretically, process delay time t_d can be measured from a system step-input response. For the system, such an approach is not feasible because system stiction and hysteresis will introduce an uncertain time delay between the system input and output and a problem of repeatability between runs. Instead, using experimental tests for

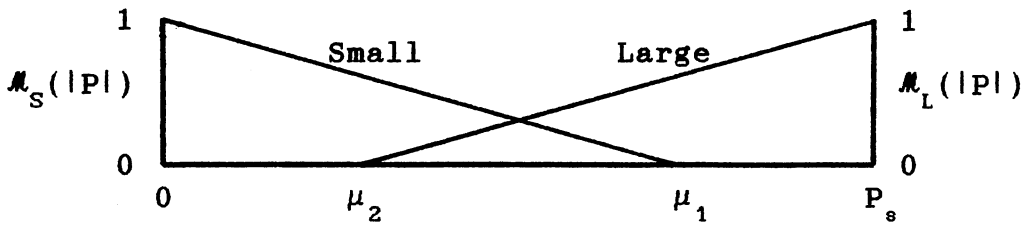

Figure 21. The Membership Functions Defined in Example 3, Chapter IV.

different possible values of t during parameter estimation process or other techniques such as correlation methods would be more feasible.

For a specific system, the value of t_d depends on sampling time interval. If sampling time interval is relatively large, the effects due to process delay can be negligible. Proper selection of sampling interval is application dependent. Nevertheless, for control applications a good rule of thumb in the selection of sampling interval is to sample between 6 to 10 data points per system natural period (i.e. inverse of system natural frequency) [20].

A Bode plot of the studied system is shown in Figure 22. From the plot of $|N(jw)/I(jw)|$, the system bandwidth is observed at approximately four Hz. Although the system bandwidth and natural frequency are pressure dependent, 20 msec sampling interval is believed adequate for system control. It was found in the above experimental tests of t_d that process delay time is negligibly small in comparison with 20 msec sampling time interval.

With the sampling interval selected, the spectral density of ∇_n-class signals can be determined. For this, some heuristic plots are shown in Figure 23. As explained in Chapter III, informative identification data may be achieved if the dominant frequency band of the input signals

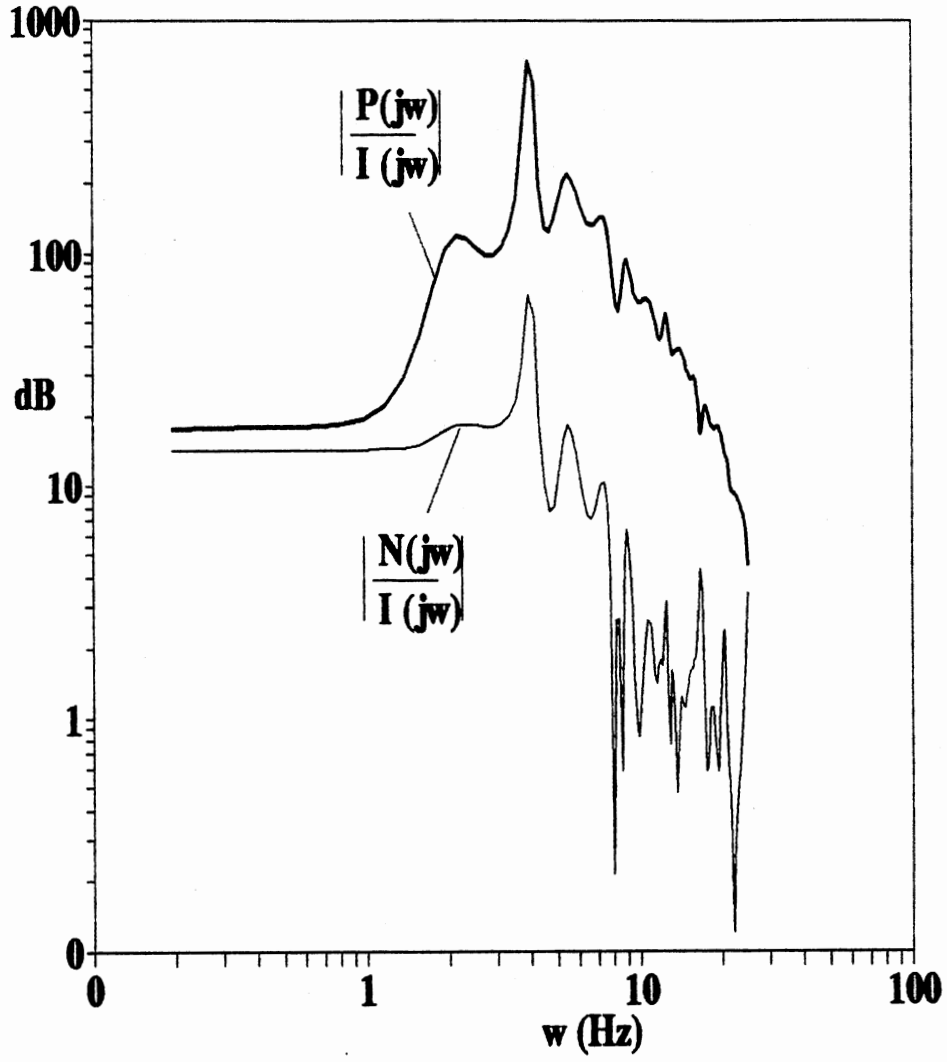

Figure 22. Bode Plot of the Hydraulic System Studied in Example 3, Chapter IV.

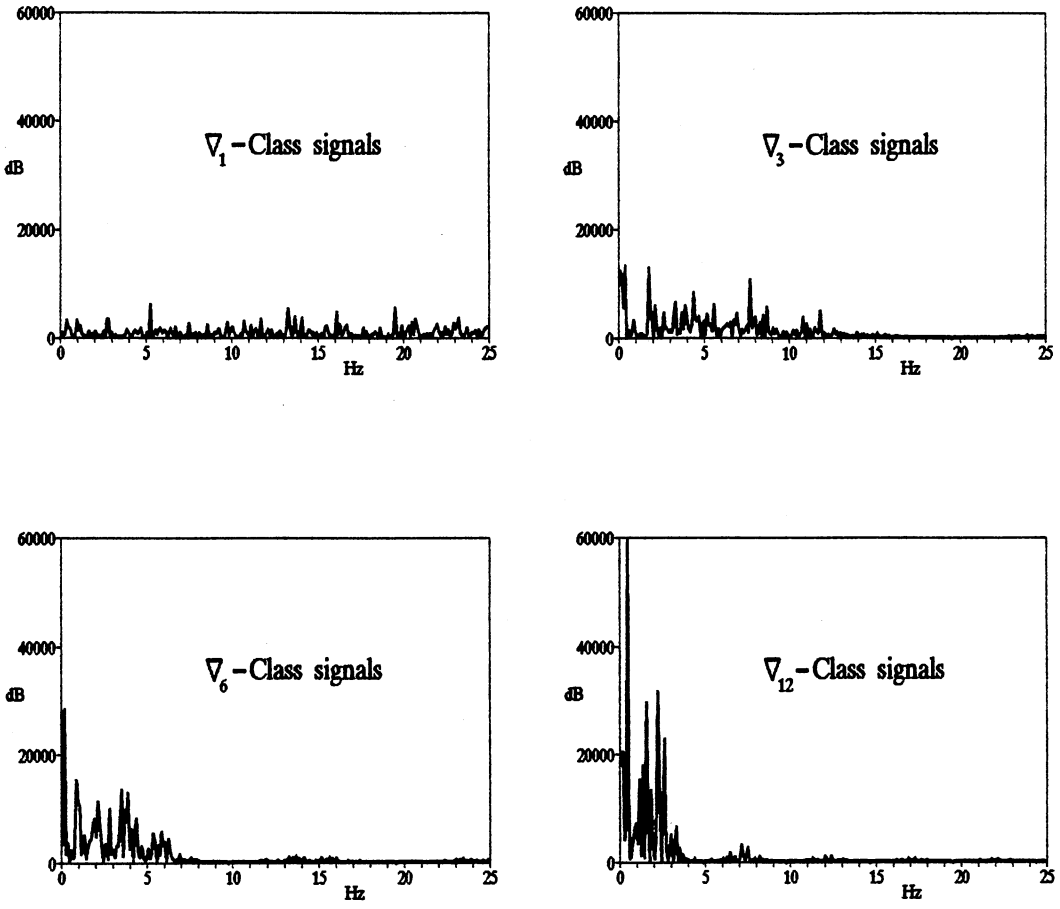

Figure 23. Power Spectral Density of Some Suggested Classes of System Input Signals (Sampling Interval = 20 msec).

coincides with the system resonant frequency. Among the classes of signals illustrated in Figure 23, ∇_{12}-class signals are the best selection as system inputs.

Indeed, the selection of input signals among ∇_n classes also can be carried out by investigating the amplitudes of $|P(t)|$ under excitations where the input signals have the same distribution range. Whenever larger amplitude of $|P(t)|$ is excited, the corresponding input signals are more likely to be persistent excitation signals.

Experimental Results

Six hundred identification data collected are plotted in Figure 24. The supply pressure P_s was set at 500 psig. Input distribution range is [0 mA, 4.5 mA] which covered the servovalve operating range.

All the data collected were used for parameter estimation purposes except that in the proposed method the first 300 data points were used for that purpose but the remaining data were used for model cross validation during the Complex Methods's optimization. The estimation results are summarized in Table VII to Table X.

For the gate function method, unacceptable EGMs were achieved as the number of quantification intervals were increased from 5 to 10 (i.e. $d = 10$ and $i \geq 6$ in Table VIII). . These EGMs have either unreasonable estimated

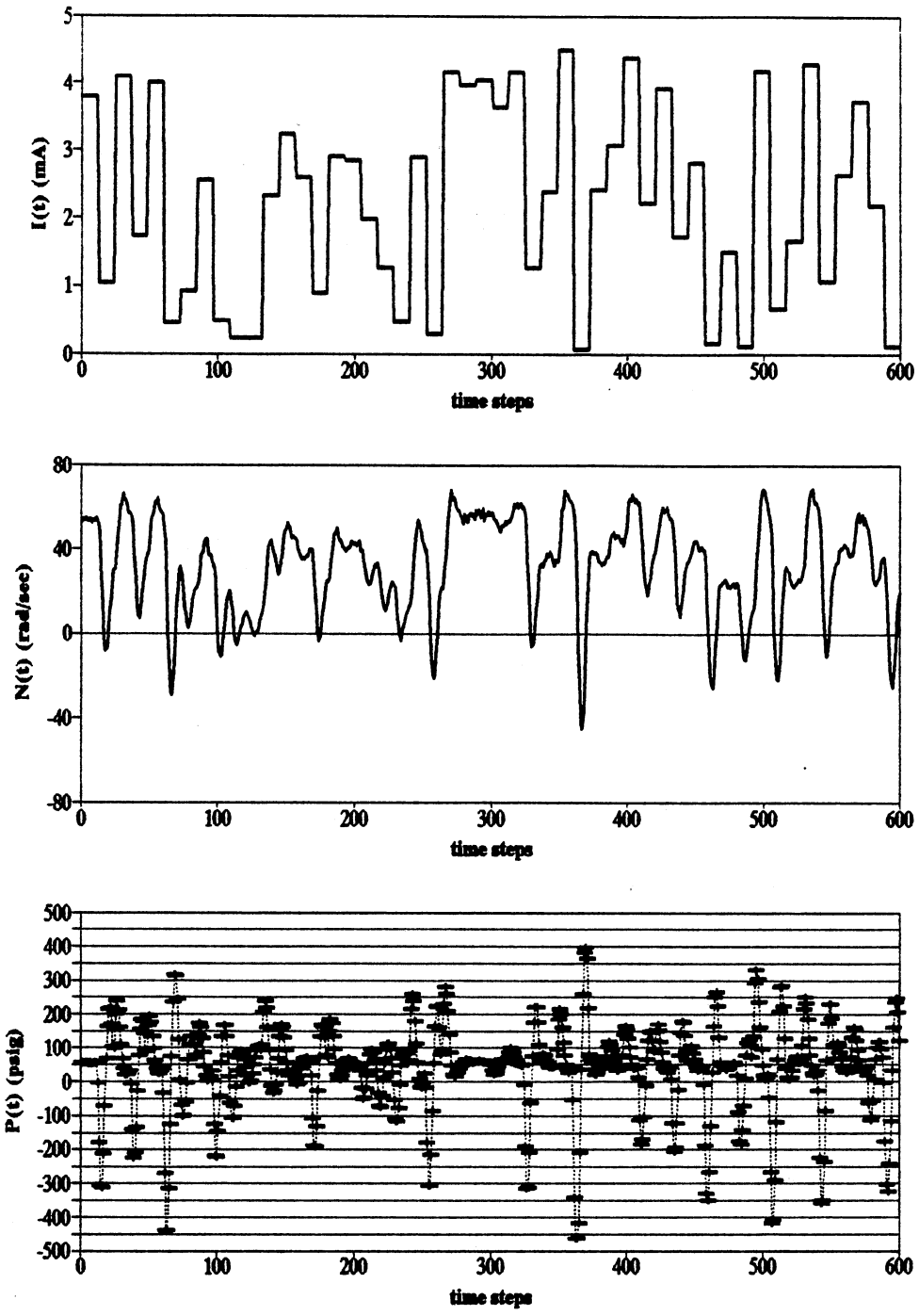

Figure 24. The Data Used for the Parameter Estimation in Example 3.

TABLE VII

A SUMMARY OF EXPERIMENTAL RESULTS OF EXAMPLE 3
(CLASSICAL LINEAR METHOD)

$\hat{a}_{11}$	$\hat{a}_{12}$	$\hat{a}_{21}$	$\hat{a}_{22}$	$\hat{b}_1$	$\hat{b}_2$
0.856	0.044	-3.627	0.802	1.237	53.135

TABLE VIII

A SUMMARY OF EXPERIMENTAL RESULTS OF EXAMPLE 3
(GATE FUNCTION METHOD)

	$\hat{a}^{[i]}_{11}$	$\hat{a}^{[i]}_{12}$	$\hat{a}^{[i]}_{21}$	$\hat{a}^{[i]}_{22}$	$\hat{b}^{[i]}_1$	$\hat{b}^{[i]}_2$
d=5						
i=1	0.910	0.033	-1.961	0.677	0.687	32.426
i=2	0.783	0.040	-4.148	0.797	2.238	58.266
i=3	0.835	0.042	-3.883	0.867	1.298	44.841
i=4	0.876	0.049	-1.105	0.946	0.415	8.628
i=5	0.823	0.054	-1.614	0.930	4.978	31.732
d=10						
i=1	0.916	0.038	-1.404	0.716	0.551	23.438
i=2	0.919	0.026	-2.446	0.719	0.748	38.420
i=3	0.699	0.036	-3.495	0.863	3.539	51.429
i=4	0.698	0.036	-2.728	0.871	3.327	36.178
i=5	0.813	0.041	-2.579	0.887	1.827	34.210
i=6	0.904	0.047	-0.649	1.012	0.083	-0.057
i=7	1.020	0.055	1.253	1.068	1.414	-22.098
i=8	0.786	0.049	-1.978	0.936	0.000	0.000
i=9	1.191	0.071	2.522	1.145	0.082	0.177
i=10	-0.001	0.014	-0.048	0.998	0.000	-0.000

TABLE IX

A SUMMARY OF EXPERIMENTAL RESULTS OF EXAMPLE 3
(POLYNOMIAL FUNCTION METHOD)

	P^0	$\|P\|$	P^2	$\|P^3\|$
$\hat{a}_{11}$	0.88502	-0.000336	-0.00000012	0.00000000
$\hat{a}_{22}$	1.14509	-0.003524	0.00001119	-0.00000001
$\hat{b}_1$	1.01462	0.001119	0.00002048	-0.00000007
$\hat{b}_2$	59.51332	-0.128545	0.00059506	-0.00000103
$\hat{a}_{12} = 0.04418$			$\hat{a}_{21} = -3.77454$	

TABLE X

A SUMMARY OF EXPERIMENTAL RESULTS OF EXAMPLE 3
(THE PROPOSED METHOD)

Without Friction		With Friction	
$\mu_1 = 342.18$		$\mu_1 = 450.16$	
$\mu_2 = 74.044$		$\mu_2 = 100.05$	
$\hat{a}_{12} = 0.045$		$\hat{a}_{12} = 0.045$	
$\hat{a}_{21} = -3.794$		$\hat{a}_{21} = -3.957$	
$\sigma_{1,1} \rightarrow \sigma_{1,8}$	$\sigma_{2,1} \rightarrow \sigma_{2,8}$	$\sigma_{1,1} \rightarrow \sigma_{1,12}$	$\sigma_{2,1} \rightarrow \sigma_{2,12}$
0.869	1.032	0.902	1.133
0.000	-0.002	0.000	-0.003
0.402	1.076	0.806	1.897
0.001	-0.001	0.000	-0.003
1.320	61.791	1.263	61.970
-0.003	-0.132	-0.001	-0.127
8.733	120.21	5.085	162.92
-0.023	-0.232	-0.013	-0.337
		1.570	-3.912
		-0.002	-0.045
		1.006	91.983
		0.000	-0.199

parameters and/or unstable poles. Such poor estimation results can be foreseen from the plot of P(t) vs. t in Figure 24. For $|P(t)| > 250$ psig, very few gated signals are useful and available for parameter estimation.

Open-Loop Step-Input Responses. All resulting models are now validated by comparing their step-input responses with those of the system for I(t) = 4 mA, 2 mA, and 0.5 mA as shown in Figures 25, 26 and 27 respectively.

In the figures, the system responses are plotted in broad solid lines. Different dynamic characteristics of the responses are achieved for the selected step inputs. Basically, the smaller is the step-input level, the less damped is the system response. Such a nonlinear phenomenon cannot be described properly by a single linear model.

As shown in Figure 26, the linear model achieved by using the classical identification method may fit into the system properly when the step input is around 2 mA. However, it is no longer adequate when the input level has large deviation from 2 mA as shown in Figures 25 and 27.

For this example, the improvement of model accuracy by using gate function method is very minor. EGMs built based on gated signals (i.e. part of identification data) would be more sensitive to measurement noise than a classical linear model built based on the whole identification data. This is

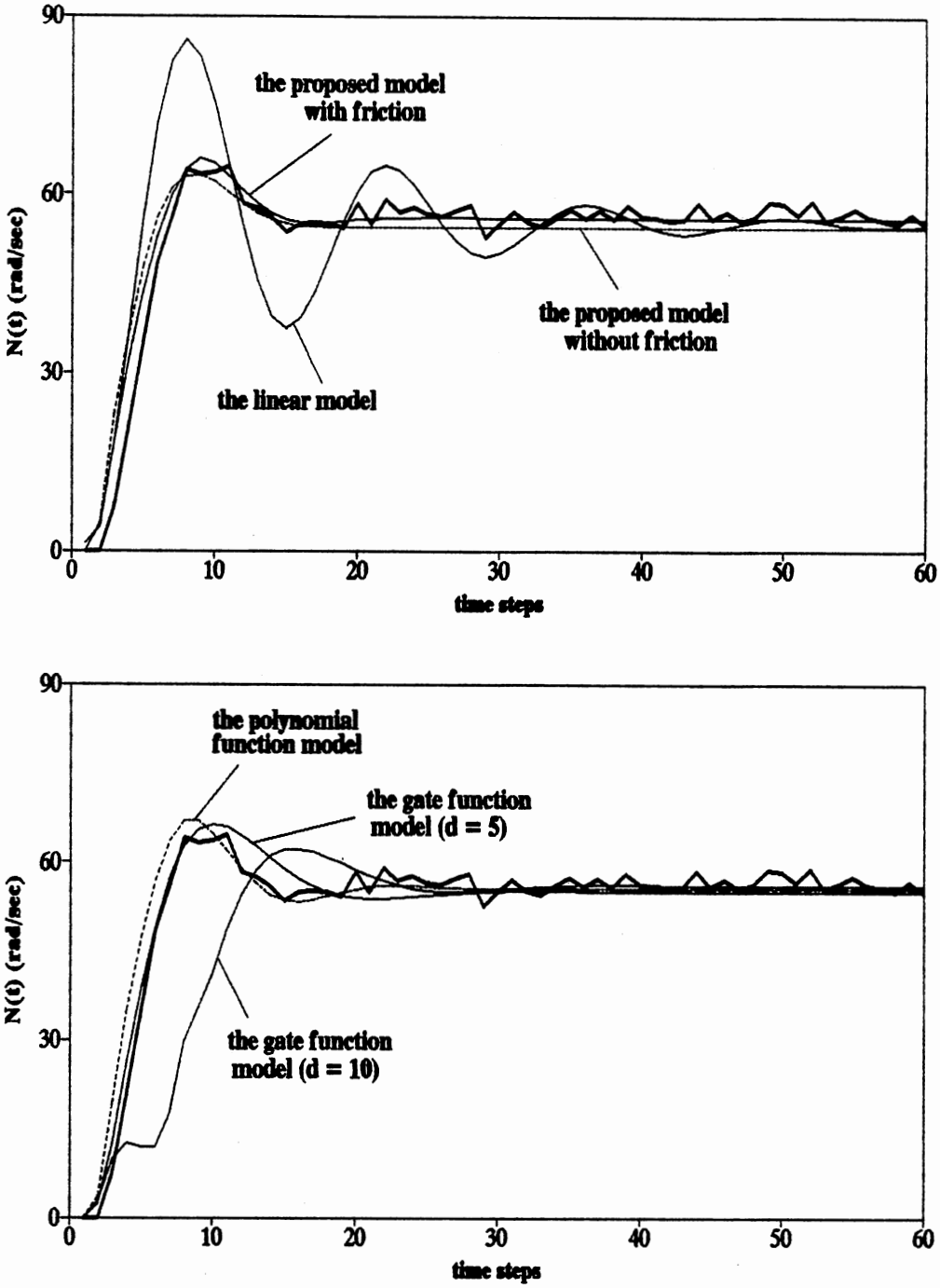

Figure 25. Measured and Simulation Step-Input Responses, I(t) = 4 mA.

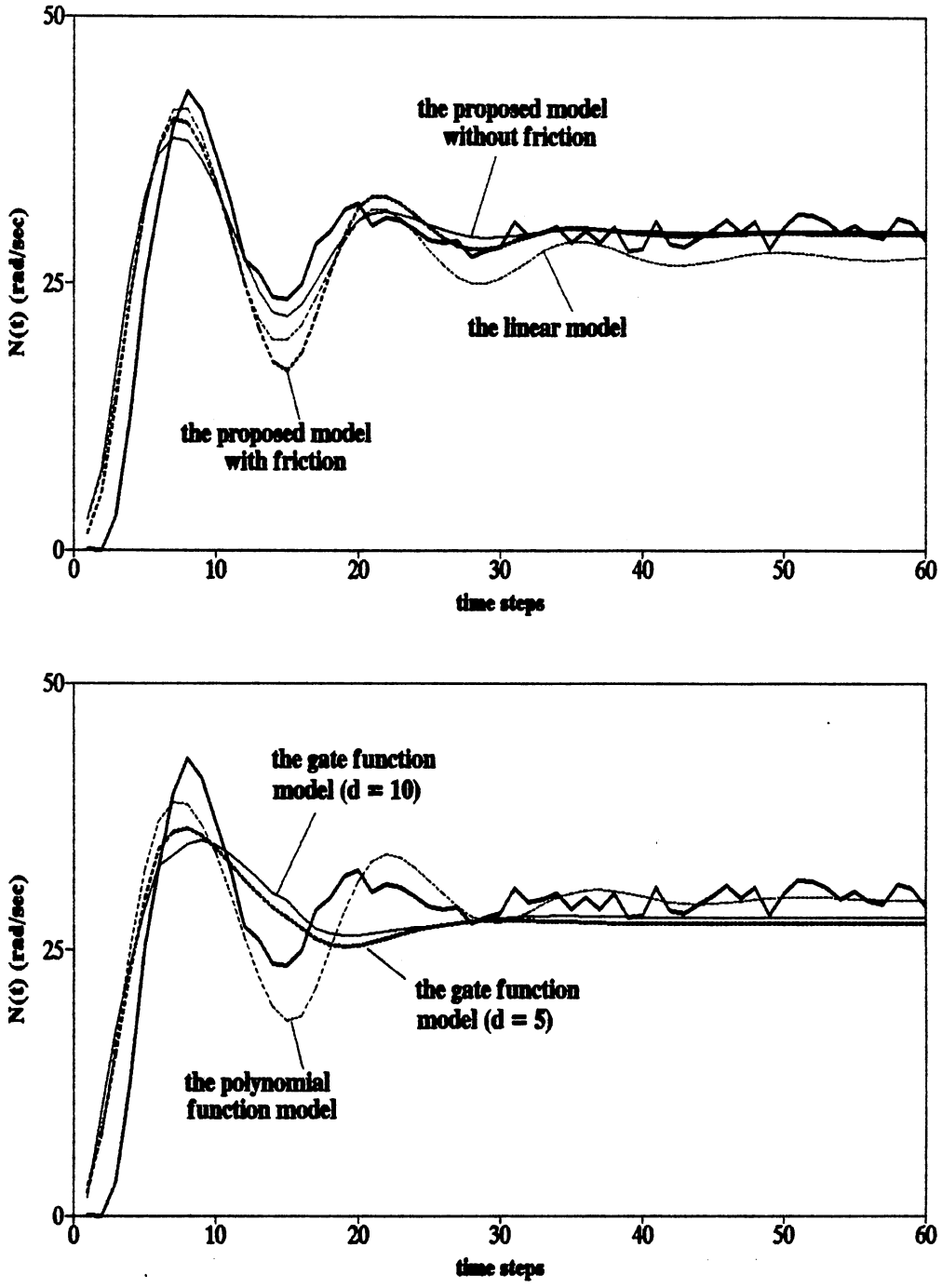

Figure 26. Measured and Simulation Step-Input Responses, I(t) = 2 mA.

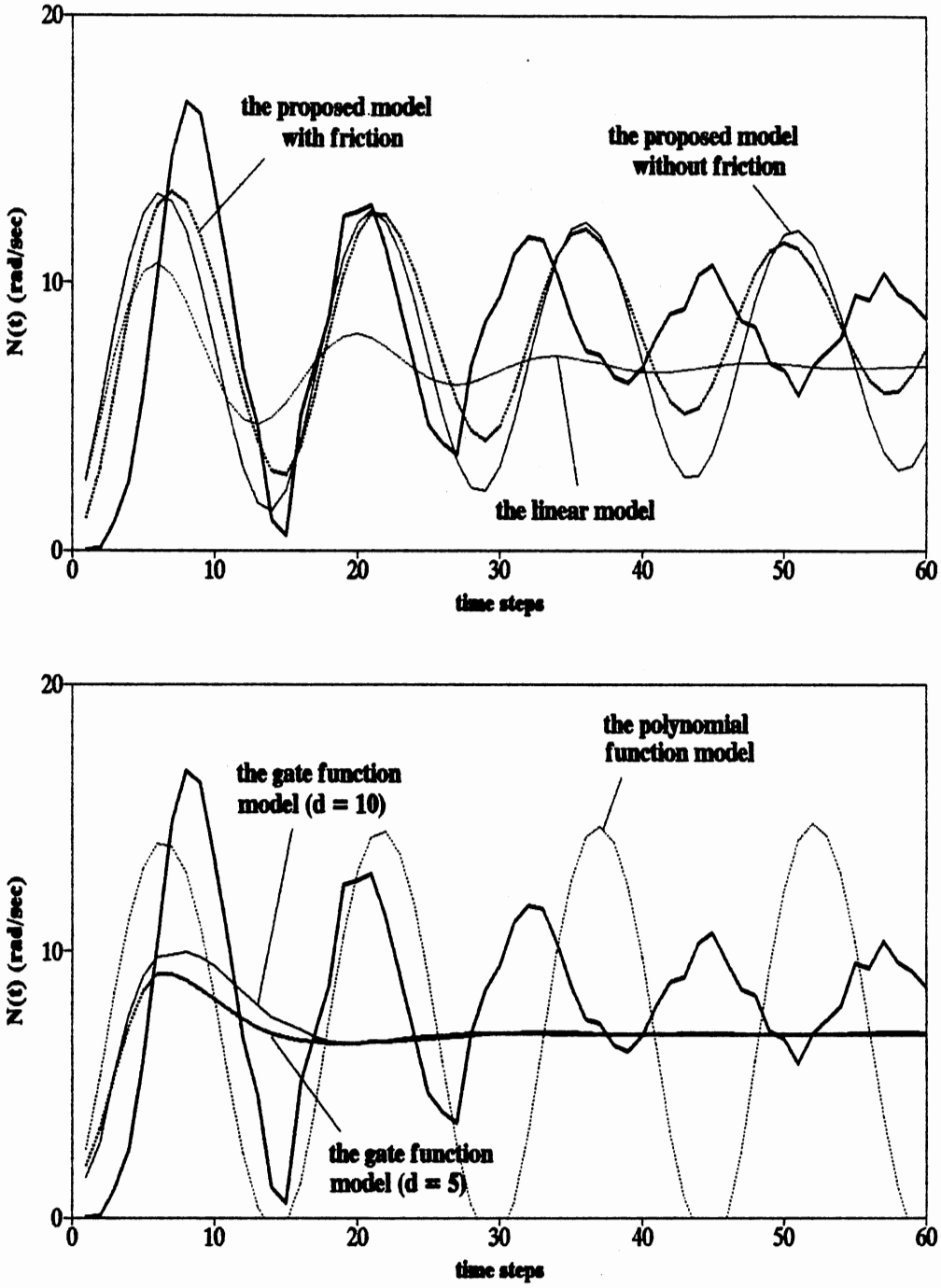

Figure 27. Measured and Simulation Step-Input Responses, I(t) = 0.5 mA.

especially true for those EGMs built based on gated signals having low |P(t)| due to the high noise-to-signal ratios. This is believed to be the main reason why the gate function method are poor in prediction of the system response for I(t) = 0.5 mA.

On the other hand, the improvement of model accuracy by using the proposed method or polynomial function method is obvious. The system nonlinear phenomenon are well predicted. Among all achieved models, the one with friction using the proposed method (called the proposed model with friction) provides the best prediction of system step-input responses. Note that in Figure 27 the phase shift between the system response and that of the proposed model with friction is primarily due to stiction.

Closed-Loop Velocity Controls. As mentioned in Chapter I, one advantage of the modeling concept using signal-dependent parameters is the ease of applying linear control theory to design nonlinear system controllers. The goal here is to improve the robustness of classical linear controllers to system signal-dependent dynamics by re-designing the controllers based on models with signal-dependent parameters. The proposed model with friction is validated against this goal.

For illustration, a linear controller called SV&UO

feedback controller (Appendix C) is used as an example.

SV&UO feedback controller with signal-dependent gains :

$$I(t) = -\underline{g}^T(t)\ \underline{x}(t) \tag{4.35a}$$

where

$$\underline{g}(t) = [g_1(t),\ g_2(t),\ g_3(t)]^T \tag{4.35b}$$

$$\underline{x}(t) = [N(t),\ P(t),\ E(t)]^T \tag{4.35c}$$

and

$$E(t+1) = E(t) + N_d(t) - N(t) \tag{4.36}$$

Substituting Equations (4.35) into Equation (4.33) with $t_d = 0$ and then with Equation (4.36),

$$\underline{x}(t+1) = \mathcal{A}(t)\ \underline{x}(t) + \underline{b}\ N_d(t) - \underline{c}(t)\ \mathrm{sgn}(N(t)) \tag{4.37a}$$

where

$$\mathcal{A} = \begin{bmatrix} \hat{a}_{11}-\hat{b}_1 g_1 & \hat{a}_{12}-\hat{b}_1 g_2 & -\hat{b}_1 g_3 \\ \hat{a}_{21}-\hat{b}_2 g_1 & \hat{a}_{22}-\hat{b}_2 g_2 & -\hat{b}_2 g_3 \\ -1 & 0 & 1 \end{bmatrix} \tag{4.37b}$$

$$\underline{b} = [0,\ 0,\ 1]^T \tag{4.37c}$$

$$\underline{c} = [\hat{c}_1,\ \hat{c}_2,\ 0]^T \tag{4.37d}$$

Let the desired closed-loop poles be the roots of Equation (C.4). After manipulation,

$$\underline{g}^T(t) = \frac{1}{\delta(t)}\ \underline{r}^T(t)\ S(t) \tag{4.38}$$

where

$$\underline{r}(t) = [\nu_1(t),\ \nu_2(t),\ \nu_3(t)]^T \tag{4.39a}$$

$$S(t) = \begin{bmatrix} \sigma_{11}(t) & \sigma_{12}(t) & s_{13} \\ \sigma_{21}(t) & \sigma_{22}(t) & \sigma_{23}(t) \\ \sigma_{31}(t) & \sigma_{32}(t) & s_{33} \end{bmatrix} \tag{4.39b}$$

$$\nu_1 = -\hat{\ell}_1\hat{\ell}_2 \tag{4.39c}$$

$$\nu_2 = \hat{\ell}_1^2 \tag{4.39d}$$

$$\nu_3 = \hat{\ell}_1(\hat{a}_{21}\hat{\ell}_1 + \hat{a}_{22}\hat{\ell}_2) - \hat{\ell}_2(\hat{a}_{11}\hat{\ell}_1 + \hat{a}_{12}\hat{\ell}_2) \tag{4.39e}$$

$$\sigma_{11} = \hat{a}_{11}^3 + \xi_1\hat{a}_{11}^2 + (2\,\hat{a}_{12}\hat{a}_{21} + \xi_2)\,\hat{a}_{11} + \hat{a}_{12}\hat{a}_{21}(\hat{a}_{22} + \xi_1) + \xi_3 \tag{4.39f}$$

$$\sigma_{12} = (\hat{a}_{11}^2 + \hat{a}_{11}\hat{a}_{22} + \hat{a}_{22}^2 + \xi_1(\hat{a}_{11} + \hat{a}_{22}) + \hat{a}_{12}\hat{a}_{21} + \xi_2)\,\hat{a}_{12} \tag{4.39g}$$

$$s_{13} = 0 \tag{4.39h}$$

$$\sigma_{21} = \sigma_{12}\hat{a}_{21} / \hat{a}_{12} \tag{4.39i}$$

$$\sigma_{22} = \hat{a}_{22}^3 + \xi_1\hat{a}_{22}^2 + (2\,\hat{a}_{12}\hat{a}_{21} + \xi_2)\,\hat{a}_{22} + \hat{a}_{12}\hat{a}_{21}(\hat{a}_{11} + \xi_1) + \xi_3 \tag{4.39j}$$

$$\sigma_{31} = -\hat{a}_{11}^2 - (1 + \xi_1)\,\hat{a}_{11} - (\hat{a}_{12}\hat{a}_{21} + 1 + \xi_1 + \xi_2) \tag{4.39k}$$

$$\sigma_{32} = -(\hat{a}_{11} + \hat{a}_{22} + 1 + \xi_1)\,\hat{a}_{12} \tag{4.39l}$$

$$s_{33} = 1 + \xi_1 + \xi_2 + \xi_3 \tag{4.39m}$$

$$\delta = (\hat{a}_{12}\hat{\ell}_2 + \hat{\ell}_1)(\hat{a}_{12}\hat{\ell}_2^2 - \hat{a}_{21}\hat{\ell}_1^2) + \hat{\ell}_1\hat{\ell}_2\hat{a}_{11}(\hat{a}_{12}\hat{\ell}_2 + \hat{\ell}_1) - \hat{\ell}_1\hat{a}_{22}(2\,\hat{a}_{12}\hat{\ell}_2^2 + \hat{\ell}_1\hat{\ell}_2 - \hat{a}_{21}\hat{\ell}_1^2) +$$

$$\hat{b}_1^2\hat{b}_2\hat{a}_{22}(\hat{a}_{22} - \hat{a}_{11}) \qquad (4.39n)$$

and ξs are the coefficients of Equation (C.4).

The control gains gs are pressure dependent. They must be updated at each sampling time instance. Equation (4.38) becomes Equation (C.5) if the signal-dependent parameters in Equation (4.33) are replaced by their corresponding ones in Equation (4.28).

The measurement of system load pressure is required in the above updating of control gains. But, the signals can be estimated using the Luenberger observer :

$$\begin{aligned}\hat{P}(t+1) = {} & \hat{a}_{22}\hat{P}(t) + \hat{a}_{21}N(t) + \hat{b}_2 I(t) - \hat{c}_2 \mathrm{sgn}(N(t)) + \\ & g_o(t)\{N(t+1) - \hat{a}_{11}N(t) - \hat{b}_1 I(t) + \\ & \hat{c}_1 \mathrm{sgn}(N(t)) - \hat{a}_{12}\hat{P}(t)\}\end{aligned} \qquad (4.40)$$

where g_o denotes the observer gain and $(\hat{a}_{22} - g_o\hat{a}_{12})$ the observer pole.

Measured angular velocity N(t) is filtered through a triple exponential digital filter (i.e. three first-order digital filters in cascade). The filtered signal is denoted by $N_f(t)$. Without further considering the filter dynamics, N(t) is replaced by $N_f(t)$ in the above controller and calculations of E(t+1) and $\hat{P}(t+1)$. A block diagram of the velocity control system is given in Figure 28.

Two cases of tracking controls which cover a range of

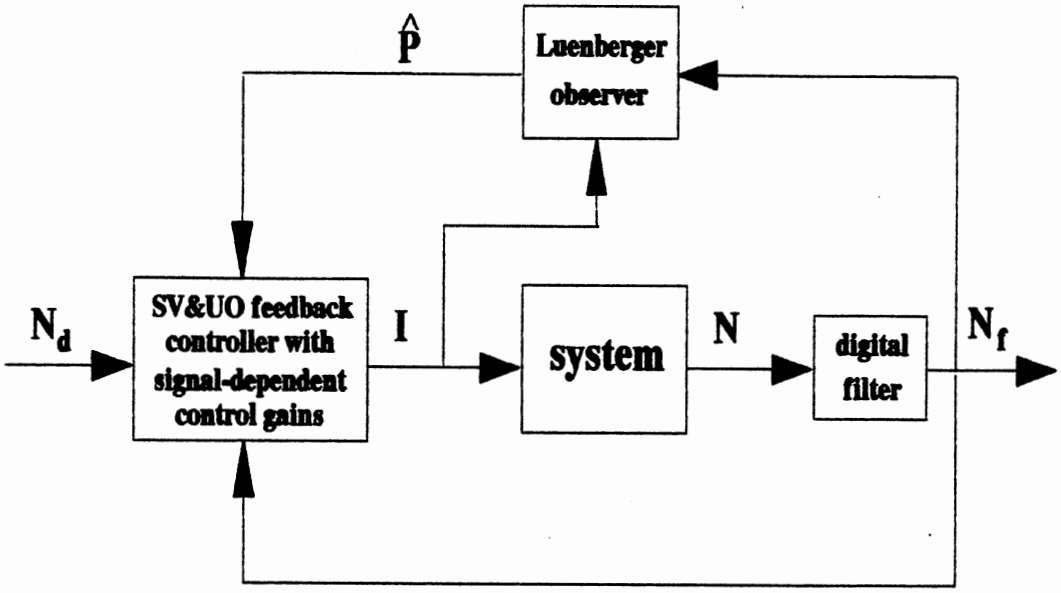

Figure 28. A Block Diagram of Velocity Control System.

working conditions were carried out experimentally. The experiments were simulated by assuming either the proposed model with friction or the classical linear model to be the system. For each case, the results are shown in Figures 29 and 30 respectively where closed-loop poles were assigned at $0.6 \pm 0.1j$ and 0.6, an observer pole assigned at 0.85, and a filter cut-off frequency of 10 Hz.

For medium-speed controls, both controllers with proper system and observer pole assignments work equally well as shown in Figure 29. Because of good matching between the models and the system as shown in Figure 26, the simulation and measured responses also reasonably match.

As the working condition changes, without re-assigning pole locations, the linear controller is no longer adequate and the measured response is shown in Figure 30(a). The compensation of system signal-dependent dynamics by using a controller with signal-dependent gains seems more feasible. As shown in Figure 30(b), the tracking accuracy has been significantly improved.

The simulation response generated by using the linear model is too idealized to predict what will happen practically, whereas the prediction by using the proposed model with friction is more reasonable. Note that the initial delay of the measured response in Figure 30(b) is due to system stiction.

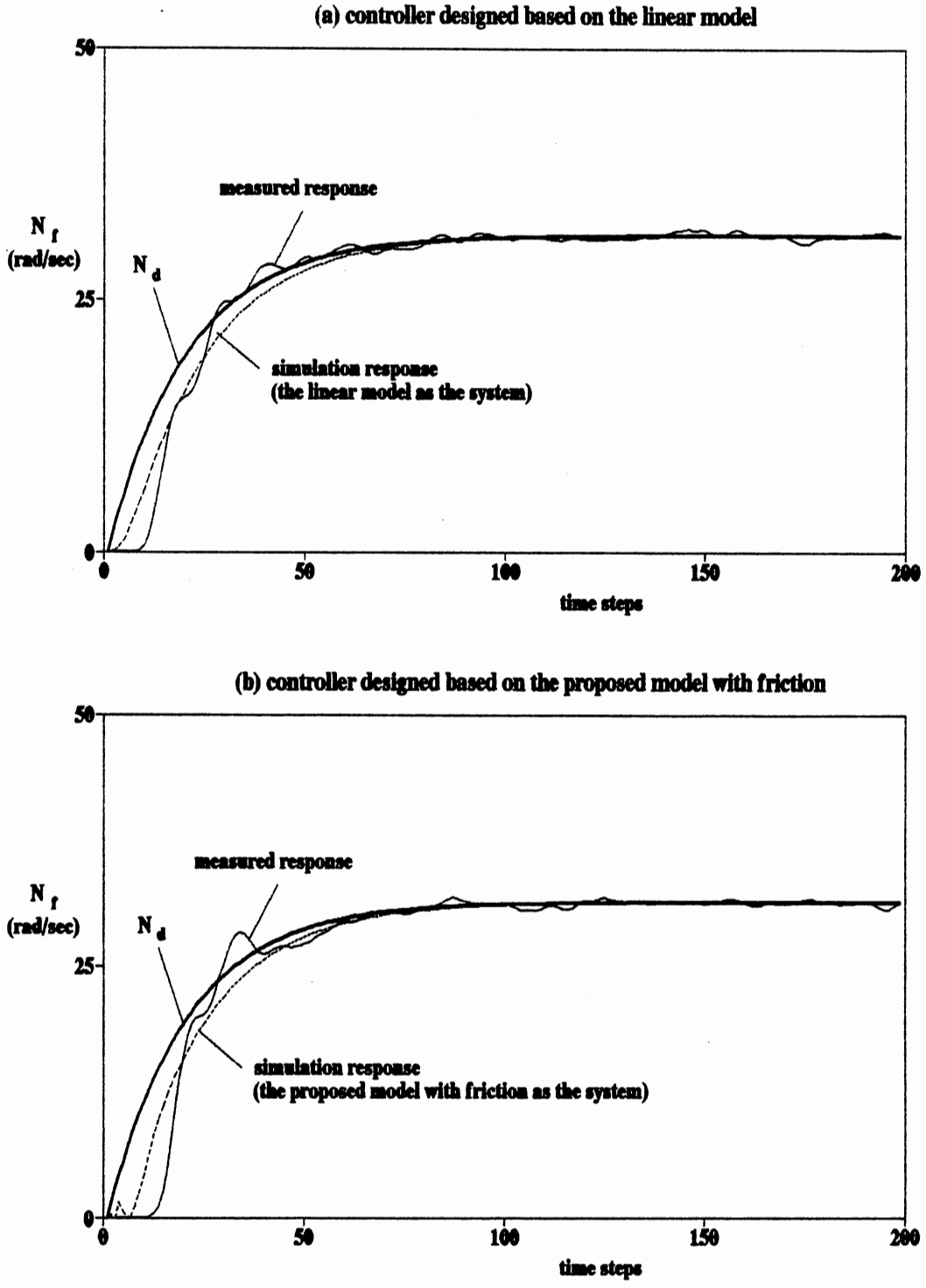

Figure 29. Measured and Simulation Responses of SV&UO Control with Luenberger Observer, Case 1.

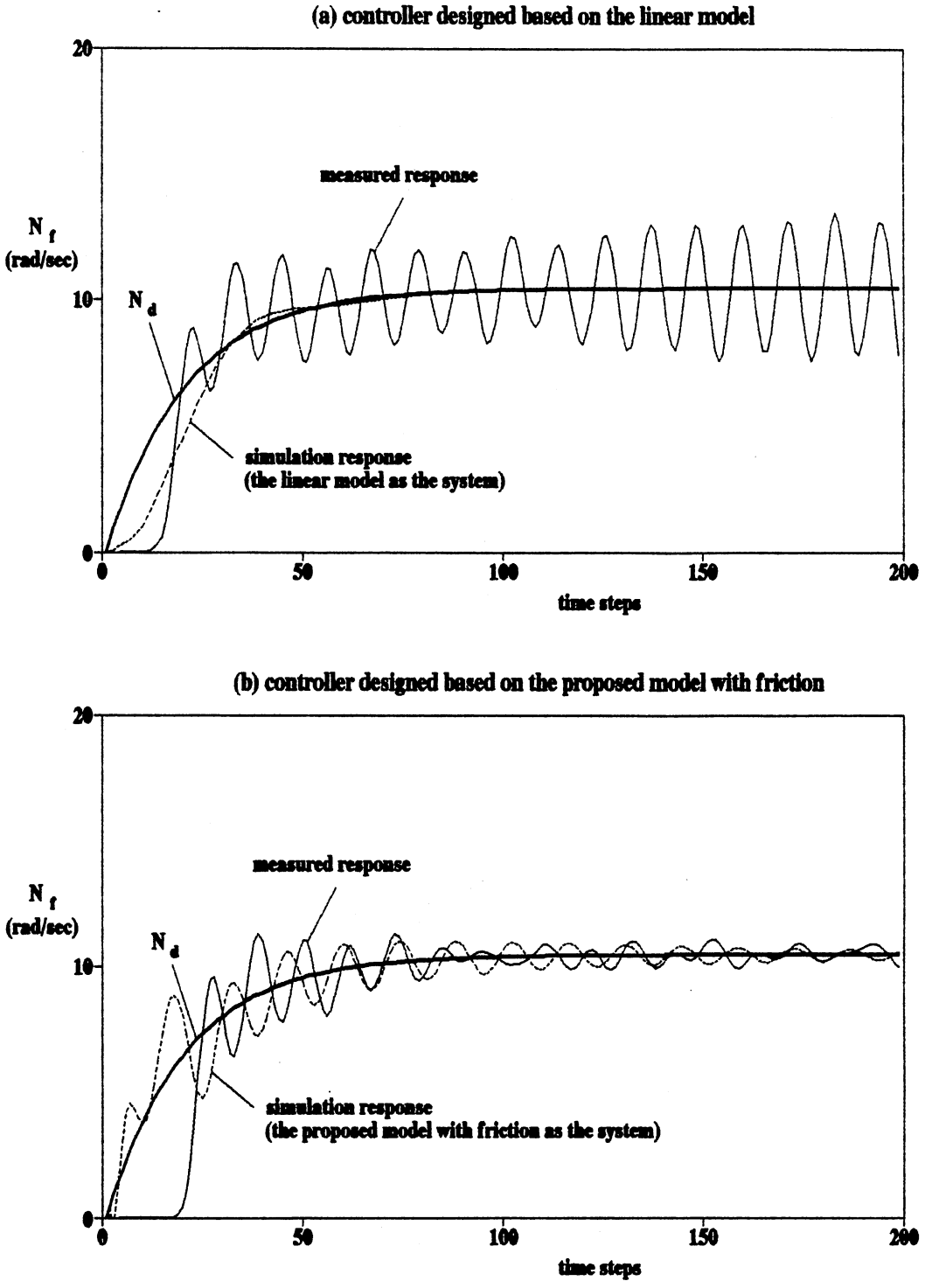

Figure 30. Measured and Simulation Responses of SV&UO Control with Luenberger Observer, Case 2.

Example 4 - Ph Process

Consider the Ph process shown in Figure 31 [50]. The notations and assumptions are introduced below. The fluid volume V of the tank is constant. The quantities Q_i, Q_r, and Q_e denote the volumetric flow rates of the influent, the chemical reagent, and the effluent. Assume that mixing in the stirred tank is perfect so that the fluid phases are homogeneous. The concentrations of H^+ and OH^- ions are denoted by C_k^+ and C_k^- where the subscript k identifies the fluid phase in question according to Figure 31. No change of specific volume of fluid occurs in the process, i.e.

$$Q_e = Q_i + Q_r \tag{4.41}$$

It is also assumed that all of the relevant acids and bases are completely dissociated in each fluid phase, and H^+ and OH^- ions react only according to the following equation :

$$H_2O \Leftrightarrow H^+ + OH^- \tag{4.42}$$

The mass balance of the ionic components of the process gives [50]

$$V \dot{C}_e^+ = - Q_e C_e^+ + Q_i C_i^+ + Q_r C_r^+ + R \tag{4.43a}$$

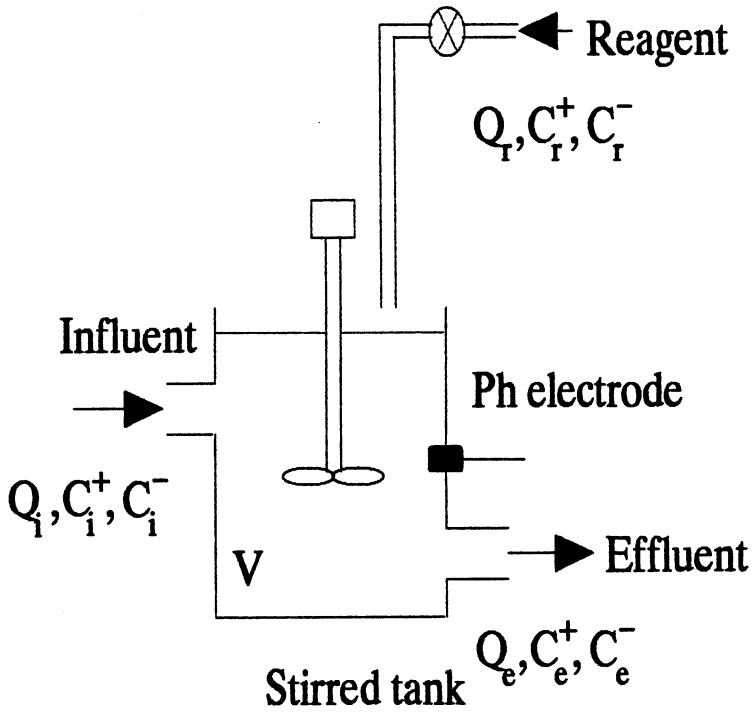

Figure 31. Schematic of a Ph Process.

$$V \dot{C}_e^- = - Q_e C_e^- + Q_i C_i^- + Q_r C_r^- + R \qquad (4.43b)$$

where R denotes the net reaction rate.

For a dilute solution, the equilibrium condition can be described by

$$C_e^+ C_e^- = K_w \qquad (4.44a)$$

and

$$K_w = 10^{-14} \text{ , for water at } 25^\circ C \qquad (4.44b)$$

Introduce $x = C_e^+ - C_e^-$. Then,

$$x = C_e^+ - K_w / C_e^+ \qquad (4.45)$$

or

$$C_e^+ = 0.5 \, (x + \sqrt{x^2 + 4 K_w}) \qquad (4.46)$$

Subtracting Equation (4.43b) from Equation (4.43a), one has

$$\dot{x} = -(q_i + q_r) x + q_r(C_r^+ - C_r^-) + q_i(C_i^+ - C_i^-) \qquad (4.47)$$

where $q_k = Q_k/V$.

Because the reagent is concentrated, its flow rate is always much smaller than that of the influent. So, Equation (4.47) is simplified to be

$$\dot{x} = -q_i x + q_r(C_r^+ - C_r^-) + q_i(C_i^+ - C_i^-) \qquad (4.48)$$

In the measurement of fluid acidity, a standard method is based on the measurement of voltage produced by a Ph electrode where the voltage is linearly dependent on the Ph value of the fluid. For convenience, the measured output denoted by y is given in units of Ph. Therefore,

$$\begin{aligned} y &= -\log_{10} C_e^+ \\ &= -\log_{10}[0.5(x + \sqrt{x^2 + 4\ K_w})] \\ &= g(x) \end{aligned} \tag{4.49}$$

Equation (4.48) provides a linear model for capturing the main features of the Ph process, whereas Equation (4.49) is the so-called titration curve. A plot of g(x) vs. x is shown in Figure 32 where $K_w = 10^{-14}$. From the figure, it is not surprising that it is difficult to neutralize the mixing fluid [36, 63].

In this example, C_i^+, C_i^-, C_r^+, C_r^-, and q_i in Equation (4.48) are assumed unknown. The titration curve g(x) in Equation (4.49) is assumed uncertain because K_w could change under different environmental temperature.

Taking the z transform of the system equations with the sampling time interval, h, results in

$$x(t+1) = a\ x(t) + b\ u(t) + c \tag{4.50a}$$

$$y(t) = g(x(t)) \tag{4.50b}$$

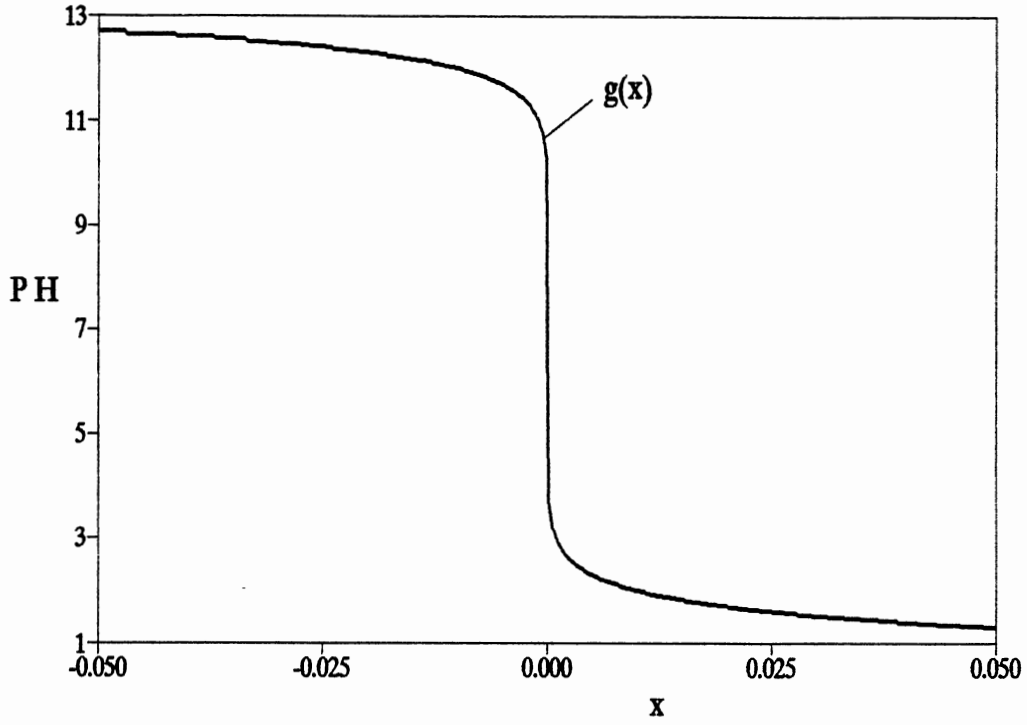

Figure 32. Titration Curve for $K_w = 10^{-14}$.

where

$$u = q_r \tag{4.50c}$$

$$a = e^{-q_i h} \tag{4.50d}$$

$$b = (1 - e^{-q_i h})(C_r^+ - C_r^-)/q_i \tag{4.50e}$$

$$c = (1 - e^{-q_i h})(C_i^+ - C_i^-) \tag{4.50f}$$

Obviously, the Ph process belongs to the class of Wiener systems, and Equations (4.50) can be arranged into the followings with signal-dependent parameters :

$$y(t) = \alpha(y(t),y(t-1))\ y(t-1) + \beta(y(t))\ u(t-1) + c(y(t)) \tag{4.51a}$$

where

$$\alpha(y(t),y(t-1)) = a\ g^*(y(t-1))/g^*(y(t)) \tag{4.51b}$$

$$\beta(y(t)) = b/g^*(y(t)) \tag{4.51c}$$

$$c(y(t)) = c/g^*(y(t)) \tag{4.51d}$$

$$g^*(y(t)) = g^{-1}(y(t))/y(t) \tag{4.51e}$$

Due to the relationship between the signal-dependent parameters, the identification of the process requires only the estimation of $\beta(y(t))$, a, and $c_b = c/b$.

Parameter values to be used for simulations are given in Table XI. For K_w given in Equation (4.44b), a plot of $\beta(y)$ vs. y is shown in Figure 33. From the figure, $\beta(y)$ is

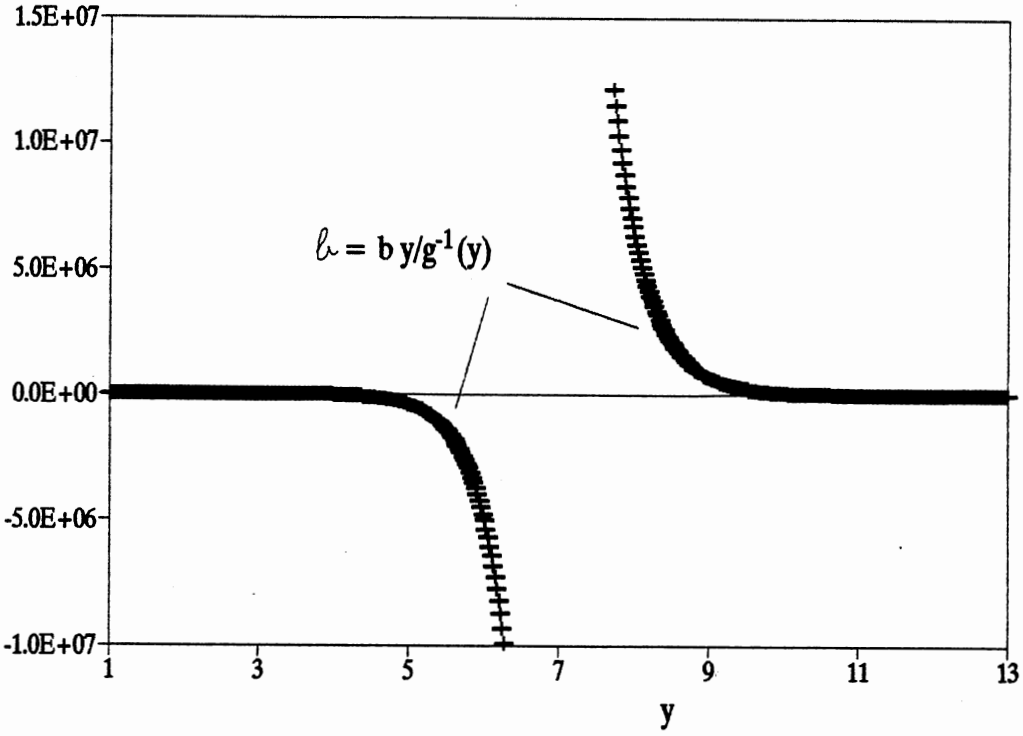

Figure 33. A System Parameter Function, Example 4.

singular at the neutral point (i.e. y = 7) around which the variation of $\mathcal{G}(y)$ is extremely large.

Obviously, from the conclusions in the previous examples, the gate function method is not suitable for the identification of systems with parameters varying abruptly. It is not adequate to parameterize $\mathcal{G}(y)$ into a polynomial because of the discontinuity of $\mathcal{G}(y)$. However, the parameterization problem can be overcome by using fuzzy linguistic rules such as Equations (4.17).

Proposed Method

Consider the following model structure :

$$y(t+1) = \hat{\mathcal{G}}(t+1)\ \{\ \hat{a}\ (y(t)-\mu_3)/\hat{\mathcal{G}}(t) + u(t) + \hat{c}_b\} + \mu_3 \qquad (4.52a)$$

If y(t) is small then

$$\hat{\mathcal{G}}(t) = \sigma_1 + \sigma_2(y(t)-\mu_3) \qquad (4.52b)$$

If y(t) is medium-1 then

$$\hat{\mathcal{G}}(t) = \sigma_3 + \sigma_4(y(t)-\mu_3) \qquad (4.52c)$$

If y(t) is medium-2 then

$$\hat{\mathcal{G}}(t) = \sigma_5 + \sigma_6(y(t)-\mu_3) \qquad (4.52d)$$

If y(t) is large then

$$\hat{\mathcal{G}}(t) = \sigma_7 + \sigma_8(y(t)-\mu_3) \qquad (4.52e)$$

where the membership functions are shown in Figure 8 and the

weighting functions are given in Equation (4.18b) through Equation (4.18j) with x_1 replaced by y.

Note that the position of the neutral point is assumed not available and it is to be estimated and determined by the value of μ_3. It was found beneficial to estimation accuracy if the scale of output variable y(t) is shifted by μ_3 as shown in Equations (4.52) which are rewritten in the following pseudo-linear regression :

$$y(t+1) = \underline{\phi}^T(t+1)\,\underline{\theta} + \mu_3 \qquad (4.53a)$$

where

$$\begin{aligned}\underline{\phi}^T(t+1) = [&\hat{\ell}(t+1)(y(t)-\mu_3)/\hat{\ell}(t),\ \pi_S(t+1)u(t),\\ &\pi_S(t+1)u(t)(y(t+1)-\mu_3),\ \pi_{M1}(t+1)u(t),\\ &\pi_{M1}(t+1)u(t)(y(t+1)-\mu_3),\ \pi_{M2}(t+1)u(t),\\ &\pi_{M2}(t+1)u(t)(y(t+1)-\mu_3),\ \pi_L(t+1)u(t),\\ &\pi_L(t+1)u(t)(y(t+1)-\mu_3),\ \hat{\ell}(t+1)]\end{aligned} \qquad (4.53b)$$

$$\underline{\theta}^T = [\hat{a},\ \sigma_1,\ \sigma_2,\ \sigma_3,\ \sigma_4,\ \sigma_5,\ \sigma_6,\ \sigma_7,\ \sigma_8,\ \hat{c}_b] \qquad (4.53c)$$

Simulation Results

∇_{20}-class input signals distributed over [-0.005, 0.005] were used. Three hundred input/output data collected are plotted in Figure 34. Simulation results are summarized in Table XII.

Since the high sensitivity of the Ph electrode to the

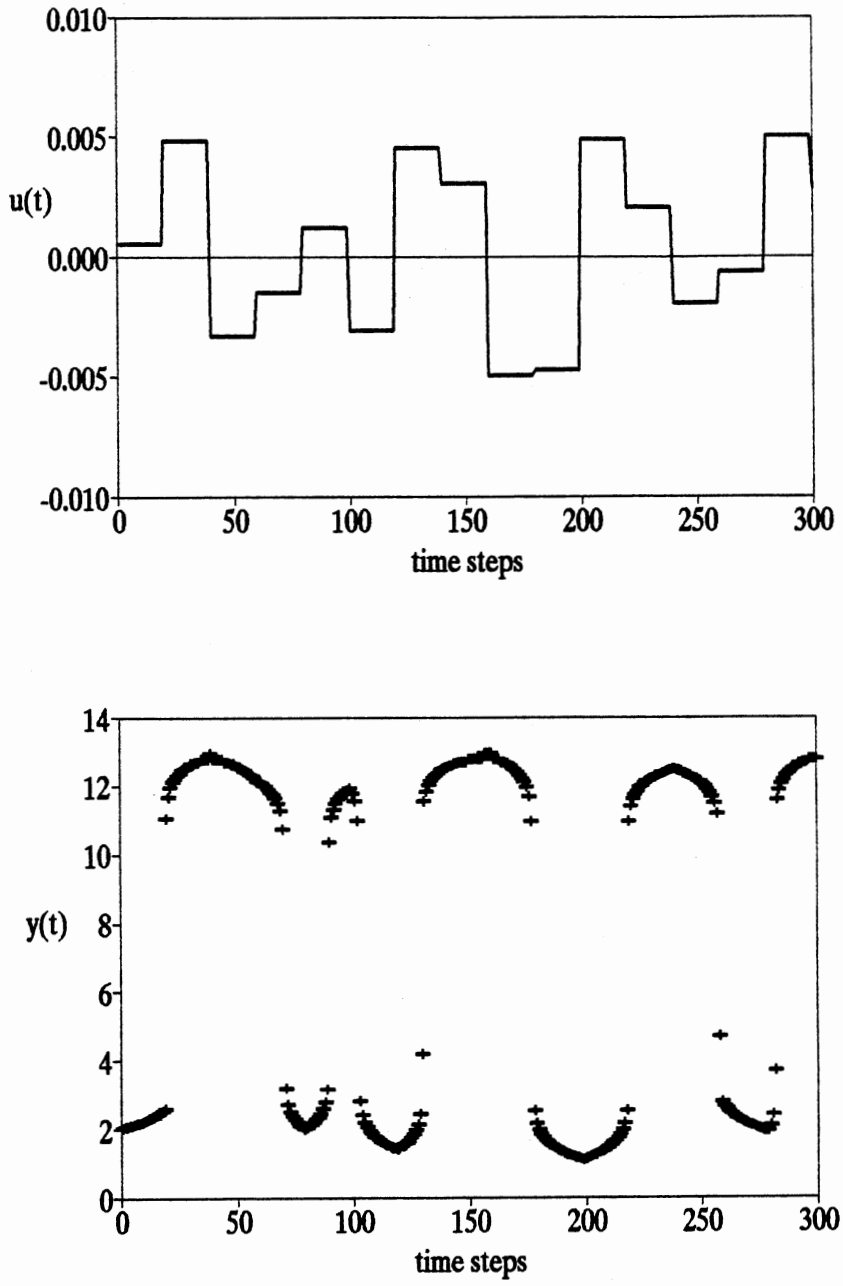

Figure 34. The Data Used for the Parameter Estimation in Example 4, Chapter IV, Where g(x) Is Given in Equation (4.49).

TABLE XI

PARAMETER VALUES FOR SIMULATIONS IN EXAMPLE 4

$h = 0.04$	$q_i = 0.1$
$C_r^+ - C_r^- = -20.0$	$C_i^+ - C_i^- = 0.01$
$a = 0.9960$	$c_b = -0.00005$

TABLE XII

A SUMMARY OF SIMULATION RESULTS OF EXAMPLE 4 FOR g(x) GIVEN IN EQUATION (4.49)

$\mu_1 \rightarrow \mu_5$	$\sigma_1 \rightarrow \sigma_4$	$\sigma_1 \rightarrow \sigma_4$
6.93428	3045.97	0.01000
3.63581	475.917	-0.01000
7.26513	6088.60	2072.34
10.0563	700.942	-359.776
9.43702		
	$\hat{a} = 0.9767$	$\hat{c}_b = -0.00061$

concentration of H^+ when the process output is around the neutral point, it is very difficult to acquire informative data about the system neutralization dynamics. As shown in Figure 34, the identification data collected do not have system dynamic information for $4 \leq y(t) \leq 10$.

The comparison between $g(x)$ and its estimate is shown in Figure 35. Basically, $\hat{g}(x)$ provides a reasonable shape about the titration curve. The curve of $\hat{g}(x)$ looks as if it were discontinuous. In fact, the value of x calculated based on the estimate of $\mathcal{G}(y)$ is out of the range shown in the figure. This means the estimate of $\mathcal{G}(y)$ is unacceptable at the dynamic interval where the discontinuous curve happens. This is due to the identification data collected not being informative.

It is concluded that the difficulty to identify a Ph process is primarily due to the high nonlinearity of the titration curve such that informative identification data cannot be easily achieved.

Since K_w depends on temperature, so does the titration curve $g(x)$. If it is possible to control environmental temperature and reduce the measurement sensitivity of the Ph electrode, good identification data are more likely to be achieved.

For example, consider the following titration curve :

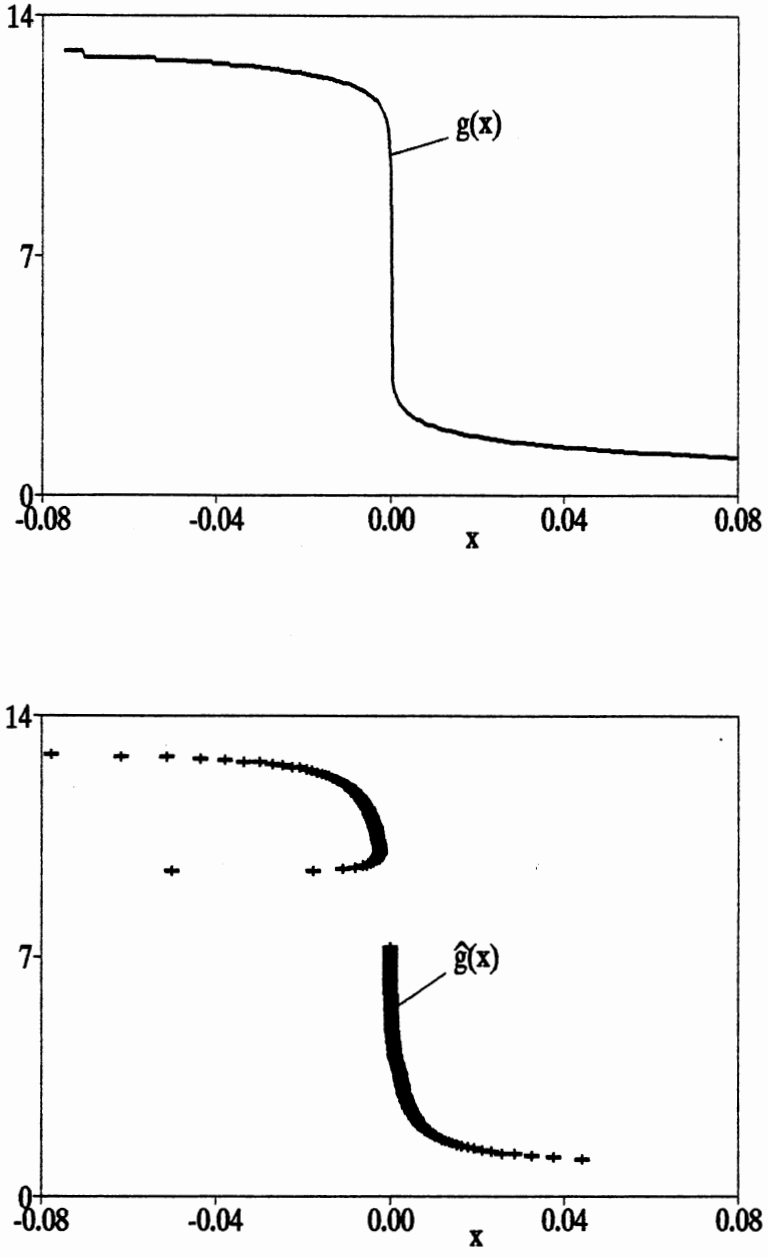

Figure 35. Comparison Between g(x) and Its Estimate in Example 4, Chapter IV, Where g(x) Is Given in Equation (4.49).

$$g(x) = 7.0 - 15.0 \, \mathrm{sgn}(x) \, |x|^{0.4} \qquad (4.54)$$

For the same input signals used above, the corresponding system outputs along with the input signals are shown in Figure 36. Compared with those in Figure 34, more data about system neutralization dynamics have been achieved.

Simulation results are summarized in Table XIII. The comparison between g(x) here and its estimate is shown in Figure 37, and good estimation of g(x) is available globally.

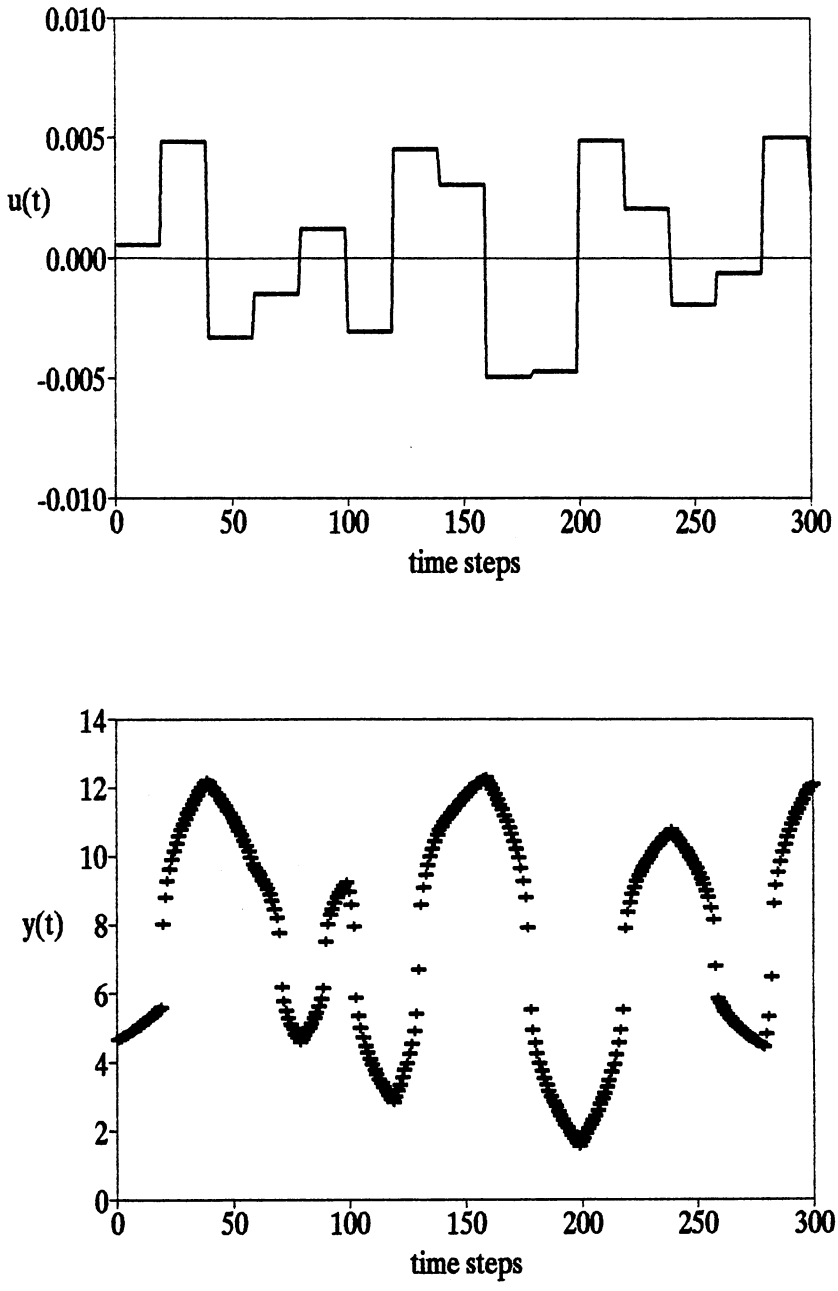

Figure 36. The Data Used for the Parameter Estimation in Example 4, Chapter IV, Where g(x) Is Given in Equation (4.54).

TABLE XIII

A SUMMARY OF SIMULATION RESULTS OF EXAMPLE 4
FOR g(x) GIVEN IN EQUATION (4.54)

$\mu_1 \rightarrow \mu_5$	$\sigma_1 \rightarrow \sigma_4$	$\sigma_1 \rightarrow \sigma_4$
6.55361	241.903	223.376
4.77047	35.7716	6.09751
6.76957	159.468	223.813
10.0425	-289.833	-30.5499
8.86962		
	$\hat{a} = 0.9661$	$\hat{c}_b = 0.000048$

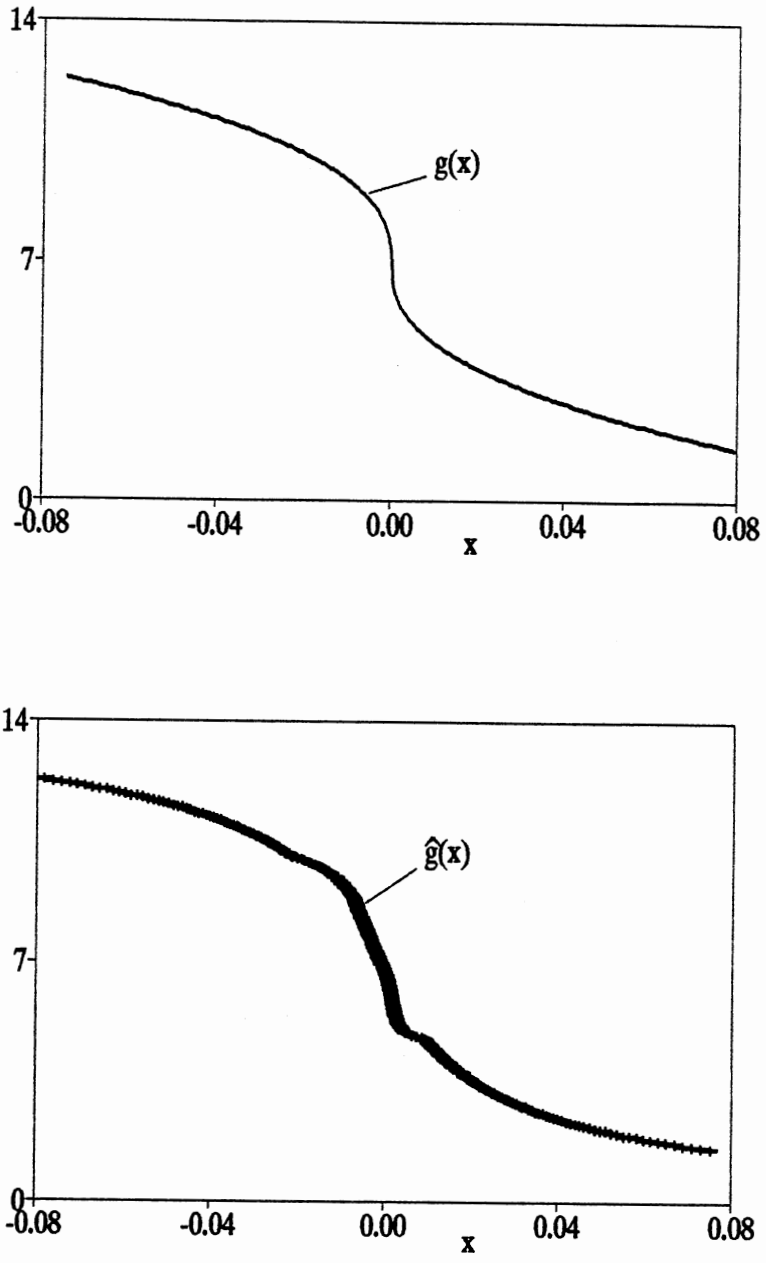

Figure 37. Comparison Between g(x) and Its Estimate in Example 4, Chapter IV, Where g(x) Is Given in Equation (4.54).

CHAPTER V

SUMMARY AND CONCLUSIONS

A new, systematic, and feasible method for the identification of "linear" systems with signal-dependent parameters is introduced in this thesis. The method involves parameterization of system parameter functions using fuzzy linguistic description. Such a parameterization approach results in model structures in pseudolinear regressions where the parameters were estimated cyclically and iteratively between the Complex Method and the recursive least-squares estimator.

In Chapter II, some physical systems which have signal-dependent parameters were mentioned. Each system can be precisely modeled in a "linear" structure but the parameters involved depend on some signal (Equations (2.1) and (2.2)). It was also mentioned that the modeling concept using signal-dependent parameters is useful in the interpretation of system nonlinear dynamics based on the well-defined linear terminology and the concept is more general than that of block-oriented modeling.

Although the dependence of system parameters on the dynamic variable could be derived, the resulting equations are usually too complicated to be useful for parameter

estimation. A practical approach is to assume the uncertainty of the signal dependence and parameterize the system parameters in the sense of a curve-fitting approximation.

Three approaches were considered to approximate system parameters in terms of piecewise constant functions, polynomial functions, and fuzzy linguistic rules, respectively. The advantage of using the first two approaches is the linear regression properties of their resulting model structures. The third was proposed as a more general approach. But, the resulting model structure is not a linear regression.

As shown in Equations (2.19) or (2.20), the proposed model structure is a combination of a "linear" model structure and linguistic description of system parameters. The determination of the "linear" model structure (i.e. the values of n and m in Equations (2.19d) and (2.19e)) is a traditional problem, whereas the determination of the linguistic rules requires proper selection of membership functions and shape functions. Such selection could be flexible. However, the use of linear membership functions (Figure 2(a)) along with polynomial shape functions (Equations (2.12) and (2.14)) are adequate for many applications.

The global identifiability of the input/output model

structure $\mathbb{R}_1$ with linear membership functions or quadratic membership functions is assured according to Theorem 2.1 and Theorem 2.2, and proofs of the theorems are given in Appendix A. It also can be shown that the global identifiability of the state-space model structure $\mathbb{R}_2$ is assured.

At the end of Chapter II, an extension of the above signal-dependent modeling concept to systems with more than one dynamic variable was mentioned briefly. But, more work is needed to investigate the identifiability of the resulting model structures.

In Chapter III, the estimation of model parameters was considered. The idea of the gate function method is to fit a nonlinear system using piecewise linear models each of which governs a local operating region. Each local model was synthesized based on a different set of gated signals which were extracted from the collected identification data through a quantification process. However, there is lack of a systematic quantification approach to guarantee the success of parameter estimation for each local model. In fact, the number of local models cannot be arbitrarily increased. Such a limitation is due to the lack of informative gated signals and/or the effect of measurement noise.

As shown in Equations (3.6), the model structure as a result of polynomial parameterization of system parameters

is linear regression in that the recursive least-squares estimator is available for the parameter estimation. Nonetheless, the polynomial function method is not feasible for systems with singular or piecewise continuous parameter functions (Examples 2 and 4, Chapter IV).

The approximation of system parameters in terms of linguistic rules showed promising flexibility to fit diverse shapes of system parameter functions. Nonetheless, the resulting model structure is a pseudolinear regression. Effort is required to develop a new parameter estimation method. The method which is cyclically iterative between the Complex Method and the recursive least-squares estimator was introduced and it showed good robustness for a range of systems.

A new point of view on the design of system inputs to achieve informative identification data was presented based on the signal-dependent modeling concept. A conclusion is that a necessary condition to achieve good identification data requires the system dynamic variable have uniform distribution over its working range. Based on this, the solution of input design is obvious for systems with input dynamic variable. For systems with non-input dynamic variable, ∇_n-class signals formed by a proper time rescaling of uniformly distributed random signals were suggested. However, such a solution is just suboptimal.

In Chapter IV, comparison studies of the identification methods discussed in Chapter III were conducted based on three simulation examples and one experimental example. A summary of the results, which show the feasibility of each method for the systems considered and the computer time required (roughly estimated), is given in Table XIV.

The gate function method was found feasible for the simplified stall/post-stall aircraft system. The resulting model gave a reasonable prediction of the system longitudinal limit cycle (d = 10, Figure 18 and Figure 19). But, the method is not recommended for the identification of other systems. The polynomial function method is only adequate for the Hammerstein system with saturating gain and may be used to identify the hydraulic system.

The superiority of the proposed identification method is obvious. The reason is the use of linguistic description of system parameter functions. Nonetheless, the proposed method takes much computer time due to the slow convergent rate of the Complex Method and the computer time required increases significantly when the number of μ parameters is increased.

Contributions of Most Significance

The concept of modeling nonlinear systems using signal-dependent parameters was not well known or widely

TABLE XIV

THE FEASIBILITY OF THE IDENTIFICATION METHODS CONSIDERED AND THE COMPUTER TIME REQUIRED FOR A RANGE OF NONLINEAR SYSTEMS

Y : Feasible N : Infeasible T : Time Unit (Computer Time)	Gate Function Method	Polynomial Function Method	Proposed Method
Hammerstein System with Saturating Gain	N	Y T	Y 5xT
Simplified Nonlinear Stall/Post-Stall Aircraft System	Y? T	N	Y 100xT
Hydraulic Servo-valve/Motor System	N	Y? T	Y 20xT
PH Process	N	N	Y?

accepted. Some advantages of such a modeling concept were not revealed. One of the contributions of this study is determining the relationship between the signal-dependent interpretation of system parameters and the design of persistent excitation signals which is important in nonlinear system identification.

Another contribution is the introduction of a new and systematic identification method which has been shown feasible and robust for a range of nonlinear systems. This thesis also conducts a comparison study to show the advantages and disadvantages of the new method versus other methods based on some simulation examples and one experimental example.

One extra contribution goes to the field of system control. Based on a "linear" model with signal-dependent parameters, the design of a system controller with signal-dependent gains was demonstrated using a linear control methodology (Appendix C). Such a controller is able to compensate the system signal-dependent dynamics which was confirmed by experiment (Example 3, Chapter IV).

Suggestions for Further Study

Following are suggestions for further study :

1. Research for improving the convergent rate of the Complex Method or find another optimization method as an

alternative.

2. Extend the comparison study conducted in this thesis to including other identification methods such as neural networks [48].
3. Consider system stochastic dynamics into models, and examine the feasibility to extend the proposed identification method to systems with dominant stochastic dynamics.
4. Extend the proposed identification method to systems with more than one dynamic variable or multiple-valued nonlinearities (e.g. stiction).

A SELECTED BIBLIOGRAPHY

[1] Ahmed, M. S. (1986), "Parameter Estimation in Bilinear Systems by Instrumental Variable Method", Int. J. Control, Vol. 44, No. 4, pp. 1177-1183.

[2] Åström, K. J. and Wittenmark, B. (1984), Computer Controlled Systems - Theory and Design, Prentice-Hall, Inc..

[3] Åström, K. J. and Wittenmark, B. (1989), Adaptive Control, Addison-Wesley Publishing Company, Inc..

[4] Billings, S. A. (1980), "Identification of Nonlinear Systems - A Survey", IEE Proc., Vol. 127, Pt. D, No. 6, pp. 272-285.

[5] Billings, S. A. and Fakhouri, S. Y. (1982), "Identification of Systems Containing Linear Dynamic and Static Nonlinear Elements", Automatica, Vol. 18, No.1, pp. 15-26.

[6] Billings, S. A. and Voon, W. S. F. (1983), "Structure Detection and Model Validity Tests in the Identification of Nonlinear Systems", IEE Proceedings, Vol. 130, Pt. D, No. 4, pp.193-199.

[7] Billings, S. A. and Voon, W. S. F. (1984), "Least Square Parameter Estimation Algorithms for Nonlinear Systems", Int. J. Systems Sci., Vol. 15, No. 6, pp. 601-615.

[8] Billings, S. A. and Voon, W. S. F. (1986), "Correlation Based Model Validity Tests for Non-Linear Models", Int. J. Control, Vol. 44, No. 1, pp. 235-244.

[9] Billings, S. A. and Chen, S. (1989), "Extended Model Set, Global Data and Threshold Model Identification of Severely Non-Linear Systems", Int. J. Control, Vol. 50, No. 5, pp. 1897-1923.

[10] Billings, S. A., Chen, S. and Korenberg, M. J. (1989), "Identification of MIMO Nonlinear Systems Using a Forward-Regression Orthogonal Estimator", Int. J. Control, Vol. 49, No. 6, pp. 2157-2189.

[11] Box, G. E. P. and Jenkin, G. M. (1976), Time Series Analysis, Holden Day, Inc..

[12] Box, M. J. (1965), "A New Method of Constrained Optimization and a Comparison with Other Methods", Computer J., 8, pp. 42-52.

[13] Chang, F. H. I. and Luus, R. (1971) "A Noniterative Method for Identification Using the Hammerstein Model", IEEE Trans. Automat. Contr., Vol. AC-16, pp. 464-468.

[14] Chen, S. and Billings, S. A. (1989), "Recursive Prediction Error Parameter Estimator for Nonlinear Models", Int. J. Control, Vol. 49, No. 2, pp. 569-594.

[15] Chen, S. and Billings, S. A. (1989), "Representations of Non-Linear Systems : the NARMAX model", Int. J. Control, Vol. 49, No. 3, pp. 1013-1032.

[16] Christensen, G. K., Conrad, F., Hansen, N. E. and Trostmann, E. (1986), "Design of Hydraulic Servos with Observer and Unity Output Feedback", 7th International Fluid Power Symposium, 16-18, September, pp. 199-209.

[17] Corlis, R. G. and Luus, R. (1969), "Use of Residuals in the Identification and Control of Two-Input, Single Output Systems", Ind. Eng. Chem. Fundamentals, Vol.8, pp. 246-253.

[18] Falkner, A. H. (1988), "Iterative Technique in the Identification of a Nonlinear System", Int. J. Control, Vol. 48, No. 1, pp. 385-396.

[19] Fnaiech, F and Ljung, L. (1987), "Recursive Identification of Bilinear Systems", Int. J. Control, Vol. 45, No. 2, pp. 453-470.

[20] Frankin, G. F. and Powell, J. D. (1980), Digital Control of Dynamic Systems, Addison-Wesley Publishing Company, Inc..

[21] Gabr, M. M. (1986), "A Recursive (On-Line) Identification of Bilinear Systems", Int. J. Control, Vol. 44, No. 4, pp. 911-917.

[22] Gallman, P. G. (1976), "A Comparison of Two Hammerstein Model Identification Algorithms", IEEE Trans. Automat. Contr., Vol. AC-21, pp. 124-126.

[23] Godfrey, K. R. and Moore, D. J. (1974), "Identification of Processes Having Direction-Dependent Responses, with Gas-Turbine Engine Application", Automatica, Vol. 10, pp. 469-481.

[24] Goodwin, G. C. and Payne, R. L. (1977), Dynamic System Identification, Experiment Design and Data Analysis, New York : Academic Press.

[25] Goodwin, G. C. and Sin, K. S. (1984), Adaptive Filtering, Prediction and Control, Prentice-Hall, Inc., Englewood Cliffs, N. J..

[26] Greblicki, W. and Pawlak, M. (1986), "Identification of Discrete Hammerstein Systems Using Kernel Regression Estimates", IEEE Trans. Automat. Contr., Vol. AC-31, No. 1, pp. 74-77.

[27] Greblicki, W. and Pawlak, M. (1987), "Hammerstein System Identification by Non-Parametric Regression Estimation", Int. J. Control, Vol. 45, No. 1, pp. 343-354.

[28] Greblicki, W. (1989), "Non-Parametric Orthogonal Series Identification of Hammerstein Systems", Int. J. System Sci., Vol. 20, No. 12, pp. 2255-2367.

[29] Haber, R. (1979), "Identification of Nonlinear Systems Having Signal-Dependent Parameters", Report, Center for Control Sciences, University of Minnesota.

[30] Haber, R., Vajk, I. and Keviczky, L. (1982), "Nonlinear System Identification by 'Linear' Systems Having Signal-Dependent Parameters", 6th IFAC Symposium on Identification and System Parameter Estimation, Washington, D.C., pp. 421-426.

[31] Haber, R. and Keviczky, L. (1985), "Identification of 'Linear' Systems Having Signal-Dependent Parameters", Int. J. Systems Sci., Vol. 16, No. 7, pp. 869-884.

[32] Haber, R., Keviczky, L. and Unbehauen, H. (1987), "Application of Adaptive Control on Nonlinear Dynamic Process - A Survey on Input-Output Approaches", IFAC Proceeding Series, 1988, Number 8, Vol. III, pp. 1-14.

[33] Haist, N. D., Chang, F. H. I. and Luus, R. (1973), "Nonlinear Identification in the Presence of Correlated Noise Using a Hammerstein Model", IEEE Trans. Automat. Contr., Vol. AC-18, pp. 552-555.

[34] Hsia, T. C. and Bailey, A. L. (1968), "Learning Model Approach for Nonlinear System Identification", IEEE Systems Science and Cybernetics Conf. Rec., pp. 228-232.

[35] Hwang, C. and Shyu, K. K. (1988), "Series Expansion Approach to the Analysis and Identification of Discrete Hammerstein Systems", Int. J. Control, Vol. 47, No. 6, pp. 1961-1972.

[36] Jacobs, O. L. R., Hewkin, P. F. and White, C. (1980), "Online Computer Control of PH in an Industrial Process", IEE Proc., Vol. 127, Pt. D, No. 4, pp. 161-168.

[37] Jiang, Z. H. (1988), "Block Pulse Function Approach for the Identification of Hammerstein Model Non-Linear Systems", Int. J. System Sci., Vol. 19, No. 12, pp. 2427-2439.

[38] Korenberg, M., Billings, S. A., Liu, Y. P. and McILROY, P. J. (1988), "Orthogonal Parameter Estimation Algorithm for Non-Linear Stochastic Systems", Int. J. Control, Vol. 48, No. 1, pp. 193-210.

[39] Krzyzak, A. (1988), "On Identification of Discrete Hammerstein Systems by the Fourier Series Regression Estimate", American Control Conference, Vol. 2, pp. 1321-1324.

[40] Leontaritis, I. J. and Billings, S. A. (1987), "Model Selection and Validation Methods for Nonlinear Systems", Int. J. Control, Vol. 45, No. 1, pp. 311-341.

[41] Leontaritis, I. J. and Billings, S. A. (1988), "Prediction Error Estimator for Non-Linear Stochastic Systems", Int. J. Systems Sci., Vol. 19, No. 4, pp. 519-536.

[42] Lin, K.C. (1990), 'A Concept for Nonlinear System Modeling and Identification', Ph.D. Proposal, MAE Department, Oklahoma State University.

[43] Ljung, L. and Söderström, T (1983), Theory and Practice of Recursive Identification, Cambridge, MA : M.I.T. Press.

[44] Ljung, L. (1987), System Identification : Theory for the User, Prentice-Hall, Inc.

[45] Merrit, H. E. (1967), Hydraulic Control Systems, John Wiley & Sons, Inc..

[46] Moore, J. B. (1982), "Global Convergence of Output Error Recursions in Colored Noise", IEEE Transactions on Automatic Control, Vol. AC-27, No. 6, pp. 1189-1199.

[47] Narendra, K. S. and Gallman, P. G. (1966), "An Iterative Method for Identification of Nonlinear Systems Using a Hammerstein Model", IEEE Trans. Automatic Control, Vol AC-11, PP. 546-550.

[48] Narendra, K. S. and Parthasarathy, K. (1990), "Identification and Control of Dynamical Systems Using Neural Networks", IEEE Trans. on Neural Networks, Vol. 1, No. 1, pp. 4-27.

[49] Newland, D. E. (1984), An Introduction to Random Vibrations and Spectral Analysis - second edition, John Wiely & Sons, Inc., New York.

[50] Orava, P. J. and Niemi, A. J. (1974), "State Model and Stability Analysis of a PH Control Process", Int. J. Control, Vol. 20, No. 4, pp. 557-567.

[51] Pajunen, G. A. (1985), "Recursive Identification of Wiener Type Nonlinear Systems", American Control Conference, Vol. 3, pp. 1365-1370.

[52] Parker, G. A. and Moore, E. L. (1982), "Practical Nonlinear System Identification Using a Modified Volterra Series Approach", Int. J. Control, Vol. 18, No. 1, pp. 85-91.

[53] Reklaitis, G. V., Ravindran, R. and Ragsdell, K. M. (1983), Engineering Optimization - Methods and Applications, John Wiely & Sons, Inc.

[54] Sagaspe, J. P. (1979), "About Non-Linear Identification using Volterra Model", IFAC, Volume 1, pp. 501-503.

[55] Söderström, T., Ljung, L. and Gustavsson, I. (1978), "A Theoretical Analysis of Recursive Identification Methods", Automatica, Vol. 14, pp. 231-244.

[56] Stalford, H., Baumann, W. T., Garrett, E. and Herdman, T. L. (1987), "Accurate Modeling of Nonlinear Systems Using Volterra Series Submodels", American Control Conference, Vol. 2, pp. 886-891.

[57] Stoica, P. and Södertröm, T. (1982), "Instrumental-Variable Methods for Identification of Hammerstein Systems", Int. J. Control, Vol. 35, No. 3, pp. 459-476.

[58] Takagi, T. and Sugeno, M. (1985), "Fuzzy Identification of Systems and Its Applications to Modeling and Control", IEEE Trans. Syst., Man, Cybern, Vol. SMC-15, No. 1, pp. 116-132.

[59] Taylor, J. H. (1983), "A Systematic Nonlinear Controller Design Approach Based on Quasilinear Models", American Control Conference, WA7-11:45, pp. 141-145.

[60] Taylor, J. H. and Strobel, K. L. (1984), "Applications of a Nonlinear Controller Design Approach Based on Quasilinear System Models", American Control Conference, San Diego, CA.

[61] Taylor, J. H. and Strobel, K. L. (1985), "Nonlinear Control System Design Based on Quasilinear System Models", American Control Conference.

[62] Volterra, V. (1930), Theory of functions, Blackie.

[63] Young, G. E. and Rao, S. (1987), "Robust Sliding-Mode Control of a Nonlinear Process with Uncertainty and Delay", ASME Journal of Dynamic Systems, Measurement and Control, Vol. 109, pp. 203-208.

[64] Zadeh, L. A. (1973), "Outline of a New Approach to the Analysis of Complex Systems and Decision Processes", IEEE Trans. Syst., Man. Cybern, Vol. SMC-3, No. 1, pp.28-44.

APPENDIX A

PROOFS OF THEOREM 2.1 AND THEOREM 2.2

Proof of Theorem 2.1

By definitions 2.1, 2.2 and 2.4, it is equivalent to proving that if Equations (2.27) hold then

$$\mu_1^{<1>} = \mu_1^{<2>} \tag{A.1a}$$

$$\mu_2^{<1>} = \mu_2^{<2>} \tag{A.1b}$$

$$\underline{\Sigma}^{<1>}_{S,a_i} = \underline{\Sigma}^{<2>}_{S,a_i} \quad \text{and} \quad \underline{\Sigma}^{<1>}_{S,b_j} = \underline{\Sigma}^{<2>}_{S,b_j} \,, \qquad i = 1,..,n \text{ and } j = 1,..,m \tag{A.1c}$$

$$\underline{\Sigma}^{<1>}_{L,a_i} = \underline{\Sigma}^{<2>}_{L,a_i} \quad \text{and} \quad \underline{\Sigma}^{<1>}_{L,b_j} = \underline{\Sigma}^{<2>}_{L,b_j} \,, \qquad i = 1,..,n \text{ and } j = 1,..,m \tag{A.1d}$$

But, owing to Equations (2.29) and (2.30),

$$\underline{\Sigma}^{<k>}_{S,a_i} \neq 0 \quad \text{or} \quad \underline{\Sigma}^{<k>}_{S,b_j} \neq 0$$
$$\exists\, i = 1,..,n \text{ or } \exists\, j = 1,..,m \,,\ k = 1,2 \tag{A.2a}$$

$$\underline{\Sigma}^{<k>}_{L,a_i} \neq 0 \quad \text{or} \quad \underline{\Sigma}^{<k>}_{L,b_j} \neq 0$$

$$\exists\, i = 1,..,n \text{ or } \exists\, j = 1,..,m\ ,\ k = 1,2 \qquad \text{(A.2b)}$$

$$\underline{\Sigma}^{<k>}_{S,a_i} \neq \underline{\Sigma}^{<k>}_{L,a_i} \quad \text{or} \quad \underline{\Sigma}^{<k>}_{S,b_j} \neq \underline{\Sigma}^{<k>}_{L,b_j}$$

$$\exists\, i = 1,..,n \text{ or } \exists\, j = 1,..,m\ ,\ k = 1,2 \qquad \text{(A.2c)}$$

Although it may exist the following relations between the parameters μ_1 and μ_2 :

$$\mu_1^{<1>} < \mu_2^{<1>} \quad \text{and} \quad \mu_1^{<2>} < \mu_2^{<2>} \qquad \text{(A.3a)}$$

$$\mu_1^{<1>} > \mu_2^{<1>} \quad \text{and} \quad \mu_1^{<2>} > \mu_2^{<2>} \qquad \text{(A.3b)}$$

$$\mu_1^{<1>} < \mu_2^{<1>} \quad \text{and} \quad \mu_1^{<2>} > \mu_2^{<2>} \qquad \text{(A.4a)}$$

$$\mu_1^{<1>} > \mu_2^{<1>} \quad \text{and} \quad \mu_1^{<2>} < \mu_2^{<2>} \qquad \text{(A.4b)}$$

Equations (A.4) indeed result in conflict with Equations (A.2a) and (A.2b) if Equations (2.27) hold. For example, it is not possible to have the function $\hat{a}_1(\mathcal{D})$ in Equation (2.16) equal to that in Equation (2.18) unless $\hat{a}_1(\mathcal{D}) = 0$. So, one just needs to investigate each condition of Equations (A.3).

1. In case Equation (A.3a) holds

Claim that Equation (A.1a) holds, otherwise there will exit an interval $[\mu_1^{<1>}, \mu_1^{<2>}]$ if $\mu_1^{<2>} > \mu_1^{<1>}$ or $[\mu_1^{<2>}, \mu_1^{<1>}]$ if $\mu_1^{<1>} > \mu_1^{<2>}$ such that

$$\mathcal{P}^{<k>}_{S,a_i}(\mathcal{D}) = \underline{\Sigma}^{T<k>}_{S,a_i}\,\underline{\Delta} = \mathcal{P}^{<k>}_{S,b_j}(\mathcal{D}) = \underline{\Sigma}^{T<k>}_{S,b_j}\,\underline{\Delta} = 0$$

$$i = 1,..,n\ ,\ j = 1,..,m\ ,\ k = 1,2 \qquad (A.5)$$

Since the elements of $\underline{\Delta}$ are mutually orthogonal, Equation (A.5) results in conflict with Equation (A.2a).

Similarly, claim Equation (A.1b) holds, otherwise there will exit an interval $[\mu_2^{<1>}, \mu_2^{<2>}]$ if $\mu_2^{<2>} > \mu_2^{<1>}$ or $[\mu_2^{<2>}, \mu_2^{<1>}]$ if $\mu_2^{<1>} > \mu_2^{<2>}$ such that

$$\mathcal{P}^{<k>}_{L,a_i}(\mathcal{D}) = \underline{\Sigma}^{T<k>}_{L,a_i}\,\underline{\Delta} = \mathcal{P}^{<k>}_{L,b_j}(\mathcal{D}) = \underline{\Sigma}^{T<k>}_{L,b_j}\,\underline{\Delta} = 0$$

$$i = 1,..,n\ ,\ j = 1,..,m\ ,\ k = 1,2 \qquad (A.6)$$

Equation (A.6) results in conflict with Equation (A.2b).

Moreover, from Equations (2.27) one has

$$\mathcal{P}^{<1>}_{S,a_i} = \mathcal{P}^{<2>}_{S,a_i}\ ,\quad \mathcal{P}^{<1>}_{S,b_j} = \mathcal{P}^{<2>}_{S,b_j}$$

$$i = 1,..,n \text{ and } j = 1,..,m \qquad (A.7a)$$

$$\mathcal{P}^{<1>}_{L,a_i} = \mathcal{P}^{<2>}_{L,a_i}\ ,\quad \mathcal{P}^{<1>}_{L,b_j} = \mathcal{P}^{<2>}_{L,b_j}$$

$$i = 1,..,n \text{ and } j = 1,..,m \qquad (A.7b)$$

Again, By applying the mutual orthogonality of the elements of $\underline{\Delta}$, Equations (A.1c) and (A.1d) obviously hold.

2. In case Equation (A.3b) holds

Claim that Equation (A.1b) holds. Otherwise consider

the intervals $[\mathcal{D}_{min}, \mu_2^{<2>}]$ and $[\mu_2^{<2>}, \mu_2^{<1>}]$ if $\mu_2^{<1>} > \mu_2^{<2>}$ (similar for the case if $\mu_2^{<2>} > \mu_2^{<1>}$). For the former interval,

$$\underline{\Sigma}^{T<1>}_{S,a_i} \underline{\Delta} = \underline{\Sigma}^{T<2>}_{S,a_i} \underline{\Delta} \quad , \quad i = 1,\ldots,n \tag{A.8a}$$

$$\underline{\Sigma}^{T<1>}_{S,b_j} \underline{\Delta} = \underline{\Sigma}^{T<2>}_{S,b_j} \underline{\Delta} \quad , \quad j = 1,\ldots,m \tag{A.8b}$$

For the latter interval,

$$\underline{\Sigma}^{T<1>}_{S,a_i} \underline{\Delta} = \pi_S^{<2>}(\mathcal{D}) \, \underline{\Sigma}^{T<2>}_{S,a_i} \underline{\Delta} + \pi_L^{<2>}(\mathcal{D}) \, \underline{\Sigma}^{T<2>}_{L,a_i} \underline{\Delta} \, , \quad i = 1,\ldots,n \tag{A.9a}$$

$$\underline{\Sigma}^{T<1>}_{S,b_j} \underline{\Delta} = \pi_S^{<2>}(\mathcal{D}) \, \underline{\Sigma}^{T<2>}_{S,b_j} \underline{\Delta} + \pi_L^{<2>}(\mathcal{D}) \, \underline{\Sigma}^{T<2>}_{L,b_j} \underline{\Delta} \, , \quad j = 1,\ldots,m \tag{A.9b}$$

From Equations (A.8) and (A.9), it is easy to show that

$$\underline{\Sigma}^{T<2>}_{S,a_i} = \underline{\Sigma}^{T<2>}_{L,a_i} \quad \text{and} \quad \underline{\Sigma}^{T<2>}_{S,b_j} = \underline{\Sigma}^{T<2>}_{L,b_j} \quad i = 1,..,n \text{ and } j = 1,..,m \tag{A.10}$$

that is in conflict with Equation (A.2c).

Similarly, claim Equation (A.1a) holds. Otherwise consider the intervals $[\mu_1^{<2>}, \mu_1^{<1>}]$ and $[\mu_1^{<1>}, \mathcal{D}_{max}]$ if $\mu_1^{<1>} > \mu_1^{<2>}$ (similar for the case if $\mu_1^{<2>} > \mu_1^{<1>}$). For the latter interval,

$$\underline{\Sigma}^{T<2>}_{L,a_i}\ \underline{\Delta} = \underline{\Sigma}^{T<1>}_{L,a_i}\ \underline{\Delta} \quad , \quad i = 1,\ldots,n \tag{A.11a}$$

$$\underline{\Sigma}^{T<2>}_{L,b_j}\ \underline{\Delta} = \underline{\Sigma}^{T<1>}_{L,b_j}\ \underline{\Delta} \quad , \quad j = 1,\ldots,m \tag{A.11b}$$

For the former interval,

$$\underline{\Sigma}^{T<2>}_{L,a_i}\ \underline{\Delta} = \mathcal{W}_S^{<1>}(\mathcal{D})\ \underline{\Sigma}^{T<1>}_{S,a_i}\ \underline{\Delta} + \mathcal{W}_L^{<1>}(\mathcal{D})\ \underline{\Sigma}^{T<1>}_{L,a_i}\ \underline{\Delta} \ , \quad i = 1,\ldots,n \tag{A.12a}$$

$$\underline{\Sigma}^{T<2>}_{L,b_j}\ \underline{\Delta} = \mathcal{W}_S^{<1>}(\mathcal{D})\ \underline{\Sigma}^{T<1>}_{S,b_j}\ \underline{\Delta} + \mathcal{W}_L^{<1>}(\mathcal{D})\ \underline{\Sigma}^{T<1>}_{L,b_j}\ \underline{\Delta} \ , \quad j = 1,\ldots,m \tag{A.12b}$$

Equations (A.11) and (A.12) further lead to

$$\underline{\Sigma}^{T<1>}_{S,a_i} = \underline{\Sigma}^{T<1>}_{L,a_i} \quad \text{and} \quad \underline{\Sigma}^{T<1>}_{S,b_j} = \underline{\Sigma}^{T<1>}_{L,b_j} \qquad i = 1,..,n \text{ and } j = 1,..,m \tag{A.13}$$

that is again in conflict with Equation (A.2c).

The reason why Equations (A.1c) and (A.1d) hold is exactly the same as that having been given for the case of Equation (A.3a). Henceforth, the proof is completed.

Proof of Theorem 2.2

Continue the proof of Theorem 2.1. With the constraint of Equation (2.15) and for $\mu_2 < \mathcal{D} < \mu_1$, one has

$$\mu_S(\mathcal{D}) > 0 \tag{A.14a}$$

$$\mu_L(\mathcal{D}) > 0 \tag{A.14b}$$

and

$$\pi_S(\mathcal{D}) + \pi_L(\mathcal{D}) = 1 \tag{A.15}$$

In Equation (A.2c), suppose that

$$\underline{\Sigma}^{<k>}_{S,a_1} \neq \underline{\Sigma}^{<k>}_{L,a_1} \quad , \quad k = 1,2 \tag{A.16}$$

By Equations (2.27), one has

$$\pi_S^{<1>}(\mathcal{D})\ \mathcal{P}^{<1>}_{S,a_1}(\mathcal{D}) + \pi_L^{<1>}(\mathcal{D})\ \mathcal{P}^{<1>}_{L,a_1}(\mathcal{D}) = \pi_S^{<2>}(\mathcal{D})\ \mathcal{P}^{<2>}_{S,a_1}(\mathcal{D}) + \pi_L^{<2>}(\mathcal{D})\ \mathcal{P}^{<2>}_{L,a_1}(\mathcal{D}) \tag{A.17}$$

Combining Equations (A.15), (A.16) and (A.17), it is straightforward to show that

$$\pi_S^{<1>}(\mathcal{D}) = \pi_S^{<2>}(\mathcal{D}) \tag{A.18}$$

Furthermore, Equations (A.14) and (A.18) lead to

$$\mu_S^{<1>}(\mathcal{D})\ \mu_L^{<2>}(\mathcal{D}) = \mu_S^{<2>}(\mathcal{D})\ \mu_L^{<1>}(\mathcal{D}) \tag{A.19}$$

where the membership functions were given in Equations (2.9) and (2.10) and are rewritten here.

$$\mathcal{M}_S^{<k>}(\mathcal{D}) = (1 - \mu_3^{<k>})\ \mathcal{L}_S^2 + \mu_3^{<k>}\ \mathcal{L}_S \quad , \quad k = 1,2 \qquad \text{(A.20a)}$$

$$\mathcal{M}_L^{<k>}(\mathcal{D}) = (1 - \mu_4^{<k>})\ \mathcal{L}_L^2 + \mu_4^{<k>}\ \mathcal{L}_L \quad , \quad k = 1,2 \qquad \text{(A.20b)}$$

where

$$\mathcal{L}_S(\mathcal{D}) = \omega_1 + \omega_2\ \mathcal{D} \qquad \text{(A.20c)}$$

$$\mathcal{L}_L(\mathcal{D}) = \omega_3 + \omega_4\ \mathcal{D} \qquad \text{(A.20d)}$$

and

$$\omega_1 = \mu_1/(\mu_1 - \mathcal{D}_{min}) \qquad \text{(A.21a)}$$

$$\omega_2 = -1/(\mu_1 - \mathcal{D}_{min}) \qquad \text{(A.21b)}$$

$$\omega_3 = -\mu_2/(\mathcal{D}_{max} - \mu_2) \qquad \text{(A.21c)}$$

$$\omega_4 = 1/(\mathcal{D}_{max} - \mu_2) \qquad \text{(A.21d)}$$

For convenience, the superscripts of μ_1 and μ_2 in Equations (A.21) have been omitted.

Substituting Equations (A.20) into Equation (A.19) and after arrangement, one has :

$$\mu_3^{<1>} + \mu_4^{<2>} - \mu_3^{<1>}\mu_4^{<2>} = \mu_3^{<2>} + \mu_4^{<1>} - \mu_3^{<2>}\mu_4^{<1>} \qquad \text{(A.22a)}$$

$$\omega_2(1-\mu_3^{<1>})\mu_4^{<2>} + \omega_4(1-\mu_4^{<2>})\mu_3^{<1>} = \omega_2(1-\mu_3^{<2>})\mu_4^{<1>} + \omega_4(1-\mu_4^{<1>})\mu_3^{<2>} \qquad \text{(A.22b)}$$

$$\omega_1(1-\mu_3^{<1>})\mu_4^{<2>} + \omega_3(1-\mu_4^{<2>})\mu_3^{<1>} + \mu_3^{<1>}\mu_4^{<2>} =$$
$$\omega_1(1-\mu_3^{<2>})\mu_4^{<1>} + \omega_3(1-\mu_4^{<1>})\mu_3^{<2>} + \mu_3^{<2>}\mu_4^{<1>} \qquad \text{(A.22c)}$$

By canceling all cross-product terms in Equations (A.22), one has

$$\mathbf{A}\begin{bmatrix} \mu_3^{<1>} \\ \mu_4^{<2>} \end{bmatrix} = \mathbf{A}\begin{bmatrix} \mu_3^{<2>} \\ \mu_4^{<1>} \end{bmatrix} \qquad \text{(A.23a)}$$

where

$$\mathbf{A} = \begin{bmatrix} \omega_2 & \omega_4 \\ \omega_1-1 & \omega_3-1 \end{bmatrix} \qquad \text{(A.23b)}$$

The proof is completed since $|\mathbf{A}| \neq 0$ and henceforth

$$\mu_3^{<1>} = \mu_3^{<2>} \qquad \text{(A.24a)}$$

$$\mu_4^{<1>} = \mu_4^{<2>} \qquad \text{(A.24b)}$$

APPENDIX B

THE COMPLEX METHOD

The Complex Method [M.J. Box 1965] is an algebraic optimization algorithm which, strictly speaking, requires a convex working space (i.e. if for any two points in the space, the line joining those two points is also in the space).

For this application, the working space is a subspace of $\mathbb{R}^n$ (also called μ-space in the context) satisfying some constraints such as Equations (2.11), (2.15) and (2.17) where n denotes the number of μs involved in the membership functions. The method begins with an initial point denoted by $\underline{\mu}^{(1)} = \{\mu_i^{(1)} | i = 1,..,n\}$ which can be arbitrarily assigned in the working space.

A summary of the Complex Method is given below [53] :

Step 1. Determine another $m - 1$ initial feasible points by using the following equation :

$$\mu_i^{(j)} = \mathcal{D}_{min} + d\,(\mathcal{D}_{max} - \mathcal{D}_{min}) \;, \qquad i = 1,\ldots,n \text{ and } j = 2,\ldots,m \qquad \text{(B.1)}$$

where d is a random number uniformly distributed over the

interval [0,1].

During the calculations of Equation (B.1), If a point $\underline{\mu}^{(j)}$ generated is not within the working space (say, an infeasible point), calculate the centroid $\underline{\mu}^{*}$ of the current set of points and reset

$$\underline{\mu}^{(j)} = 0.5\ (\underline{\mu}^{*} + \underline{\mu}^{(j)}) \qquad (B.2)$$

Repeat and until $\underline{\mu}^{(j)}$ becomes feasible.

For each feasible point $\underline{\mu}^{(j)}$, a corresponding model within the working model structure can be formed by incorporating the Least-Squares estimator (see also Chapter III). Henceforth, each feasible point indeed comes with an associated model performance index $\vartheta(\underline{\mu}^{(j)})$.

Step 2. Determine the point $\underline{\mu}^{(o)}$ which results in the poorest performance index (say, ϑ_{max}). Calculate the centroid $\underline{\mu}^{*}$ and the new point $\underline{\mu}^{(n)}$.

$$\underline{\mu}^{(n)} = \underline{\mu}^{*} + \alpha\ (\underline{\mu}^{*} - \underline{\mu}^{(o)}) \qquad (B.3)$$

where α is a reflection constant.

(a) If $\underline{\mu}^{(n)}$ is feasible but $\vartheta(\underline{\mu}^{(n)}) > \vartheta_{max}$, retract half the distance to the centroid. Continue until $\vartheta(\underline{\mu}^{(n)}) < \vartheta_{max}$ and then go to Step 4.

(b) If $\mu^{(n)}$ is feasible and $\vartheta(\underline{\mu}^{(n)}) < \vartheta_{max}$, go to Step 4.

(c) If $\underline{\mu}^{(n)}$ is infeasible, go to Step 3.

Step 3. Adjust for feasibility.

(a) If $\underline{\mu}^{(n)} > \mathcal{D}_{max}$, set $\underline{\mu}^{(n)} = \mathcal{D}_{max}$.

If $\underline{\mu}^{(n)} < \mathcal{D}_{min}$, set $\underline{\mu}^{(n)} = \mathcal{D}_{min}$.

(b) If $\underline{\mu}^{(n)}$ is infeasible, retract half the distance to the centroid. Continue until $\underline{\mu}^{(n)}$ is feasible and then go to Step 4.

Step 4. Check for termination. If

$$|\vartheta_{max} - \vartheta_{min}| \leq \varepsilon_i \tag{B.4a}$$

and/or

$$\| \underline{\mu}^{(j)} - \underline{\mu}^{*} \|_{max} \leq \varepsilon_d \ , \ j = 1,\ldots,m \tag{B.4b}$$

terminate. Otherwise go to Step 2. ε_i and ε_d are small numbers.

Remark B1. In Step 2(a), during the retracting process the condition $\vartheta(\underline{\mu}^{(n)}) < \vartheta_{max}$ could be never met. A proper modification of this step is suggested below in case the condition still doesn't be met after a pre-set number of times of retracting :

Determine the point which has the corresponding best performance index ϑ_{min}. *Retract all the other points half the distance to the "best" point. Repeat until the conditions* (B.4) *are met and then terminate.*

Remark B2. According to the numerical experiments [M.J. Box 1965], $\alpha = 1.3$ and $m = 2n$ are recommended. However, good results could be achieved by choosing $\alpha = 1.3$ and $m = n + 2$.

Remark B3. Upper and lower bounds of the dynamic variable x_i must be known to carry out Step 1. If such bounds do not naturally arise as part of the problem formulation, then it is necessary to provide some estimated values, and for computational efficiency the bounds should be as tight as possible.

Remark B4. The Complex Method does not require continuity of the problem functions, since it makes no use of function value difference. That's why the proposed identification method is able to deal with systems with discontinuous parameter functions.

APPENDIX C

STATE VARIABLE & UNITY OUTPUT (SV&UO) FEEDBACK CONTROL

State variable feedback control based on pole assignment is a well-known technique to shape system transient dynamics. For tracking control applications, the technique was extended by introducing a co-state in the feedforward path along with an unity output feedback [Christensen et. al. 1986].

A block diagram of SV&UO feedback controller is shown in Figure C.1.

SV&UO feedback controller :

$$I(t) = - \underline{g}^T \underline{x}(t) \qquad (C.1a)$$

where

$$\underline{g} = [g_1, g_2, g_3]^T \qquad (C.1b)$$

$$\underline{x}(t) = [N(t), P(t), E(t)]^T \qquad (C.1c)$$

and

$$E(t+1) = E(t) + N_d(t) - N(t) \qquad (C.2)$$

The reason to introduce the co-state E(t) is to

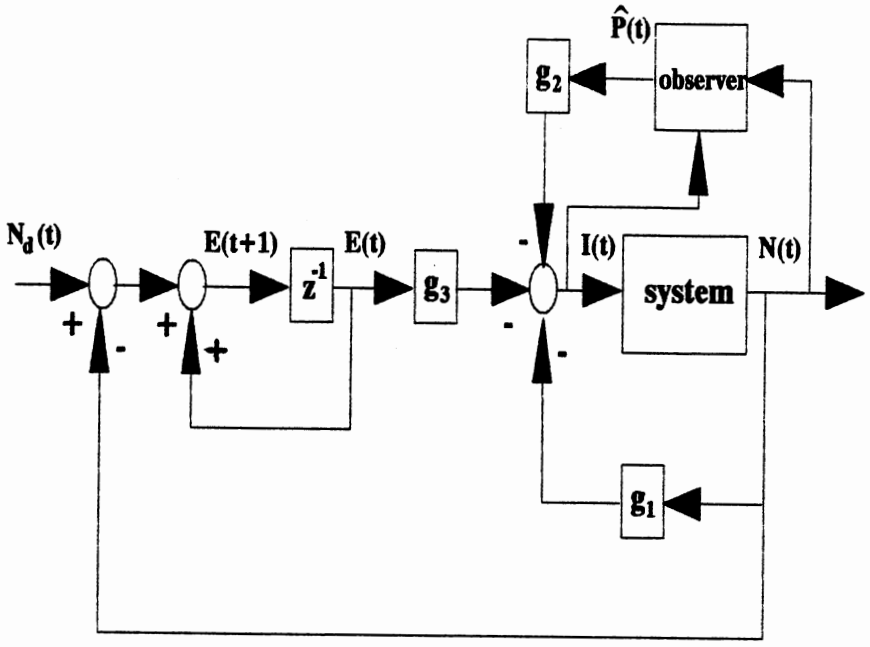

Figure C.1. A Block Diagram of SV&UO Feedback Control with Observer [Christensen et. al. 1986].

guarantee that the system output N(t) will track the desired output $N_d(t)$, so long as the closed-loop system is stable or the feedforward loop reaches steady state (i.e. E(t+1) = E(t), as $t \rightarrow \infty$).

Substituting Equations (C.1) into Equation (4.28) with $t_d = 0$ and then with Equation (C.2), one has

$$\underline{x}(t+1) = \mathbf{A}\, \underline{x}(t) + \underline{b}\, N_d(t) \tag{C.3a}$$

where

$$\mathbf{A} = \begin{bmatrix} \hat{a}_{11}-\hat{b}_1 g_1 & \hat{a}_{12}-\hat{b}_1 g_2 & -\hat{b}_1 g_3 \\ \hat{a}_{21}-\hat{b}_2 g_1 & \hat{a}_{22}-\hat{b}_2 g_2 & -\hat{b}_2 g_3 \\ -1 & 0 & 1 \end{bmatrix} \tag{C.3b}$$

$$\underline{b} = [0,\ 0,\ 1]^T \tag{C.3c}$$

Let the desired closed-loop poles be the roots of the following characteristic equation :

$$1 + \xi_1 q^{-1} + \xi_2 q^{-2} + \xi_3 q^{-3} = 0 \tag{C.4}$$

Then, after manipulation, one has the following for calculation of the control gains gs in Equation (C.1b) :

$$\underline{g}^T = \frac{1}{\delta}\, \underline{r}^T\, \mathbf{S} \tag{C.5}$$

where

$$\underline{r} = [r_1,\ r_2,\ r_3]^T \tag{C.6a}$$

$$S = \begin{bmatrix} s_{11} & s_{12} & s_{13} \\ s_{21} & s_{22} & s_{23} \\ s_{31} & s_{32} & s_{33} \end{bmatrix} \tag{C.6b}$$

$$r_1 = -\hat{b}_1\hat{b}_2 \tag{C.6c}$$

$$r_2 = \hat{b}_1^2 \tag{C.6d}$$

$$r_3 = \hat{b}_1(\hat{a}_{21}\hat{b}_1 + \hat{a}_{22}\hat{b}_2) - \hat{b}_2(\hat{a}_{11}\hat{b}_1 + \hat{a}_{12}\hat{b}_2) \tag{C.6e}$$

$$s_{11} = \hat{a}_{11}^3 + \xi_1\hat{a}_{11}^2 + (2\,\hat{a}_{12}\hat{a}_{21} + \xi_2)\hat{a}_{11} + \hat{a}_{12}\hat{a}_{21}(\hat{a}_{22} + \xi_1) + \xi_3 \tag{C.6f}$$

$$s_{12} = (\hat{a}_{11}^2 + \hat{a}_{11}\hat{a}_{22} + \hat{a}_{22}^2 + \xi_1(\hat{a}_{11} + \hat{a}_{22}) + \hat{a}_{12}\hat{a}_{21} + \xi_2)\,\hat{a}_{12} \tag{C.6g}$$

$$s_{13} = 0 \tag{C.6h}$$

$$s_{21} = s_{12}\hat{a}_{21} / \hat{a}_{12} \tag{C.6i}$$

$$s_{22} = \hat{a}_{22}^3 + \xi_1\hat{a}_{22}^2 + (2\,\hat{a}_{12}\hat{a}_{21} + \xi_2)\,\hat{a}_{22} + \hat{a}_{12}\hat{a}_{21}(\hat{a}_{11} + \xi_1) + \xi_3 \tag{C.6j}$$

$$s_{31} = -\hat{a}_{11}^2 - (1 + \xi_1)\,\hat{a}_{11} - (\hat{a}_{12}\hat{a}_{21} + 1 + \xi_1 + \xi_2) \tag{C.6k}$$

$$s_{32} = -(\hat{a}_{11} + \hat{a}_{22} + 1 + \xi_1)\,\hat{a}_{12} \tag{C.6l}$$

$$s_{33} = 1 + \xi_1 + \xi_2 + \xi_3 \tag{C.6m}$$

$$\delta = (\hat{a}_{12}\hat{b}_2 + \hat{b}_1)(\hat{a}_{12}\hat{b}_2^2 - \hat{a}_{21}\hat{b}_1^2) + \hat{b}_1\hat{b}_2\hat{a}_{11}(\hat{a}_{12}\hat{b}_2 + \hat{b}_1) - \hat{b}_1\hat{a}_{22}(2\,\hat{a}_{12}\hat{b}_2^2 + \hat{b}_1\hat{b}_2 - \hat{a}_{21}\hat{b}_1^2) + \hat{b}_1^2\hat{b}_2\hat{a}_{22}(\hat{a}_{22} - \hat{a}_{11}) \tag{C.6n}$$

P(t) is required to measure in the above controller. However, it can be estimated by using Luenberger observer

and the observer dynamics are determined independently as below :

$$\hat{P}(t+1) = \hat{a}_{22}\hat{P}(t) + \hat{a}_{21}N(t) + \hat{b}_2 I(t) + g_o\{N(t+1) - \hat{a}_{11}N(t) - \hat{b}_1 I(t) - \hat{a}_{12}\hat{P}(t)\} \qquad (C.7)$$

where g_o denotes the observer gain.

APPENDIX D

A SUMMARY OF THE PROPOSED SYSTEM IDENTIFICATION METHOD

As mentioned in Chapter I, the process of system identification includes three stages which are system modeling, parameter estimation, and model validation. In this appendix, the proposed method for each stage is defined in a block diagram as shown in Figure D.1.

In the stage of system modeling, a "linear" model structure with signal-dependent parameters such as Equations (2.19) or (2.20) is proposed. The model structure is a combination of "linear" dynamic equation(s) and fuzzy linguistic rules which describe the signal dependence of the system parameters (Chapter II).

In the stage of parameter estimation, the proposed method is a combination of the Complex Method and the recursive least-squares estimator. Basically, the model parameters are divided into two sets; in one set the parameter values are optimized in the sense of the Complex Method whereas in the other set the parameter values are estimated using the recursive least-square estimator.

Since in the optimization process of the Complex

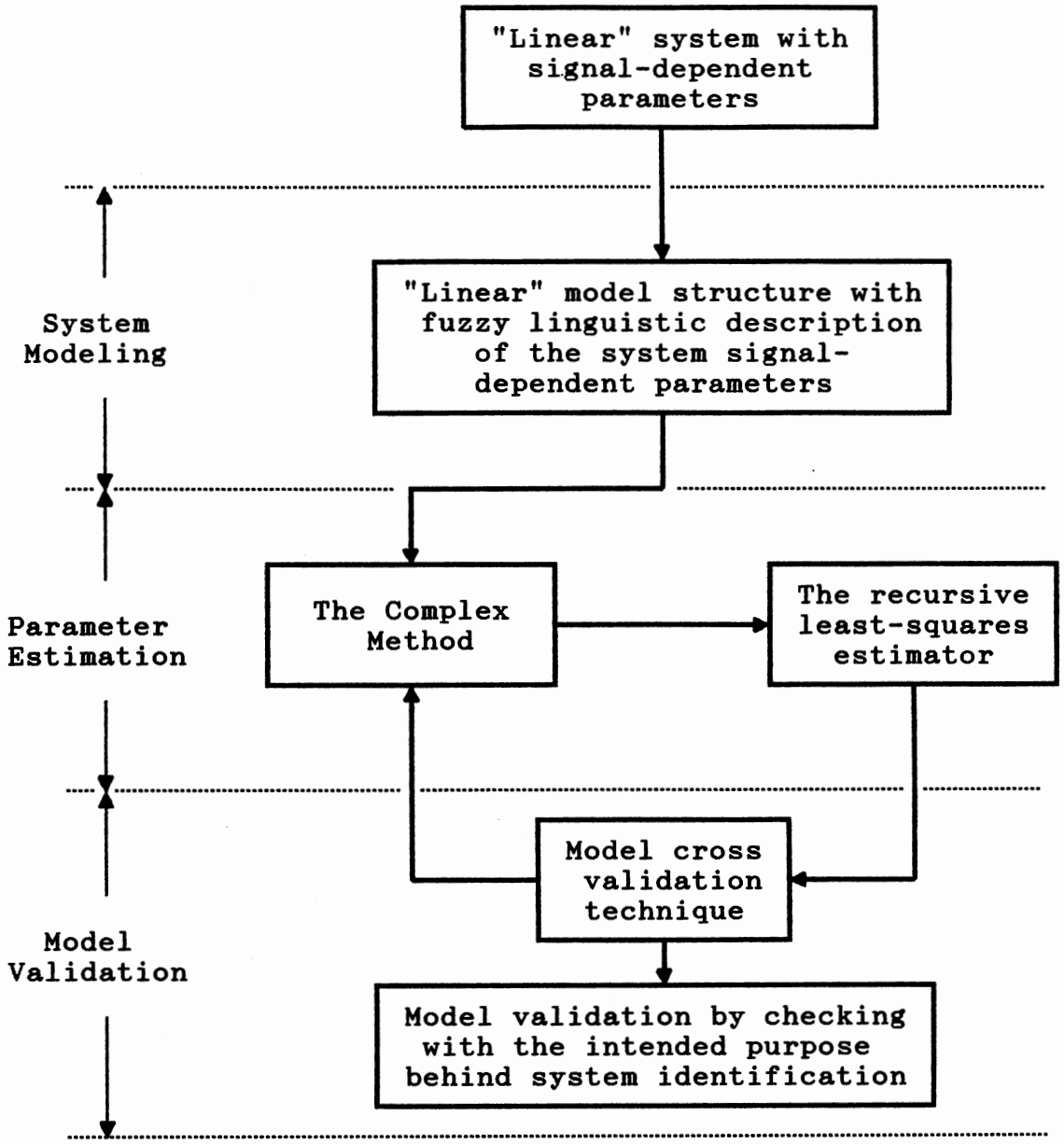

Figure D.1. A Block Diagram of the Proposed System Identification Method.

Method, a technique to evaluate model performance is required. In this respect, one called model cross validation is applied. Finally, the model resulting from the previous two stages is validated by checking with the intended purpose behind system identification such as for system control.

VITA

KU-CHIN LIN

Candidate for the Degree of

Doctor of Philosophy

Thesis: AN APPROACH TO MODELING AND IDENTIFICATION OF SYSTEMS WITH SIGNAL-DEPENDENT PARAMETERS

Major Field: Mechanical Engineering

Biographical:

Personal Data: Born in Taiwan, R. O. C., April 24, 1958, the son of Yi-zhi Lin and Kou Lyou. Married to Tsuey-Fang Chi on March 21, 1987.

Education: Graduated from Fongson High School, Taiwan, R. O. C., in June, 1976; received Bachelor of Science degree in Marine Engineering from National Taiwan College of Marine Science and Technology in June 1981; received Master of Science degree from National Taiwan Cheng Kung University in June, 1984; completed requirements for the Doctor of Philosophy degree at Oklahoma State University in May, 1992.

Professional Experience: Lecturer, Nan-Kai Institute of Technology, August, 1986, to August, 1987; Teaching Assistant, Department of Mechanical Engineering, Oklahoma State University, August, 1988, to May, 1989; Research Assistant, Department of Mechanical Engineering, Oklahoma State University, May, 1988, to May, 1992.